Effects of damming and reservoir operation on hydrodynamics and thermal regimes in large cascade reservoirs of the Yangtze River, China

by
Lianghong Long
Born in Hubei, China

Accepted Dissertation thesis for the partial fulfillment of the requirements for a
Doctor of Natural Sciences
Fachbereich 7: Natur- und Umweltwissenschaften
Universität Koblenz-Landau

Thesis examiners:

Prof. Dr. Andreas Lorke, Landau

Prof. Dr. Zhengjian Yang, Landau

Date of the oral examination: 22 December 2020

This dissertation is based on the following manuscripts/publications (ordered by date):

Lianghong L., Daobin J., Defu L., Zhenjian Y., A., Lorke (2019). Effect of Cascading Reservoirs on the Flow Variation and Thermal Regime in the Lower Reaches of the Jinsha River. Water, 11(5): 1008. doi.org/10.3390/w11051008

Lianghong L., Daobin J., Zhengjian Y., A., Lorke (2019). Density driven water circulation in typical tributary of the Three Gorges Reservoir, China. River Research and Applications, 35: 833–843. doi.org/10.1002/rra.3459

Lianghong L., Daobin J., Zhenjian Y., Defu L., Heqing C., Zhongyong, Y., Liu, L., A. Lorke (2020). Tributary oscillations generated by diurnal discharge regulation in Three Gorges Reservoir. Environmental Research Letters, 15(8): 084011. doi.org/10.1088/1748-9326/ab8d80

Lianghong L., Zhenjian Y., Liu, L., Daobin J., A., Lorke. Recent changes of the thermal structure in Three Gorges Reservoir and its ecological impacts on tributary bays. Submitted to Science of Total Environment (4 November 2020), under review

Table of Contents

Abstract

Rivers play an important role in the global water cycle, support biodiversity and ecological integrity. However, river flow and thermal regimes are heavily altered in dammed rivers. These impacts are being exacerbated and become more apparent in rivers fragmented by multiple dams. Recent studies mainly focused on evaluating the cumulative impact of cascade reservoirs on flow or thermal regimes, but the role of upstream reservoirs in shaping the hydrology and hydrodynamics of downstream reservoirs remains poorly understood. To improve the understanding of the hydrodynamics in cascade reservoirs, long-term observational data are used in combination with numerical modeling to investigate the changes in flow and thermal regime in three cascade reservoirs at the upper reach of the Yangtze River. The three studied reservoirs are Xiluodu (XLD), Xiangjiaba (XJB) and Three Gorges Reservoir (TGR). In addition, the effects of single reservoir operation (at seasonal/daily time scale) on hydrodynamics are examined in a large tributary of TGR. The results show that the inflow of TGR has been substantially altered by the two upstream reservoirs with a higher discharge in spring and winter and a reduced peak flow in summer. XJB had no obvious contribution to the variations in inflow of TGR. The seasonal water temperature of TGR was also widely affected by the upstream two reservoirs, i.e., an increase in winter and decrease in spring, associated with a delay in water temperature rise and fall. These effects will probably be intensified in the coming years due to the construction of new reservoirs. The study also underlines the importance of reservoir operation in shaping the hydrodynamics of TGR. The seasonal dynamics of density currents in a tributary bay of TGR are closely related to seasonal reservoir operations. In addition, high-frequency water level fluctuations and flow velocity variations were observed in response to periodic tributary bay oscillations, which are driven by the diurnal discharge variations caused by the operation of TGR. As another consequence of operation of cascade reservoirs, the changes in TGR inflow weakened spring thermal stratification and caused warming in spring, autumn and winter. In response to this change, the intrusions from TGR occurred more frequently as overflow and earlier in spring, which caused a sharp reduction in biomass and frequency of phytoplankton blooms in tributary bays of TGR. This study suggests that high-frequency bay oscillations can

potentially be used as an efficient management strategy for controlling algal blooms, which can be included in future multi-objective ecological conservation strategies.

1 Introduction

1.1 The accelerating hydropower development in the globe

1.1.1 Global boom of hydropower development

For thousands of years, dams have been built to control and manage water resources in the world for benefits of human society, and the number has increased markedly over the past 60 years (Lehner et al., 2011). The 20th century experienced a bloom in dam construction. By early 21st century, > 50,000 dams that are higher than 15 m had been built in the world (Berga et al., 2006), among which about 8,600 dams were primarily designed for hydropower generation (International Commission on Large Dams (2011)). Future hydropower development is mainly concentrated in developing countries and emerging economies of Southeast Asia, South America, and Africa (Zarfl et al., 2014). In recent years, ability of dams to change natural river hydrology has increased in many river basins (Jiao et al., 2020; Magilligan and Nislow, 2005; Yan et al., 2010). On a global basis, 48% of rivers are moderately-to-severely affected by either flow regulation, fragmentation, or both, and the impacts might be doubled when currently planned dams are constructed by 2030 (Grill et al., 2015).

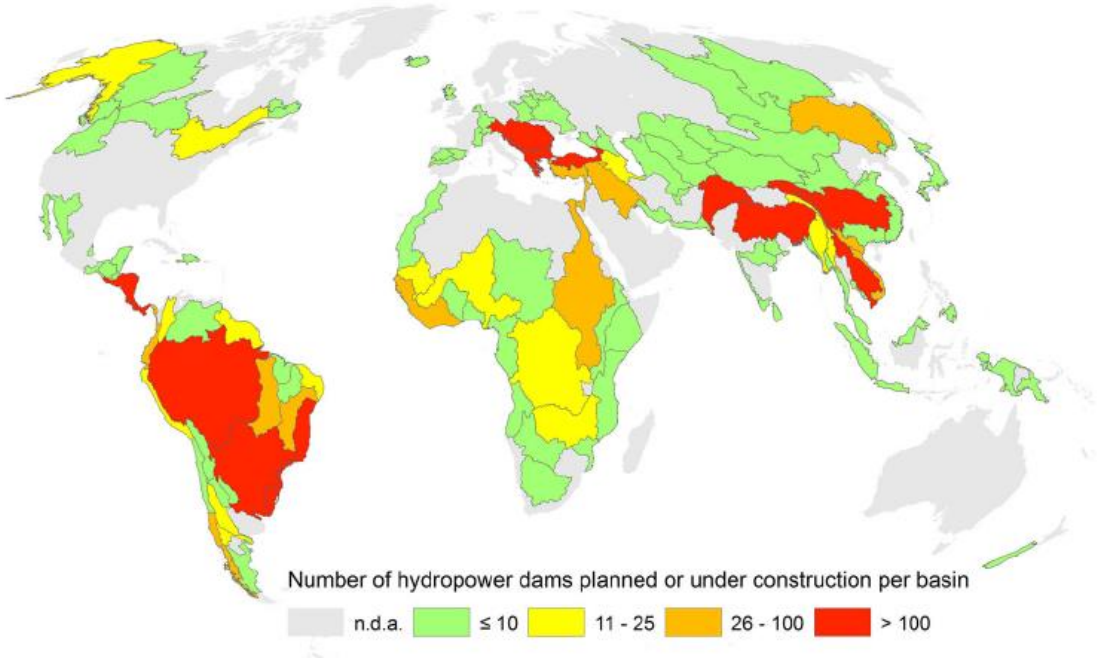

Figure 1. The global distribution of future hydropower dams planned or under construction per basin (Red > 100, Orange: 26–100, Yellow: 11–25, Green ≤ 10, Gray no data available, adapted from Zarfl et al.,

2014)

1.1.2 Overview of the area of interest (Yangtze River Basin)

China plays an important role in global hydropower development. The Yangtze River in China is an example for ongoing development of large cascading hydropower reservoirs, with a lot of large-scale hydropower projects planned, under construction, and completed (Yao et al., 2006) (Figure 2). The installed capacity of the hydropower station in the Yangtze River Basin accounts for 53.2% of the country's total. Recently, in the lower reach of Jinsha River (upper reach of Yangtze River), four cascade hydropower reservoirs (Xiangjiaba, Xiluodu, Wudongde and Baihetan) had been built. The first two reservoirs have been in operation since 2012, 2013, respectively, and the other two are currently under construction at upstream of Xiluodu (Table 1). The large number of dams and their associated environmental alterations resulted in a number of changes in hydrology (Wang et al., 2018; Xu and Zhang, 2018), water temperature (He et al., 2020; Wang et al., 2020), sediment load (Ren et al., 2020), greenhouse gases emissions (Li et al., 2020b) and fish communities (Yu et al., 2019). Thus, how to best assess the environmental impacts of these cascade reservoirs has become a burning issue.

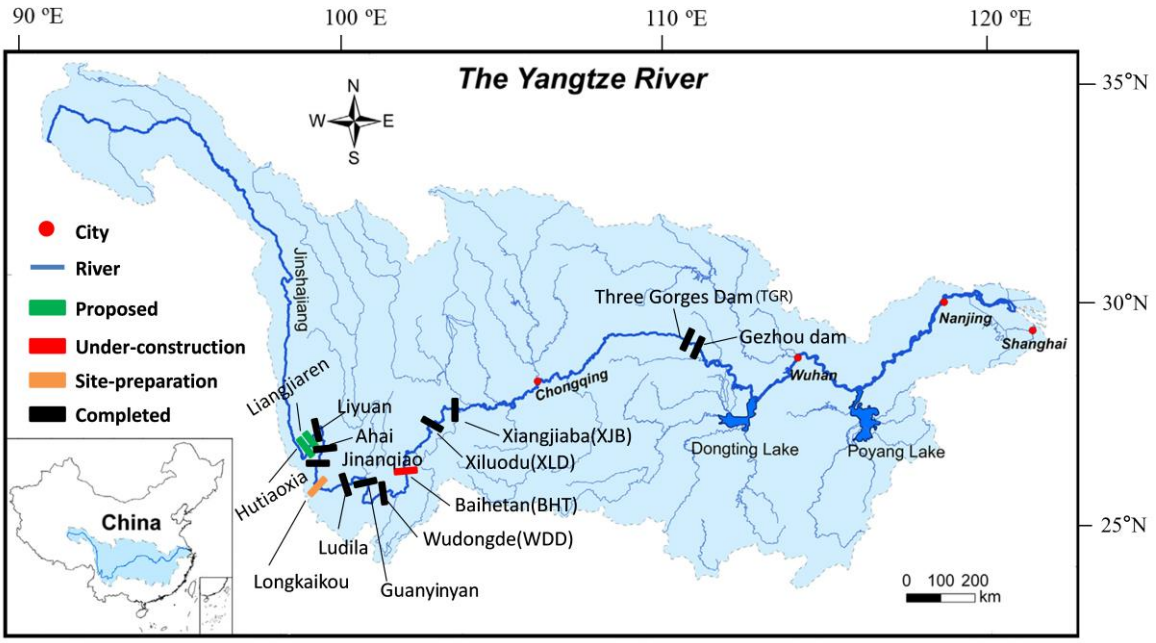

Figure 2. Map of the Yangtze River basin with names of proposed, under-construction, site-preparation, and completed hydropower dams in the main river. The lower left inset map shows the location of the studied region in China. The catchment area is marked by light blue color. The fiver dams (Wudongde, Baihetan, Xiluodu, Xiangjiaba and Three Gorges) mentioned in the study with an abbreviation in bracket, and major cities are marked by red filled circles, respectively.

Table 1. Main features of the studied cascade hydropower reservoirs (* denotes dams under construction). Dead water level refers to the lowest water level that allows the reservoir to operate under normal operation. m a.s.l. is abbreviation of meter above sea level).

Reservoir	Hydropower capacity (MW)	Dam height (m)	Normal Water level (m a.s.l.)	Dead water level (m a.s.l.)	Storage capacity (10^8 m^3)	Hydraulic residence time (days)	Operation year
Three Gorges (TGD)	22500	185	175	145	393	~36	2003
Xiangjiaba (XJB)	7750	162	380	370	52	~16	2012
Xiluodu (XLD)	13860	285.5	600	540	129	~37	2013
Baihetan (BHT)*	16000	289	820	760	179	-	2022
Wudongde (WDD)	10200	270	950	920	43	-	2020

1.2 The impacts of damming on flow and thermal regimes

1.2.1 Dam-induced flow alteration

Rivers play important roles in global cycle of water and biogeochemistry, sustaining aquatic biodiversity and ecological integrity (Arthington et al., 2006; Li et al., 2020a). In recent years, the river flow regimes were widely altered due to intensified dam constructions (Gierszewski et al., 2020; Poff and Matthews, 2013). Generally, most of dams operate with the goal to suppress peak flows, to compensate low flows, or to store or divert river flows. As a consequence, flow regimes in the downstream river can be seasonally modified in a way that the flow peaks are reduced during the flood season and the low flows in dry season are considerably enhanced (Jiang et al., 2014; Maingi and Marsh, 2002). These flow redistributions in time by dams can have far-reaching influences on river production, biodiversity, and ecosystem function (Nilsson et al., 2005). Thus, it is essential to gain a good understanding of the flow regime of rivers for ecological hydropower development as well as for reservoir operation.

Recent studies over the past decade have discussed flow regime alterations caused by dams in many basins, e.g., Amazon River (Timpe and Kaplan, 2017), Mekong River (Hecht et al., 2019), and Yellow River (Yang et al., 2012). Long-term hydrological observations (Duan et al., 2016; Yang et al., 2008) and integrated modeling approaches (Wang et al., 2018; Xu and Zhang, 2018) are commonly applied in assessing dam-induced flow alterations. The

regional-scale flow alterations of individual or cascade dams at a basin scale are well documented (Gao et al., 2013; Hecht et al., 2019; Mp et al., 1996), along with the disturbances caused by climate change (Mittal et al., 2014; Yang et al., 2008). Dams are known to alter and homogenize regional flow regimes by comparing the pre-impoundment period (Poff et al., 2007). Compared to the seasonal hydrologic response to dam (Cui et al., 2020), climate change causes gradual changes in the basin or global scale (Van Oorschot et al., 2018). However, an important unresolved question is the intrinsic connection between flow alterations and downstream thermal regime or water quality.

1.2.2 Dam-induced changes in river thermal regime

The thermal regime of rivers plays an important role in the overall health of aquatic ecosystems, affecting water quality and the distribution of aquatic species in the river environment (Caissie, 2006). Damming can greatly modify riverine thermal regimes (Olden and Naiman, 2010), especially in stratified reservoirs, where the vertical density gradient acts as a barrier suppressing mixing of the water column (Moreno-Ostos et al., 2008) and affects the vertical transfer of heat and thermal structure (Elçi, 2008). Furthermore, the discharged water differs greatly in temperature to that occurring naturally in the river (Caissie, 2006) and adversely alters downriver biotic conditions. It is therefore important to understand the thermal dynamics of rivers and related stratification processes in reservoirs.

Reservoirs in general alter the downstream river water temperature with two main features (Liu et al., 2005; Long et al., 2019; Preece and Jones, 2002; Wang et al., 2020): i) homogenization effect – reduction in the annual and daily fluctuations of water temperature; ii) hysteresis effect – delay in water temperature rise and fall (spring cooling and winter warming) (Olden and Naiman, 2010). The degree of alteration depends largely on stratification behavior of the reservoir and selective withdrawl depth (Olden and Naiman, 2010). Many large reservoirs with strong thermal stratification, e.g., Tahtali Reservoir (Çalışkan and Elçi, 2009) and Kouris reservoir (Ma et al., 2008), can selectively alter downstream river water temperature by releasing hypolimnetic (cold) or epilimnetic (warm) water. Well-mixed reservoirs can also directly modify a river's thermal regimes by distorting and blunting the definite synchronous behavior of interacting air and water temperature (Kędra and Wiejaczka, 2016; Poole and Berman, 2001). In addition, flow reduction and/or flow alteration can also

contribute to changes in downstream river water temperature (Caissie, 2006; Sinokrot and Gulliver, 2000). Given the important role of water temperature for biotic responses, the dynamics of stratification and reservoir operation on discharge are crucial to downstream river ecology and therefore should be better understood.

1.3 The response of hydrodynamics to reservoir operation

After the reservoir is filled, enlarged cross-sectional area causes a general reduction in flow velocity (Vörösmarty et al., 2003). The drastic changes in hydrodynamics (from lotic to lentic) (Agostinho et al., 2008; Casamitjana et al., 2003) are strongly related to the location and height of dam, volume of reservoir and water residence time (Schmutz and Sendzimir, 2018). Water residence time can be calculated as the ratio of reservoir storage capacity to discharge (Straškraba et al., 1995), which is closely related to mixing and transport processes, and seasonal changes in thermal stratification (Andradóttir et al., 2012; Rueda et al., 2006).

Seasonal and inter-annual cycle of flow regulation and water level fluctuations (WLFs) are important features of reservoirs. Hydropower reservoirs generally free their storage capacity prior to flood seasons (for flood control) and refill before dry seasons (for power generation). Seasonal WLFs are a key physical process that affects thermal stratification and ecosystem functioning in reservoirs (Geraldes and Boavida, 2005; Jin et al., 2019; Litvinov and Roshchupko, 2007). In addition to seasonal flow regulations, short-term reservoir hydrodynamics are also noticeably affected by various withdrawal schemes (Çalışkan and Elçi, 2009; Carr et al., 2020). Changing the schedule of discharge depth can alter vertical mixing regime (Johnson et al., 2004), which has large impacts on heat transport, distribution of dissolved oxygen and nutrients cycling (Meghan K. Carr et al., 2020). It has been simulated by numerical modeling that deep-water withdrawals tend to facilitate heat transfer in the water column and deepen the water mixing layer (Ma et al., 2008), in contrast to surface withdrawals that shrink the metalimnion and result in less mass transfer from the epilimnion to the hypolimnion (Zouabi-Aloui et al., 2015).

Recently, artificial hydrodynamics processes have been observed and simulated in reservoirs as a result of periodical discharge management (Sha et al., 2015; Xie et al., 2019). This periodic reservoir operation has been proven to be able to generate internal waves in

reservoirs (Bocaniov et al., 2014) and cause daily variations of water temperature (Xie et al., 2019). In stratified waters, internal waves are an important forcing mechanism for vertical energy and mass transport and shown to have a number of ecological effects (Boehrer, 2000; Hodges et al., 2000). In comparison to most commonly observed wind-driven internal waves (Stevens, 1999; Vidal et al., 2005; Vidal et al., 2007), the reservoir oscillations caused by discharge regulations are still poorly studied. In addition, the understanding of physical properties of artificial waves in reservoirs and their ecological impacts is still limited. Therefore, it is of great significance to conduct detailed hydrodynamic monitoring and quantify the impacts of reservoir operation.

1.4 Cumulative impacts in cascade reservoirs

With the number of dams increasing globally, the joint operations of cascade reservoirs has been widely adopted. In a cascade reservoirs system, the hydrodynamics in downstream reservoirs are not only affected by the size, location, operation of itself, but also affected by the water discharged from upstream reservoirs because of changes in flow rates (temperature). For example, inflow water often form a density current along the channel bottom due to lower temperature of the releasing water from upstream reservoirs (Chen et al., 2016a). The resulting hydrodynamics and thermal regime can both differ from that of a solitary reservoir (Chen et al., 2016a; Hocking and Straškraba, 1994). Compared to the individual impacts of dam, multiple dams can have cumulative impacts on the ecological environment (Dos Santos et al., 2018; Wang et al., 2014).

The cumulative environmental impacts induced by cascade hydropower reservoirs induce the superposition of impacts on the ecosystems that can be both spatial and temporal (Cooper and Sheate, 2002; Culp et al., 2000). However, the superposition of impacts is not a simple addition because of each other's interference. The influences can be either positive or negative mainly depending on diversion of the dams (Hou et al., 2011; Ma et al., 2018; Yi et al., 2019), which can develop via a supra-additive process (greater than the sum of the individual effects) or an infra-additive process (less than the sum of the individual effects). This indicates the integrated impacts from multiple dams can be diverse and multifactorial. For example, the impacts on hydrology can depend largely on the operational rules and,

naturally, size of reservoir, and on the actual number and location of the dams (Lauri et al., 2012). The few existing observations revealed an increase of the overall degree of cumulative effect in response to the joint operation of cascade reservoirs (Ouyang et al., 2011; Song et al., 2018). However, in most cases, the mechanisms how alterations propagate and potentially accumulate along the cascade are poorly understood. This may prevent us from having a systematic understanding of the ecological effects of dams in a cascade reservoir system.

1.5 Current research and knowledge gaps in the study area

The effects of dam on hydrologic regime (Duan et al., 2016), thermal regime (Wang et al., 2020; Xie et al., 2017) have been discussed in detail by field observation and model simulation in the Yangtze River. For example, TGR changed the magnitude of extreme flows, leading to increase of annual minimum flows and reduction of annual maximum flows (Chen et al., 2016b; Gao et al., 2013). And the annual cycle of water temperature experienced a damped response to air temperature and a marked seasonal alteration: spring cooling and winter warming (Cai et al., 2018; Tao et al., 2020). Previous studies examined the effect of TGR on downstream water temperature by simply comparing to pre-dam period (Dai et al., 2012; Long et al., 2016), but it remains difficult to accurately evaluate the dynamic effects of dam on river because some key processes have been overlooked: 1) Little is known about the response of thermal regime to different operational stages; 2) The thermal and ecological impacts of the two upstream newly-built large reservoirs on TGR are poorly explored.

Recently, the impacts of cascade reservoirs on the natural flow regime and water temperature in the Yangtze River have been investigated based on field observation by Chen et al., (2016) and hydrological model by Wang et al., (2020), and they found that ecological flows would be strongly influenced and the delays in temperature cycle will be further exacerbated when more reservoirs are involved. Nevertheless, both studies overlooked the mechanisms of alterations propagation and potentially accumulative process along the reservoir cascade. The role of individual reservoir in the cascade reservoirs system is poorly understood. Thus, it is of great significance to improve our understanding of flow alteration, thermal regime changes in cascade reservoirs, and reveal the impacts of upstream dams on hydrodynamics in downstream reservoirs.

In addition to hydrological and thermal regimes alteration, water quality and algal blooms in TGR have caught the attention of researchers from the globe (Fu et al., 2010; Stone,

2008; Xu et al., 2013). The main source of nutrients and other pollutants in tributary bays is the mainstream of the Yangtze River, which can intrude the tributary bays as a density current (Ma et al., 2015). The type of bidirectional density currents in the tributaries have great influence in nutrient and pollutant transport (Holbach et al., 2014), algal blooms (Yang et al., 2018), water quality (Xia et al., 2018). Thus, it is important to understand the dynamics of density currents and their impacts on hydrodynamics in tributary bays. Despite the large number of site-specific measurements and simulations in TGR and its tributaries (Xiong et al., 2013; Yang et al., 2010; Zhao et al., 2013; Zheng et al., 2011), direct long-term observations of density current are sparse and restricted to daily resolution. Besides, the response of the hydrodynamics in tributaries to high frequency (sub-daily) WLFs and the potential success of related mitigation measures remain speculative. Thus, a better understanding of ecological impacts of reservoir operation is needed with a more detailed study.

2 Hypotheses and research questions

The one goal of this PhD thesis is to improve understanding of the stratification and hydrodynamics in three cascade reservoirs (XLD, XJB, and TGR, Fig. 2), figure out the downriver flow alteration, thermal regime change, and cumulative impacts. Besides, the other goal is to reveal the effect of upstream two dams and TGR operation on hydrodynamic and algal blooms in the eutrophic tributary (Xiangxi bay) of TGR. In order to achieve our goals, the following three research questions should be answered corresponding to three hypotheses.

Question 1: How do the seasonal flow, thermal regimes, and stratification changes along the three cascade reservoirs?

Hypothesis 1.1: The seasonal river flow variability are significantly affected by the XLD and XJB in the upper reach of Yangtze River, with maximum flows being reduced during the flood season and minimum flows being increased in dry season.

Hypothesis 1.2: The river thermal regimes in the upper reach of Yangtze River are significantly altered by three above-mentioned reservoirs, with two features: i) homogenization effect; ii) hysteresis effect.

Hypothesis 1.3: The stratifications gradually get weakened along the reservoir cascade.

Question 2: What is the role of seasonal and diurnal operation scheduling in hydrodynamics in TGR?

Hypothesis 2.1: While seasonal operations that imply the large WLFs are closely related to the dynamics and shift of density currents among underflow, interflow, and overflow in tributary of TGR.

Hypothesis 2.2: Diurnal operation causes high-frequency WLFs and velocity variations by the formation of internal wave.

Question 3: What are the changes in hydrodynamics, and algal blooms in downstream reservoir (TGR) in response to the cascade reservoir operation?

Hypothesis 3.1: The upstream dams weaken the spring stratification in the downstream reservoir by significantly increasing in discharge rates.

Hypothesis 3.2: The recent changes of the thermal structure in Three Gorges Reservoir cause the shift of density currents and decrease the risk of algal bloom in tributary.

3 Outline

The field investigation and numerical modelling used to answer the research questions are divided into three parts and the findings are presented in 4 articles. The articles, attached as Appendices, either have been published / accepted or are under review. The research approaches to answer three questions addressed in each part are outlined below.

Part 1

Long-term daily observations of discharge and water temperature in the Yangtze River before and after damming were conducted to evaluate the impacts of dams on downstream river flow and water temperature (Q 1). A two-dimensional, laterally averaged, hydrodynamic model (CE-QUAL-W2) was applied to simulate the spatial and temporal distribution of water temperature in the upstream two reservoirs.

Appendix I -

Lianghong Long, Daobin Ji, Defu Liu, Zhengjian Yang, Andreas Lorke (2019). Effect of Cascading Reservoirs on the Flow Variation and Thermal Regime in the Lower Reaches of the Jinsha River. Water, 11(5): 1008. doi.org/10.3390/w11051008

Appendix IV-

Lianghong Long, Zhengjian Yang, Liu Liu, Daobin Ji, Defu Liu, Andreas Lorke (2020). Recent changes of the thermal structure in Three Gorges Reservoir and its ecological impacts on tributary bays. Submitted to Science of Total Environment (4 November 2020), under review

Part 2

CE-QUAL-W2 was applied to simulate the hydrodynamics in a eutrophic tributary bay (Xiangxi Bay) of TGR and examine the seasonal dynamics of density currents in recent years (Q 2). High-frequency measurements of flow velocity and water level in Xiangxi Bay, as well as hourly outflow from TGR, were performed to examine the hydrodynamics in tributary bay of TGR in response to sub-daily operation (Q 2).

Appendix II -

Lianghong Long, Daobin Ji, Zhengjian Yang, Scott A. Wells, Jun Ma, Defu Liu (2019). Density driven water circulation in typical tributary of the Three Gorges Reservoir, China. River Research and Applications, 35: 833–843. doi.org/10.1002/rra.3459

Appendix III-

Lianghong Long, Daobin Ji, Zhengjian Yang, Defu Liu, Heqing Cheng, Zhongyong Yang, Liu Liu, Andreas Lorke (2020). Tributary oscillations generated by diurnal discharge regulation in Three Gorges Reservoir. Environmental Research Letters 15(8): 084011. doi.org/10.1088/1748-9326/ab 8d80

Part 3

The seasonal variations of water temperature and discharge in the mid reaches of the Yangtze River were investigated by synthesizing multi-year (2004-2018) hydrological and meteorological data (Q 3). The effects of upstream dams on the stratification of TGR were investigated by examining water temperature depth profiles near the dam. The dynamics of spring density currents are analysed by a two-dimensional, laterally averaged, hydrodynamic model (CE-QUAL-W2) and eager to link up with spring phytoplankton blooms (represented by surface chlorophyll-a concentration) (Q 3).

Appendix IV-

Lianghong Long, Zhengjian Yang, Liu Liu, Daobin Ji, Defu Liu, Andreas Lorke (2020). Recent changes of the thermal structure in Three Gorges Reservoir and its ecological impacts on tributary bays. Submitted to Science of Total Environment (4 November 2020), under review

4 Discussion

The present work advances our understanding of effects of damming and reservoir operation on hydrodynamics and thermal regimes in large cascade reservoirs of the Yangtze River. In order to answer proposed research questions, the thesis presents the achievements and discussions in three parts. Three main achievements shown in figure 3 include: (I) these three deep reservoirs presented a gradual weakening stratification, and the seasonal river flow have been significantly modified with higher discharge in spring and a reduction in summer. In addition, downstream river water temperature in the upstream two reservoirs experienced the significant warming in winter and cooling in spring and impose a noticeable hysteresis effect on water temperature rising and falling processes; (II) the study reveals and underlines the importance of reservoir operation on hydrodynamic at different time scale. The seasonal operations are closely related to the seasonal dynamics of density currents in tributary bay (XXR) of TGR, while diurnal discharge operation caused high-frequency WFLs and velocity variations by the tributary oscillation (barotropic wave with a period of 2 h); (III) after three cascade reservoirs operation, the spring stratification in TGR weakened and reservoir got warm, further resulting in the changes of density current and algal blooms in tributary bay (XXR) of TGR.

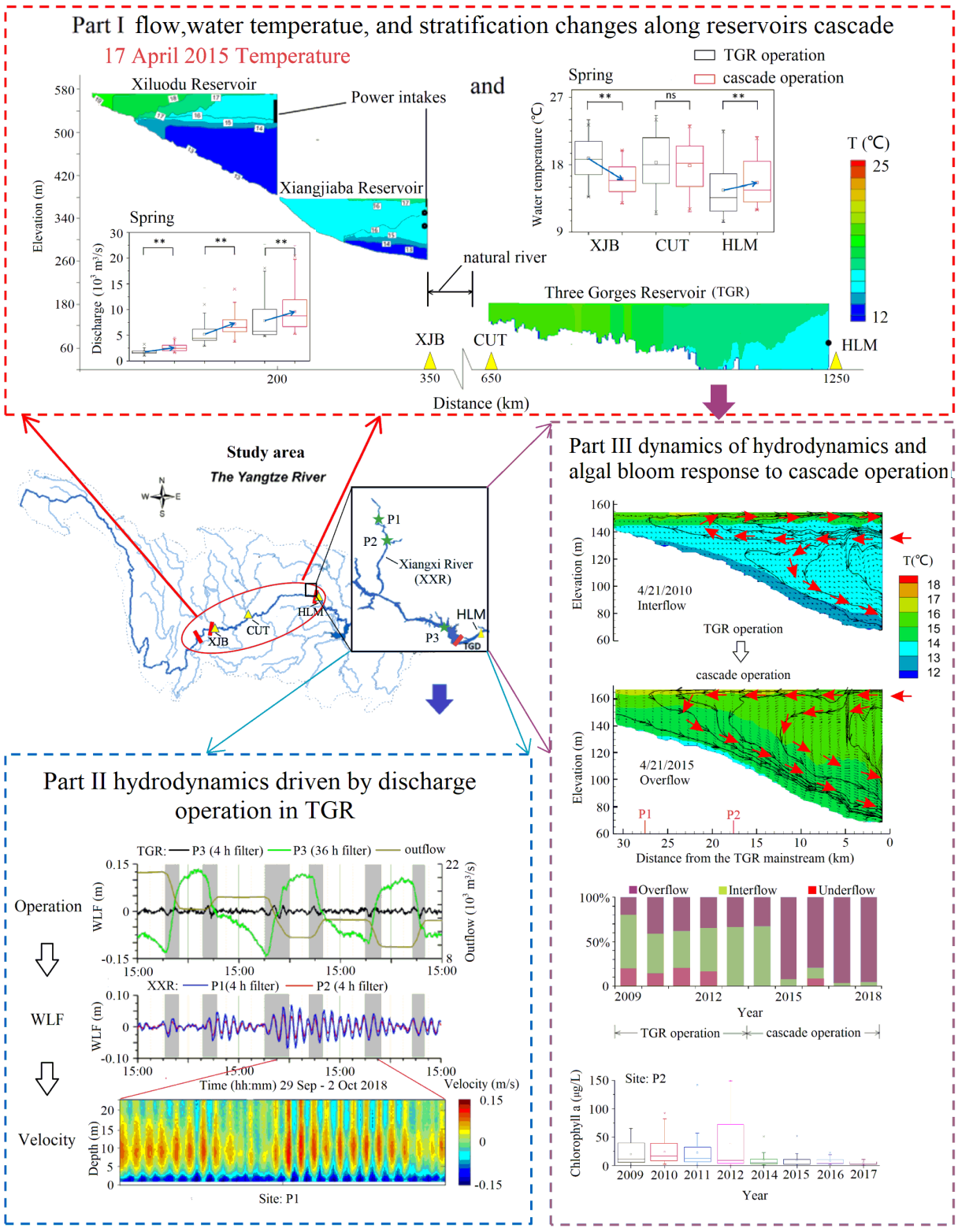

Figure 3. Summary of the main achievements in studying the effect of damming and reservoir operation on hydrodynamics and thermal regimes in large cascade reservoirs of the Yangtze River, China.

4.1 Effects of reservoir on river flow and thermal regime

The seasonal river flow in mid reach of Yangtze River have been substantially modified due to the formation of cascade reservoirs with increased discharge in spring and reduced discharge in summer. In addition, downstream river water temperature in the three reservoirs experienced significant warming in winter and cooling in spring (Appendix I). This is consistent with previous studies (Lu et al., 2013; Tao et al., 2020) in addition to the superimposed hysteresis effect on seasonal water temperature cycle (Appendix I). These results supported our hypothesis that river flow and thermal regimes were altered significantly by the three cascade reservoirs (H 1.1-1.2).

The seasonal outflow variability at the downstream of XJB was significantly affected by the larger upstream Xiluodu Reservoir (XLD, Fig. 2). In contrast, the smaller reservoir XJB did not significantly alter the seasonal flow regimes due to the milder water-level management strategy (Appendix I). This suggests that the reservoir operation of XJB did not contribute to cumulative effect in terms of downstream discharge variations. At the most downstream TGR, an increase of annual minimum flows and reduction of the annual maximum flows downstream were reported (Gao et al., 2013; Tian et al., 2019). This study further explored new changes in flow regimes after the formation of the two new reservoirs (XLD and XJB), e.g.,, a recent significant increase in spring averaged inflow of TGR at CUT, or a drop in summer discharge by ~2000 $m^3 s^{-1}$ (Appendix IV). That results indicated the flow alterations from upstream reservoirs can directly affect the inflow conditions of downstream reservoir.

Besides, this study also found the three deep reservoirs with a maximum depth of > 100 m presented a gradual weakening of thermal stratifications (Fig. 3, H 1.3). In accordance with previous numerical simulations of the thermal structure in XLD (Xie et al., 2017), the formation of vertical temperature stratification in XLD is mainly due to density currents, i.e., an underflow during winter but a near-surface flow during spring-summer (Appendix I). In XJB, in contrast, a steep thermocline could not be observed with a brief and weakened stratification due to the shorter residence time and strong vertical mixing. Observations in TGR showed the vertical temperature differences were less pronounced only with a short-term stratification in April-May. In despite of the differences of stratification, the

homogenization effects from three reservoirs are similar. For example, monthly mean water temperature at XJB station was found to be smaller (- 2.8 ℃) in April, and warmer (+ 3.2 ℃) in December, while these effects of these two reservoirs (XLD and XJB) are slight smaller than the impacts of single operation of TGR, e.g., a decrease of 4.3 ℃ in April and an increase of 3.7 ℃ in December (Deng et al., 2016). The difference of alterations may be due to the twice storage capacity in TGR. After the formation of the two upstream reservoirs, mean outflow water temperature in TGR increased by 1.1 ℃ in spring and further by 0.8 ℃ in winter (Appendix IV). These changes indicated the cumulative effect of cascade reservoirs is not simply linear addition.

In addition, the study showed in summer the outflows from the three cascade reservoirs were slightly different (mostly < 1 ℃) to the natural river temperature before the formation of the reservoirs (Appendix I, (Long et al., 2016)). This negligible summer cooling effect is in contrast to many other stratified reservoirs, e.g., a decrease by 3 ℃ in Hills Creek Dam (Angilletta Jr et al., 2008), and even by 5-6 ℃ in the regulated Lyon River (Jackson and Gibbins, 2007), caused by discharging (cold) hypolimnetic water. Contrasting patterns, i.e., an increase of summer discharge temperature, have been observed in small reservoirs where the release depth was located in the epilimnion (Lessard and Hayes, 2003). But in these studied reservoirs, the temperature of the discharged water in summer was not modified significantly by reservoirs because water was released from the well-mixed epilimnion (Appendix I, Fig. 3). Another noticeable change in temperature is the delay in the seasonal cycle. The nearly a month offset-time of water temperature was in close agreement with the hydraulic residence time in weak stratified XJB and mixed TGR. On the contrary, the delay of the annual cycle (~22 days) in the partially stratified XLD was only approximately half of its residence time due to limited mixing of the inflowing water with the hypolimnion in the reservoir (Appendix I). That suggests the residence time and stratification are the important factors in the delay of annual cycle and hysteresis effect.

4.2 Importance of reservoir operation on hydrodynamic

Appendix II and III suggest the importance of seasonal and diurnal reservoir operation in hydrodynamics in TGR. The seasonal operations with the large WLFs are closely related to

the seasonal dynamics of density currents in tributary bays of TGR, and more frequent transformations of density-driven water circulation could facilitate mixing in tributary bays (H 2.1, Appendix II), while diurnal operation caused high-frequency WLFs and flow velocity variations by the tributary oscillations (H 2.2). But it is different to the above-mentioned hypothesis 2.2, this tributary oscillation with a period of 2 h is a barotropic wave, and represents a so far overlooked hydrodynamic feature of tributaries bays in large reservoirs (Appendix III).

Previous studies (Ji et al., 2010; Yang et al., 2010) have revealed the ubiquitous density currents in TGR mainly caused by the temperature differences between mainstream and tributaries, and the density currents presented a frequent transformation among overflow, interflow and underflow (Appendix II, Ma et al., 2015). Field measurements showed a change in the intrusion depth from TGR from mid depth to the water surface in response to a rapid water level rise (Liu et al., 2012). Ji et al. (2017) also found larger daily WLFs and a longer duration of water level rise would create an advantageous density-driven water circulation to prevent algal blooms. These studies indicate that the water level management is likely to play an important role on the hydrodynamics in tributary bays by changing density currents. Besides, compared to single operation of TGR, the findings in Appendix IV also showed the spring warming which caused by the variation in discharge, induced lift-up of the intrusion from interflow to overflow one month earlier operation and caused a three-fold increase of the frequency of occurrence of overflows. This change in density current further led to alterations of the mixing regime in the tributary bay, i.e., deepening of the surface mixed layer (Appendix II). The deeper mixed layer results in a reduction of the ratio of thickness of euphotic zone to mixing depth and therewith to unfavourable conditions for phytoplankton bloom in the XXR and potentially also in other tributary bays (Appendix III).

In addition to seasonal density current changes, the recent high-frequency observations of WLFs and flow velocity in a large tributary bay of TGR revealed standing waves with 2 h period which was generated by diurnal discharge regulation in TGR, represents a so far overlooked hydrodynamics in TGR (Appendix IV). As an important finding, the bay oscillations had a strong effect on the temporal dynamics and vertical distribution of flow velocity in the tributary. The periodic wave caused a frequent reversal of the density current

transporting water from TGR into the bay and resulted in a pulsating inflow of the river along the bed. This can cause more vertical mixing driven by shear production of turbulent kinetic energy at the velocity gradient at the edge of the density-driven intrusion (Ellison and Turner, 2006). So the wave can be expected to provide an important control on the exchange of momentum, heat and solutes between both water masses (Sha et al., 2015), and then have a far-reaching impact on water quality (Shilei et al., 2020). Thus, accurately and timely understanding of the impacts of reservoir operation on hydrodynamics is important for assessing the impacts of hydropower development on the riverine ecosystem. To better conserve riverine ecology, this study suggests that an adaptive discharge management, whether in seasonal scale or daily scale, may provide an efficient mean to improve water quality and combat harmful algae blooms.

4.3 Importance of cumulative impacts and its ecological implication in cascade dam operation

As stated above, this study not only confirms the differences of stratifications along the reservoir cascade (H 1), but also reveals the impact mechanism of upstream dams on the development of thermal stratification in the downstream reservoir (H 3.1). In addition, this thesis also examined that the recent dynamics of density current and algal blooms in the tributary (XXR) of TGR are related to recent changes of thermal structure (H 3.2, Appendix IV).

By comparing observations of cumulative impact induced by the cascade hydropower reservoirs in the other dammed rivers (Ouyang et al., 2011; Peng et al., 2014; Sabo et al., 2017; Song et al., 2018), this study further reveals the interaction between cascade reservoirs and highlight the importance of cumulative impacts. Cumulative effects are not simply added by individual impacts because reservoirs may be inter-dependent in cascade dammed river (Appendix I). Compared to a single reservoir, inflow water often forms a density current along the sloping bottom due to lower temperature of the discharged water from the upstream reservoir (Chen et al., 2016a), and the increase or decrease in inflow discharge both can affect the stratification in the downstream reservoir. In these cases, the results showed that upstream reservoirs can weaken the development of thermal stratification in downstream reservoirs (Appendix I, Appendix IV). For example, in TGR, spring stratification becomes weak due to

the increase of inflow after upstream dam operation.

In addition, the change in thermal stratification had far-reaching ecological impacts in the tributary of TGR (H 3.2), which was exemplified by the modified patterns of density currents and the reduced risk of algal blooms in tributary bays of TGR (Appendix IV). Previous studies demonstrated that density currents have significant impacts on the hydrodynamics, thermal structure, and phytoplankton blooms in the tributaries of TGR (Ji et al., 2017; Liu et al., 2012; Yang et al., 2010). As stated above, compared to standalone operation of TGR, the spring warming during cascade operation period caused a new hydrodynamics regime in the tributary bay, e.g., the earlier occurrence of overflow in spring and a three-fold increase in the occurrence frequency (Appendix IV). Since 2012, flow regulation with large WLFs had been proposed in TGR for the purpose of phytoplankton control (Liu et al., 2012), and then the scheduling scheme with WLF patterns of different "tide-types" was formulated (Yang et al., 2013), because this flow regulation can affect the density-driven water circulation in tributary. However, large manmade WLFs are difficult to implement constrained by the strict rules for flood control. The study suggests the operation of upstream reservoirs is a potential and effective way to improve water quality by affecting the hydrodynamic in downstream reservoir, and the ecological operation of the multi-reservoirs have application prospect in future.

In future, with the joint operation of two new reservoirs (WDD and BHT) upstream of XLD, new hydrological and thermal regimes can form (Wang et al., 2020; Wang et al., 2018). By recognizing the comparable large storage capacities of the reservoirs (Liu, 2007), the two new reservoirs can potentially develop thermal stratification and intensify the changes in the flow and temperature regime in the coming years as predicted by He et al., (2020). This thesis identified the importance of incorporating also longer-term variability and trends into assessments and process-based analysis of the hydrological, thermal, biogeochemical and ecological impacts of cascade reservoirs. Future research should overcome site-specific assessments in cascade reservoirs, which are typically associated with upstream reservoir operation. The interactions of individual reservoir with up- and downstream located reservoirs should be taken into consideration systematically.

5 Conclusion

This thesis advances our understanding of the effects of reservoir cascade on river flow and thermal regimes and highlights the importance of reservoir operation. The joint operations of cascade reservoirs substantially altered the hydrology of TGR: higher discharge in spring and lower discharge in summer were observed, while XJB, the reservoir directly upstream of TGR had no obvious contribution to the discharge variations in TGR. The outflow water temperature of the three reservoirs experienced significant winter warming and spring cooling (except for TGR), in addition to a noticeable hysteresis effect on the seasonal water temperature cycle.

This study also underlines the importance of reservoir operation in reservoir hydrodynamics. The seasonal dynamics of density currents in tributary bays of TGR are closely related to seasonal hydrological cycle of TGR. Meanwhile, high-frequency WLFs and flow velocity variations in tributary bays were attributable to bay oscillations (barotropic wave with a period of 2 h) that were excited by diurnal discharge regulations of TGR.

Furthermore, as a consequence of joint operations of cascade reservoirs, the changes in inflow weakened thermal stratification and caused warming in TGR. It further had far-reaching effects on hydrodynamics and algal blooms in tributary bays, e.g., earlier and extended time period of occurrence of overflow and a sharp reduction in phytoplankton blooms. In future studies, cumulative effects of cascade reservoirs should be systematically investigated.

Reference

Agostinho, A., Pelicice, F., Gomes, L., 2008. Dams and the fish fauna of the Neotropical region: Impacts and management related to diversity and fisheries. Brazilian journal of biology = Revista brasleira de biologia, 68: 1119-32. DOI:10.1590/S1519-69842008000500019

Andradóttir, H.Ó., Rueda, F.J., Armengol, J., Marcé, R., 2012. Characterization of residence time variability in a managed monomictic reservoir. Water Resources Research, 48: W11505. DOI:10.1029/2012wr012069

Angilletta Jr, M.J. et al., 2008. Big dams and salmon evolution: changes in thermal regimes and their potential evolutionary consequences. Evolutionary Applications, 1(2): 286-299. DOI:10.1111/j.1752-4571.2008.00032.x

Arthington, A., Bunn, S., Poff, N., Naiman, R., 2006. The Challenge of Providing Environmental Flow Rules to Sustain River Ecosytem. Ecological applications : a publication of the Ecological Society of America, 16: 1311-8. DOI:10.1890/1051-0761(2006)016[1311:TCOPEF]2.0.CO;2

Berga, L. et al., 2006. Dams and Reservoirs, Societies and Environment in the 21st Century. Two Volume Set. London: CRC Press, . DOI:10.1201/b16818

Bocaniov, S.A., Ullmann, C., Rinke, K., Lamb, K.G., Boehrer, B., 2014. Internal waves and mixing in a stratified reservoir: Insights from three-dimensional modeling. Limnologica, 49: 52-67. DOI:10.1016/j.limno.2014.08.004

Boehrer, B., 2000. Modal response of a deep stratified lake: western Lake Constance. Journal of Geophysical Research: Oceans, 105(C12): 28837-28845. DOI:10.1029/2000JC900125

Cai, H. et al., 2018. Quantifying the impact of the Three Gorges Dam on the thermal dynamics of the Yangtze River. Environmental Research Letters, 13(5): 054016. DOI:10.1088/1748-9326/aab9e0

Caissie, D., 2006. The Thermal Regime of Rivers: A Review. Freshwater Biology, 51: 1389-1406. DOI:10.1111/j.1365-2427.2006.01597.x

Çalışkan, A., Elçi, Ş., 2009. Effects of Selective Withdrawal on Hydrodynamics of a Stratified Reservoir. Water Resources Management, 23(7): 1257-1273. DOI:10.1007/s11269-008-9325-x

Carr, M.K., Sadeghian, A., Lindenschmidt, K.E., Rinke, K., Morales-Marin, L., 2020. Impacts of Varying Dam Outflow Elevations on Water Temperature, Dissolved Oxygen, and Nutrient Distributions in a Large Prairie Reservoir. Environmental engineering science, 37(1): 78-97. DOI:10.1089/ees.2019.0146

Casamitjana, X., Serra, T., Colomer, J., Baserba, C., Perez Losada, J., 2003. Effects of water withdrawal in the stratification patterns of a reservoir. Hydrobiologia, 504: 21-28. DOI:10.1023/B:HYDR.0000008504.61773.77

Chen, G., Fang, X., Devkota, J., 2016a. Understanding flow dynamics and density currents in a river-reservoir system under upstream reservoir releases. Hydrological Sciences Journal, 61(13): 2411-2426. DOI:10.1080/02626667.2015.1112902

Chen, J. et al., 2016b. Changes in monthly flows in the Yangtze River, China – With special reference to the Three Gorges Dam. Journal of Hydrology, 536: 293-301. DOI:https://doi.org/10.1016/j.jhydrol.2016.03.008

Cooper, L.M., Sheate, W.R., 2002. Cumulative effects assessment: A review of UK environmental impact statements. Environmental Impact Assessment Review, 22(4): 415-439. DOI:10.1016/S0195-9255(02)00010-0

Cui, T., Tian, F., Yang, T., Wen, J., Khan, M.Y.A., 2020. Development of a comprehensive framework for assessing the impacts of climate change and dam construction on flow regimes. Journal of Hydrology, 590: 125358. DOI:10.1016/j.jhydrol.2020.125358

Culp, J.M., Cash, K.J., Wrona, F.J., 2000. Cumulative effects assessment for the Northern River Basins Study. Journal of Aquatic Ecosystem Stress and Recovery, 8(1): 87-94. DOI:10.1023/A:1011404209392

Dai, L., Dai, H., Jiang, D., 2012. Temporal and spatial variation of thermal structure in Three Gorges Reservoir: A simulation approach. Journal of Food Agriculture & Environment, 10(2): 1174-1178.

Deng, Y., Xiao, Y., Tuo, Y., He, T., 2016. Influence of Three Gorges Reservoir on water temperature between Yichang and Jianli. 27: 551-560. DOI:10.14042/j.cnki.32.1309.2016.04.009

Dos Santos, N.C.L. et al., 2018. Cumulative ecological effects of a Neotropical reservoir cascade across multiple assemblages. Hydrobiologia, 819(1): 77-91. DOI:10.1007/s10750-018-3630-z

Duan, W., Guo, S., Wang, J., Liu, D., 2016. Impact of Cascaded Reservoirs Group on Flow Regime in the Middle and Lower Reaches of the Yangtze River. Water, 8(6): 218. DOI:10.3390/w8060218

Elçi, Ş., 2008. Effects of thermal stratification and mixing on reservoir water quality. Limnology, 9(2): 135-142. DOI: 10.1007/s10201-008-0240-x

Ellison, T.H., Turner, J.S., 2006. Turbulent entrainment in stratified flows. Journal of Fluid Mechanics, 6(3): 423-448. DOI:10.1017/S0022112059000738

Fu, B. et al., 2010. Three Gorges Project: Efforts and challenges for the environment. Progress in Physical Geography: Earth and Environment, 34(6): 741-754. DOI:10.1177/0309133310370286

Gao, B., Yang, D., Yang, H., 2013. Impact of the Three Gorges Dam on flow regime in the middle and lower Yangtze River. Quaternary International, 304: 43-50. DOI:10.1016/j.quaint.2012.11.023

Geraldes, A.M., Boavida, M.-J., 2005. Seasonal water level fluctuations: Implications for reservoir limnology and management. Lakes & Reservoirs: Science, Policy and Management for Sustainable Use, 10(1): 59-69. DOI:10.1111/j.1440-1770.2005.00257.x

Gierszewski, P.J., Habel, M., Szmańda, J., Luc, M., 2020. Evaluating effects of dam operation on flow regimes and riverbed adaptation to those changes. Science of The Total Environment, 710: 136202. DOI:10.1016/j.scitotenv.2019.136202

Grill, G. et al., 2015. An index-based framework for assessing patterns and trends in river fragmentation and flow regulation by global dams at multiple scales. Environmental Research Letters, 10(1): 015001. DOI:10.1088/1748-9326/10/1/015001

He, T., Deng, Y., Tuo, Y., Yang, Y., Liang, N., 2020. Impact of the Dam Construction on the Downstream Thermal Conditions of the Yangtze River. Int J Environ Res Public Health, 17(8): 2973. DOI:10.3390/ijerph17082973

Hecht, J.S., Lacombe, G., Arias, M.E., Dang, T.D., Piman, T., 2019. Hydropower dams of the Mekong River basin: A review of their hydrological impacts. Journal of Hydrology, 568: 285-300. DOI:10.1016/j.jhydrol.2018.10.045

Hocking, G., Straškraba, M., 1994. An analysis of the effect of an upstream reservoir by means of a mathematical model of reservoir hydrodynamics. Water Science and Technology, 30: 91-98. DOI:10.2166/wst.1994.0032

Hodges, B.R., Imberger, J., Saggio, A., Winters, K.B., 2000. Modeling basin-scale internal waves in a stratified lake. Limnology and oceanography, 45(7): 1603-1620. DOI:10.4319/lo.2000.45.7.1603

Holbach, A. et al., 2014. Three Gorges Reservoir: Density Pump Amplification of Pollutant Transport into Tributaries. Environmental Science & Technology, 48(14): 7798-7806. DOI:10.1021/es501132k

Hou, B., Wu, Y., Li, J., 2011. Environmental cumulative effects assessment of cascade hydropower development in the main stream of the upper typical reaches in Minjiang River, 2011 International Conference on Remote Sensing, Environment and Transportation Engineering, pp. 304-309. DOI:10.1109/RSETE.2011.5964274

Jackson, H., Gibbins, C., 2007. Role of discharge and temperature variation in determing invertebrate community structure in a regulated river. River Research and Applications, 23: 651-669. DOI:10.1002/rra.1006

Ji, D., Liu, D., Yang, Z., Xiao, S., 2010. Hydrodynamic characteristics of Xiangxi Bay in Three Gorges Reservoir. Sci China-Phys Mech Astron, 40(1): 101-112 (in Chinese).

Ji, D. et al., 2017. Impacts of water level rise on algal bloom prevention in the tributary of Three Gorges Reservoir, China. Ecological Engineering, 98: 70-81. DOI:10.1016/j.ecoleng.2016.10.019

Jiang, L., Ban, X., Wang, X., Cai, X., 2014. Assessment of Hydrologic Alterations Caused by the Three Gorges Dam in the Middle and Lower Reaches of Yangtze River, China. Water, 6(5): 1419-1434. DOI:10.3390/w6051419

Jiao, D., Wang, D., Lv, H., 2020. Effects of human activities on hydrological drought patterns in the Yangtze River Basin, China. Natural Hazards, 104(1): 1111-1124. DOI:10.1007/s11069-020-04206-2

Jin, J. et al., 2019. Effects of water level fluctuation on thermal stratification in a typical tributary bay of Three Gorges Reservoir, China. PeerJ, 7: e6925. DOI:10.7717/peerj.6925

Johnson, B.M. et al., 2004. Effects of Climate and Dam Operations on Reservoir Thermal Structure. Journal of Water Resources Planning and Management, 130(2): 112-122. DOI:doi:10.1061/(ASCE)0733-9496(2004)130:2(112)

Kędra, M., Wiejaczka, Ł., 2016. Disturbance of water-air temperature synchronisation by dam reservoirs. Water and Environment Journal, 30(1-2): 31-39. DOI:10.1111/wej.12156

Lauri, H. et al., 2012. Future changes in Mekong River hydrology: impact of climate change and reservoir operation on discharge. Hydrol. Earth Syst. Sci., 16(12): 4603-4619. DOI:10.5194/hess-16-4603-2012

Lehner, B. et al., 2011. High-resolution mapping of the world's reservoirs and dams for sustainable river-flow management. Frontiers in Ecology and the Environment, 9(9): 494-502. DOI:10.1890/100125

Lessard, J.L., Hayes, D.B., 2003. Effects of elevated water temperature on fish and macroinvertebrate communities below small dams. River Research and Applications, 19(7): 721-732. DOI:10.1002/rra.713

Li, M. et al., 2020a. Evaluation of Reservoir-Induced Hydrological Alterations and Ecological Flow Based on Multi-Indicators. Water, 12(7): 2069. DOI:10.3390/w12072069

Li, Z. et al., 2020b. The net GHG emissions of the China Three Gorges Reservoir: I. Pre-impoundment GHG inventories and carbon balance. Journal of Cleaner Production, 256: 120635. DOI:https://doi.org/10.1016/j.jclepro.2020.120635

Litvinov, A.S., Roshchupko, V.F., 2007. Long-term and seasonal water level fluctuations of the Rybinsk Reservoir and their role in the functioning of its ecosystem. Water Resources, 34(1): 27-34. DOI:10.1134/s0097807807010034

Liu, B., Yang, D., Ye, B., Berezovskaya, S., 2005. Long-term open-water season stream temperature variations and changes over Lena River Basin in Siberia. Global and Planetary Change, 48(1-3): 96-111. DOI:10.1016/j.gloplacha.2004.12.007

Liu, F., 2007. Introduction of the planed hydroelectric engineering on the lower Jinshajiang Construction of Water Resources & Hydroelectric Engineering, 3: 153-155 (in Chinese).

Liu, L., Liu, D., Johnson, D.M., Yi, Z., Huang, Y., 2012. Effects of vertical mixing on phytoplankton blooms in Xiangxi Bay of Three Gorges Reservoir: Implications for management. Water Research, 46(7): 2121-2130. DOI:10.1016/j.watres.2012.01.029

Long, L.-H. et al., 2016. Characteristic of the water temperature lag in Three Gorges Reservoir and its effect on the water temperature structure of tributaries. Environmental Earth Sciences, 75: 1459. DOI:10.1007/s12665-016-6266-1

Long, L., Ji, D., Liu, D., Yang, Z., Lorke, A., 2019. Effect of Cascading Reservoirs on the Flow Variation and Thermal Regime in the Lower Reaches of the Jinsha River. Water, 11(5): 1008. DOI:10.3390/w11051008

Lu, S.S., Dai, L.Q., Dai, H.C., Mao, J.Q., 2013. Effect of Release Temperature from Three Gorges Reservoir on the Procreation of Chinese Sturgeons. Applied Mechanics & Materials, 361-363: 958-961. DOI:10.4028/www.scientific.net/AMM.361-363.958

Ma, J. et al., 2015. Modeling density currents in a typical tributary of the Three Gorges Reservoir, China. Ecological Modelling, 296: 113-125. DOI:10.1016/j.ecolmodel.2014.10.030

Ma, Q., Li, R., Feng, J., Lu, J., Zhou, Q., 2018. Cumulative effects of cascade hydropower stations on total dissolved gas supersaturation. Environmental science and pollution research international, 25(14): 13536-13547. DOI:10.1007/s11356-018-1496-2

Ma, S., Kassinos, S.C., Fatta Kassinos, D., Akylas, E., 2008. Effects of selective water withdrawal schemes on thermal stratification in Kouris Dam in Cyprus. Lakes & Reservoirs: Science, Policy and Management for Sustainable Use, 13(1): 51-61. DOI:10.1111/j.1440-1770.2007.00353.x

Magilligan, F.J., Nislow, K.H., 2005. Changes in hydrologic regime by dams. Geomorphology, 71(1): 61-78. DOI:10.1016/j.geomorph.2004.08.017

Maingi, J., Marsh, S., 2002. Quantifying Hydrologic Impacts Following Dam Construction Along the Tana River, Kenya. Journal of Arid Environments, 50(1): 53-79. DOI:10.1006/jare.2000.0860

Meghan K. Carr, Amir Sadeghian, Karl-Erich Lindenschmidt, Karsten Rinke, Morales-Marin, L., 2020. Impacts of Varying Dam Outflow Elevations on Water Temperature, Dissolved Oxygen, and Nutrient Distributions in a Large Prairie Reservoir. Environmental engineering science, 37(1): 78-97. DOI:10.1089/ees.2019.0146

Mittal, N., Mishra, A., Singh, R., Bhave, A.G., van der Valk, M., 2014. Flow regime alteration due to anthropogenic and climatic changes in the Kangsabati River, India. Ecohydrology & Hydrobiology, 14(3): 182-191. DOI:10.1016/j.ecohyd.2014.06.002

Moreno-Ostos, E., Marcé, R., Ordóñez, J., Dolz, J., Armengol, J., 2008. Hydraulic Management Drives Heat Budgets and Temperature Trends in a Mediterranean Reservoir. International Review of Hydrobiology, 93(2): 131-147. DOI:10.1002/iroh.200710965

Mp, C., Webb, R., Schmidt, J., 1996. Dams and Rivers: A Primer on the Downstream Effects of Dams. U.S. Geological Survey Circular, 1126. DOI:10.3133/cir1126

Nilsson, C., Reidy, C.A., Dynesius, M., Revenga, C., 2005. Fragmentation and Flow Regulation of the World's Large River Systems. Science, 308(5720): 405-408. DOI:10.1126/science.1107887

Olden, J.D., Naiman, R.J., 2010. Incorporating thermal regimes into environmental flows assessments: modifying dam operations to restore freshwater ecosystem integrity. Freshwater Biology, 55(1): 86-107. DOI:10.1111/j.1365-2427.2009.02179.x

Ouyang, W., Hao, F., Song, K., Zhang, X., 2011. Cascade Dam-Induced Hydrological Disturbance and Environmental Impact in the Upper Stream of the Yellow River. Water Resources Management, 25(3): 913-927. DOI:10.1007/s11269-010-9733-6

Peng, Y., Ji, C., Gu, R., 2014. A Multi-Objective Optimization Model for Coordinated Regulation of Flow and Sediment in Cascade Reservoirs. Water Resources Management, 28(12): 4019-4033. DOI:10.1007/s11269-014-0724-x

Poff, N.L., Matthews, J.H., 2013. Environmental flows in the Anthropocence: past progress and future prospects. Current Opinion in Environmental Sustainability, 5(6): 667-675. DOI:10.1016/j.cosust.2013.11.006

Poff, N.L., Olden, J.D., Merritt, D.M., Pepin, D.M., 2007. Homogenization of regional river dynamics by dams and global biodiversity implications. Proceedings of the National Academy of Sciences, 104(14): 5732-5737.

DOI:10.1073/pnas.0609812104

Poole, G.C., Berman, C.H., 2001. An ecological perspective on in-stream temperature: natural heat dynamics and mechanisms of human-caused thermal degradation. Environmental management, 27(6): 787-802. DOI:10.1007/s002670010188

Preece, R.M., Jones, H.A., 2002. The effect of Keepit Dam on the temperature regime of the Namoi River, Australia. River Research and Applications, 18(4): 397-414. DOI:10.1002/rra.686

Ren, J. et al., 2020. Impact of the construction of cascade reservoirs on suspended sediment peak transport variation during flood events in the Three Gorges Reservoir. CATENA, 188: 104409. DOI:10.1016/j.catena.2019.104409

Rueda, F., Moreno-Ostos, E., Armengol, J., 2006. The residence time of river water in reservoirs. Ecological Modelling, 191(2): 260-274. DOI:10.1016/j.ecolmodel.2005.04.030

Sabo, J. et al., 2017. Designing river flows to improve food security futures in the Lower Mekong Basin. Science, 358: eaao1053. DOI:10.1126/science.aao1053

Schmutz, S., Sendzimir, J., 2018. Riverine Ecosystem Management. Springer, Cham, Switzerland. DOI:10.1007/978-3-319-73250-3

Sha, Y., Wei, Y., Li, W., Fan, J., Cheng, G., 2015. Artificial tide generation and its effects on the water environment in the backwater of Three Gorges Reservoir. Journal of Hydrology, 528: 230-237. DOI:10.1016/j.jhydrol.2015.06.020

Shilei, Z. et al., 2020. Reservoir water stratification and mixing affects microbial community structure and functional community composition in a stratified drinking reservoir. Journal of Environmental Management, 267: 110456. DOI:10.1016/j.jenvman.2020.110456

Sinokrot, B., Gulliver, J., 2000. In-Stream Flow Impact on River Water Temperatures. Journal of Hydraulic Research, 38(5): 339-349. DOI:10.1080/00221680009498315

Song, X., Zhuang, Y., Wang, X., Li, E., 2018. Combined Effect of Danjiangkou Reservoir and Cascade Reservoirs on Hydrologic Regime Downstream. Journal of Hydrologic Engineering, 23(6): 05018008. DOI:doi:10.1061/(ASCE)HE.1943-5584.0001660

Stevens, C.L., 1999. Internal waves in a small reservoir. Journal of Geophysical Research: Oceans, 104(C7): 15777-15788. DOI:10.1029/1999jc900098

Stone, R., 2008. Three Gorges Dam: Into the Unknown. Science, 321(5889): 628-632. DOI:10.1126/science.321.5889.628

Straškraba, M., Dostálková, I., Hejzlar, J., Vyhnálek, V., 1995. The Effect of Reservoirs on Phosphorus Concentration. Internationale Revue der gesamten Hydrobiologie und Hydrographie, 80(3): 403-413. DOI:10.1002/iroh.19950800304

Tao, Y. et al., 2020. Quantifying the impacts of the Three Gorges Reservoir on water temperature in the middle reach of the Yangtze River. Journal of Hydrology, 582: 124476. DOI:10.1016/j.jhydrol.2019.124476

Tian, J. et al., 2019. Influence of Three Gorges Dam on downstream low flow. Water, 11(1): 65. DOI:10.3390/w11010065

Timpe, K., Kaplan, D., 2017. The changing hydrology of a dammed Amazon. Science Advances, 3(11): e1700611. DOI:10.1126/sciadv.1700611

Van Oorschot, M., Kleinhans, M., Buijse, T., Geerling, G., Middelkoop, H., 2018. Combined effects of climate change and dam construction on riverine ecosystems. Ecological Engineering, 120: 329-344. DOI:10.1016/j.ecoleng.2018.05.037

Vidal, J., Casamitjana, X., Colomer, J., Serra, T., 2005. The internal wave field in Sau reservoir: Observation and modeling of a third vertical mode. Limnology and Oceanography, 50(4): 1326-1333. DOI:10.4319/

lo.2005.50.4.1326

Vidal, J., Rueda, F.J., Casamitjana, X., 2007. The seasonal evolution of high vertical-mode internal waves in a deep reservoir. Limnology and Oceanography, 52(6): 2656-2667. DOI:10.4319/lo.2007.52.6.2656

Vörösmarty, C. et al., 2003. Anthropogenic Sediment Retention: Major Global Impact from Registered River Impoundments. Global and Planetary Change, 39(1-2): 169-190. DOI:10.1016/S0921-8181(03)00023-7

Wang, H., Xia, K., Song, D.P., Tang, Y., 2014. Cumulative Effect of Cascade Hydropower Development on Water Quantity Process in the Upper Wu River of Western China. Advanced Materials Research, 955-959: 2973-2978. DOI:10.4028/www.scientific.net/AMR.955-959.2973

Wang, Y., Zhang, N., Wang, D., Wu, J., 2020. Impacts of cascade reservoirs on Yangtze River water temperature: Assessment and ecological implications. Journal of Hydrology, 590: 125240. DOI:10.1016/j.jhydrol. 2020.125240

Wang, Y., Zhang, N., Wang, D., Wu, J., Zhang, X., 2018. Investigating the impacts of cascade hydropower development on the natural flow regime in the Yangtze River, China. Science of The Total Environment, 624: 1187-1194. DOI:10.1016/j.scitotenv.2017.12.212

Xia, J. et al., 2018. Tempo-Spatial Analysis of Water Quality in the Three Gorges Reservoir, China, after its 175-m Experimental Impoundment. Water Resources Management, 32(9): 2937-2954. DOI:10.1007/s11269-018-1918-4

Xie, K., Liu, Z., Chen, Y., Chen, X., 2019. Investigation on internal wave due to hydro-peaking in a deep run-of-the-river reservoir. Journal of Hydroelectric Engineering, 38(1): 41-51(in chinese).

Xie, Q. et al., 2017. Understanding the Temperature Variations and Thermal Structure of a Subtropical Deep River-Run Reservoir before and after Impoundment. Water, 9(8): 603. DOI:10.3390/w9080603

Xiong, C.J. et al., 2013. The Influence of Hydrodynamic Conditions on Algal Bloom in the Three Gorges Reservoir Tributaries. Applied Mechanics and Materials, 295-298: 1981-1990. DOI:10.4028/www.scientific.net /AMM.295-298.1981

Xu, C., Zhang, D., 2018. Impact of the operation of cascade reservoirs in upper Yangtze River on hydrological variability of the mainstream. Proc. IAHS, 379: 421-432. DOI:10.5194/piahs-379-421-2018

Xu, X., Tan, Y., Yang, G., 2013. Environmental impact assessments of the Three Gorges Project in China: Issues and interventions. Earth-Science Reviews, 124: 115-125. DOI:10.1016/j.earscirev.2013.05.007

Yan, Y., Yang, Z., Liu, Q., Sun, T., 2010. Assessing effects of dam operation on flow regimes in the lower Yellow River. Procedia Environmental Sciences, 2(6): 507-516. DOI:10.1016/j.proenv.2010.10.055

Yang, T. et al., 2008. A spatial assessment of hydrologic alteration caused by dam construction in the middle and lower Yellow River, China. Hydrological Processes, 22(18): 3829-3843. DOI:10.1002/hyp.6993

Yang, Z., Liu, D., Ji, D., Xiao, S., 2010. Influence of the impounding process of the Three Gorges Reservoir up to water level 172.5 m on water eutrophication in the Xiangxi Bay. Science China Technological Sciences, 53(4): 1114-1125. DOI:10.1007/s11431-009-0387-7

Yang, Z. et al., 2013. An eco-environmental friendly operation: An effective method to mitigate the harmful blooms in the tributary bays of Three Gorges Reservoir. Science China Technological Sciences, 56(6): 1458-1470. DOI:10.1007/s11431-013-5190-9

Yang, Z. et al., 2018. Hydrodynamic mechanisms underlying periodic algal blooms in the tributary bay of a subtropical reservoir. Ecological Engineering, 120: 6-13. DOI:10.1016/j.ecoleng.2018.05.003

Yang, Z., Yan, Y., Liu, Q., 2012. Assessment of the flow regime alterations in the Lower Yellow River, China. Ecological Informatics, 10: 56-64. DOI:10.1016/j.ecoinf.2011.10.002

Yao, Y., Zhang, B., Ma, X., Ma, P., 2006. Large-scale Hydroelectric Projects and Mountain Development on the Upper Yangtze River. Mountain Research and Development, 26(2): 109-114. DOI:10.1659/0276-4741

(2006)26[109:LHPAMD]2.0.CO;2

Yi, Y. et al., 2019. The effects of cascade dam construction and operation on riparian vegetation. Advances in Water Resources, 131: 103206. DOI:10.1016/j.advwatres.2018.09.015

Yu, M., Yang, D., Liu, X., Li, Q., Wang, G., 2019. Potential Impact of a Large-Scale Cascade Reservoir on the Spawning Conditions of Critical Species in the Yangtze River, China. Water, 11(10): 2027. DOI:10.3390/w11102027

Zarfl, C., Lumsdon, A.E., Berlekamp, J., Tydecks, L., Tockner, K., 2014. A global boom in hydropower dam construction. Aquatic Sciences, 77(1): 161-170. DOI:10.1007/s00027-014-0377-0

Zhao, P., Tang, X., Tang, J., Wang, C., 2013. Assessing water quality of Three Gorges Reservoir, China, over a five-year period from 2006 to 2011. Water Resources Management, 27(13): 4545-4558. DOI:10.1007/s11269-013-0425-x

Zheng, T., Mao, J., Dai, H., Liu, D., 2011. Impacts of water release operations on algal blooms in a tributary bay of Three Gorges Reservoir. Science China Technological Sciences, 54(6): 1588-1598. DOI:10.1007/s11431-011-4371-7

Zouabi-Aloui, B., Adelana, S.M., Gueddari, M., 2015. Effects of selective withdrawal on hydrodynamics and water quality of a thermally stratified reservoir in the southern side of the Mediterranean Sea: a simulation approach. Environmental Monitoring and Assessment, 187(5): 292. DOI:10.1007/s10661-015-4509-3

Author contributions

This thesis is based on four original research articles provided in Appendix I-IV which were conceived by all of the authors. I am the lead author of all articles and the contributions of all authors are explained in the following:

Appendix I -

Lianghong Long, Daobin Ji, Defu Liu, Zhengjian Yang, Andreas Lorke (2019). Effect of Cascading Reservoirs on the Flow Variation and Thermal Regime in the Lower Reaches of the Jinsha River. Water, 11(5): 1008. doi.org/10.3390/w11051008

Conceptualization: L. Long and D. Liu

Investigation: L. Long, D. Ji, and Z. Yang

Methodology: L. Long and D. Ji

Formal analysis: L. Long and A. Lorke

Writing the manuscript: L. Long

Revising the manuscript: L. Long and A. Lorke

Appendix II -

Lianghong Long, Daobin Ji, Zhengjian Yang, Scott A. Wells, Jun Ma, Defu Liu (2019). Density driven water circulation in typical tributary of the Three Gorges Reservoir, China. River Research and Applications, 35: 833–843. doi.org/10.1002/rra.3459

Conception and design: D. Ji and D. Fu

Data acquisition: D. Ji and Z. Yang

Model design: L. Long, S. A. Wells, and J. Ma

Interpretation of results: L. Long and D. Ji

Writing the manuscript: L. Long

Revising the manuscript: S. A. Wells

Appendix III –

Lianghong Long, Daobin Ji, Zhengjian Yang, Defu Liu, Heqing Cheng., Zhongyong Yang, Andreas Lorke (2020). Tributary oscillations generated by diurnal discharge regulation in Three Gorges Reservoir. Environmental Research Letters 15(8): 084011. doi.org/10.1088/1748-9326/ab 8d80

Conception and design: L. Long and A. Lorke

Funding: D. Ji and A. Lorke

Data acquisition: L. Long, Z. Yang, and H. Cheng

Data analysis: L. Long and A. Lorke

Interpretation of results: L. Yang and A. Lorke

Writing the manuscript: L. Long

Revising the manuscript: L. Long, L. Liu, and A. Lorke

Appendix IV -

Lianghong Long, Zhengjian Yang, Liu Liu, Daobin Ji, Defu Liu, Andreas Lorke (2020). Recent changes of the thermal structure in Three Gorges Reservoir and its ecological impacts on tributary bays. Submitted to Science of Total Environment (4 November 2020), under review

Conception and design: L. Long and A. Lorke

Data acquisition: L. Long, Z. Yang, and D. Ji

Data analysis: L. Long and A. Lorke

Interpretation of results: L. Yang and A. Lorke

Writing the manuscript: L. Long

Revising the manuscript: Z. Yang, L. Liu, and A. Lorke

Declaration

I hereby declare that the thesis entitled "*Effect of damming and reservoir operation on hydrodynamics and thermal regimes in large cascade reservoirs of the Yangtze River, China*" is the result of my own work except where otherwise indicated. It has not been submitted for any other degree at another university or scientific institution.

Landau, 10 November 2020 ……

Lianghong Long

Curriculum Vitae

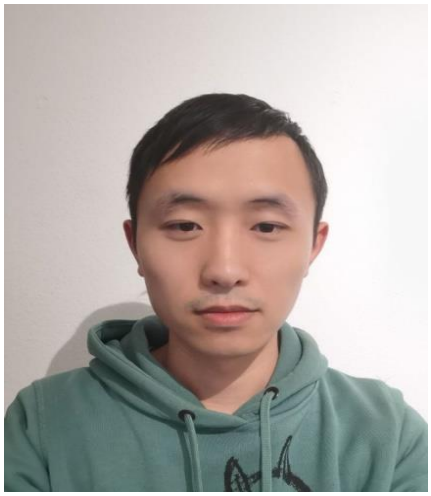

Lianghong Long (龙良红)

Date of birth	21 January 1992
Place of birth	Hubei, China
Nationality	China
Current address	Thomas-Nast-Str. 61 76829 Landau, Germany
Email	long@uni-landau.de

Since August 2017	PhD candidate, Institute for Environmental Sciences, University of Koblenz-Landau, Germany
September 2014 - July 2017	MSc, College of Hydraulic & Environmental Engineering, China Three Gorges University, China
September 2010 - July 2014	BSc, College of Hydraulic & Environmental Engineering, China Three Gorges University, China
September 2007 - July 2010	Senior High School of Dangyang No. 1, Hubei, China

Acknowledgements

Three years of doctoral career is coming to an end, at this moment, all kinds of scenes like the lens flashed through the mind, which is exciting, bitter, regret, but more grateful!

First of all, deeply thank my supervisor, Andreas Lorke, for his strict requirements, careful guidance, constant support and encouragement in three years. I appreciate the maximum freedom he provided a good platform to carry out my research, as well as taught me a lot of scientific methods, and guided me into the rigorous academic attitude. I most respect him not only because of his profound knowledge, excellent academic achievements, keen academic insight, but also his enthusiasm for research. The unforgettable time in the discussions during our meetings, in the field with you, in the travelling with you, is the priceless treasure in my whole lifetime.

Second, thanks to Angelika Holderle, the secretary of our group, help me solve daily-life issues. Without her kind assistances in office, in apartment, in bank…, I can't imagine in this German-speaking city what the life will be like. I also appreciate Christoph Bors, the technician in our group, supported me from the lab to the field. Thanks to Liu Liu, Sofya Guseva, Gerrit Rau, Carolin Ganglo, Lorenzo Rovelli, Lediane Marcon, and everyone in Environmental Physics group at Uni Landau. It is really great time being with all of you. Certainly, I have to say thank you to Mayra Ishikawa, who is my valuable dictionary in Germany. It's my luck working with her in the same room.

Then, I am deeply grateful to teachers and students who have provided selfless help in my field work. They are Prof. Defu Liu and Jun Ma working at Hubei University of Technology, Daobin Ji and Zhengjian Yong, Shangbin Xiao working at China Three Gorges University. Thanks to Xingxing Zhao, Zaiqiang cheng who supported me in field for instrument deployed. Thanks also to Liu Liu, and Clara Mendoza-Lera for critically proofreading the first draft of the thesis. The thesis is impossible to complete without their help.

At last but not least, I would like to thank my family for their love and support, particularly to my wife Hui Xu. We're thousands of miles apart after our wedding. Thank her for sacrificing her study time to care for and manage our son alone. For over a thousand days and nights, my life will have no luster, no hope without her encouragement and support. Thanks also to my parents in China who always unconditionally back me up. Thank to myself because I never give up. The end of PhD study time also means a new beginning for my life. Finally, send this message to my future self: It does not matter how slowly you go as long as you do not stop.

Appendices

Appendix I

Effect of cascading reservoirs on the flow variation and thermal regime in the lower reaches of the Jinsha River

Lianghong Long [1]; Daobin Ji [2*]; Defu Liu [3]; Zhengjian Yang [2]; Andreas Lorke [1, *]

[1] *Institute for Environmental Sciences, University of Koblenz-Landau, Fortstrasse 7, 76829 Landau, Germany*

[2] *College of Hydraulic and Environmental Engineering, China Three Gorges University, 443002 Yichang City, Hubei Province, China*

[3] *Hubei Key Laboratory of River-lake Ecological Restoration and Algal Utilization , Hubei University of Technology,430068 Wuhan City, Hubei Province, China*

***** Correspondence: lorke@uni-landau.de (Andreas Lorke)

Please click the following link to read the publication

https://www.mdpi.com/2073-4441/11/5/1008

https://doi.org/10.3390/w11051008

Article

Effect of cascading reservoirs on the flow variation and thermal regime in the lower reaches of the Jinsha River

Lianghong Long [1]; Daobin Ji [2]*; Defu Liu [3]; Zhengjian Yang [2]; Andreas Lorke [1,]*

1. Institute for Environmental Sciences, University of Koblenz-Landau, Fortstrasse 7, 76829 Landau, Germany
2. College of Hydraulic and Environmental Engineering, China Three Gorges University, 443002 Yichang City, Hubei Province, China
3. Hubei Key Laboratory of River-lake Ecological Restoration and Algal Utilization , Hubei University of Technology,430068 Wuhan City, Hubei Province, China

* Correspondence: lorke@uni-landau.de; dbji01101@ctgu.edu.cn

Abstract: We analyze the alteration of discharge and water temperature caused by two newly established reservoirs in the lower reaches of the Jinsha River. In comparison to longer-term observations from the pre-impoundment period, the seasonal flow variability was significantly affected by the larger, upstream-located Xiluodu reservoir, with higher discharge in spring and reduced discharge in summer. The smaller, downstream located Xiangjiaba reservoir did not contribute significantly to the total hydrological alteration caused by the reservoir cascade. Thermal stratification occurred in spring and summer in Xiluodu reservoir, but was not observed in Xiangjiaba reservoir. The vertical structure and seasonal dynamics of thermal stratification was mainly governed by the water temperature of the inflow and the depth of the water outlet. Despite the different thermal structure, both reservoirs reduced the amplitude of annual temperature variations and delayed the seasonal temperature cycle in the downstream river water. In contrast to discharge variation, thermal effects were accumulative along the cascading reservoirs. Homogenization and delay effects can be expected to increase further with the completion of ongoing reservoir construction upstream of the two studied reservoirs. Based on our findings, we discuss the larger-scale impacts of cascading hydropower developments and emphasize the need for taking water temperature and its variation into account when developing optimized operation or mitigation strategies for these systems.

Keywords: Flow alteration; thermal regime; stratification; cascading reservoirs; cumulative effect

1. Introduction

Reservoirs provide comprehensive ecosystem services to the human society, such as flood control, electricity generation, navigation, irrigation and drinking water storage, and have been promoting economic and social development [1,2]. However, dam construction and reservoir operation are associated with drastic changes of the physical environment in the impounded water body (reservoir), as well as in downstream river reaches, with globally significant impacts on biodiversity [3,4], biogeochemical cycling [5,6] and greenhouse gas emissions [7,8].

Flow velocity and its temporal dynamics are among the primarily affected physical characteristics of the impounded river. Enlarged cross-sectional area causes a general reduction of the flow velocity, an increase of water residence time [9], and often changes the characteristics of the water body from lotic to lentic [10,11]. In consequence, reservoirs can develop seasonal or diurnal thermal stratification, depending mainly on residence time and water depth [12,13]. Vertical density stratification acts as a barrier restraining mixing of the water column [14] and affects the vertical

distribution of suspended and dissolved material, including nutrients, algae and oxygen [15,16]. Downstream of reservoirs, river discharge is strongly altered, with higher dry season flows and reduced flood peaks [17,18]. Furthermore, downstream water temperature and its seasonal dynamics can differ strongly from the pre-impoundment conditions [19]. Common alterations include a reduction in the annual and daily fluctuations of water temperature, lower summer maximum temperature, and a delay in the annual cycle of temperature variations [20].

With the number of dams increasing globally [21], cascading reservoir configurations, where the inflowing water into impoundments is already affected by upstream dam operation, become more frequent. Although the few existing observations revealed an increase of the overall degree of hydrological alteration for the combined operation of cascading reservoirs [22,23], the mechanisms by which alterations propagate and potentially accumulate along cascading reservoirs are poorly understood. The impact of reservoir operations on hydrology depends largely on the operation rules applied and, naturally, on the actual number and location of the dams [24]. The hydrodynamics in reservoirs, which receive inflowing water from upstream impoundments, is not only affected by flow regulation, but also by discharge temperature. Inflowing water often form a density current along the channel bottom due to lower release temperature of the upstream reservoir. The resulting thermal regime can therefore differ from that of a solitary reservoir [25,26]. Most studies on the impact of cascading reservoirs on river systems have mainly been focusing on discharge and sediment transport, whereas the impact of reservoir operation on the thermal regime in downstream reservoirs and river reaches has rarely been studied.

The Jinsha River, which is the upper stretch of the Yangtze River in China, is an example for ongoing development of cascading reservoir construction. The upper Yangtze River is extensively used for hydropower production, with seven large-scale hydropower projects planned, two being under construction, and two recently completed dams [27]. Xiluodu and Xiangjiaba hydroelectric power stations are located in the lower reaches of the Jinsha River. Xiangjiaba is the most downstream located reservoir at the Jinsha River and started operation in 2012. Xiluodu reservoir is located upstream of Xiangjiaba and started operation in 2013. Two additional reservoirs are currently under construction upstream of Xiluodu. The environmental impacts of cascading reservoirs in the Jinsha River have been studied in respect to the hydrologic regime [28,29], the thermal regime [30], fish diversity [31], dissolved gas pressure [32], sediment accumulation or siltation [33,34], and water quality [35]. Studies on alterations of downstream flow and thermal regime, however, are sparse and were mostly based on design data, without validation by field measurements. Recently, Xie et al, (2017) analyzed the water temperature characteristics and the formation of thermal stratification in Xiluodu reservoir. The accumulation of the hydrological and thermal impacts of the combined operation of Xiluodu and Xiangjiaba reservoir, however, were not considered.

This study aims at improving current understanding of the cumulative effects of cascading reservoirs by analyzing the thermal regime and flow alteration in two newly constructed reservoirs in the lower reaches of the Jinsha River (Xiluodu and Xiangjiaba). We used field measurements of water temperature in both reservoirs and combined these with longer-term observations of discharge and temperature in the Jinsha River during pre-impoundment conditions. A set of indices are used to evaluate the accumulation effect of water temperature after impoundment of both reservoirs and to analyze flow alteration from 1980 to 2015. We used the measured data to calibrate a two-dimensional hydrodynamic model (CE-QUAL-W2), which we applied to analyze the spatial and temporal distribution of water temperature and the formation of thermal stratification in both reservoirs.

2. Materials and Method

2.1. Study Site

Xiluodu and Xiangjiaba reservoirs are the most downstream located reservoirs in the Jinsha River (Fig. 1). Their main functions include hydropower generation, flood control, and increase of shipping and commerce in the region. Two additional reservoirs (Baihetan (BHT) and Wudongde (WDD)) are

currently under construction upstream of Xiluodu and are planned to be put into operation in 2020-2022. The basins of Xiluodu and Xiangjiaba are a typical canyon-shaped and the slope of the riverbed is around 1.12 ‰ and 0.77 ‰, respectively. The length of Xiluodu reservoir is about 200 km and its width varies between 150 and 1000 m. The impoundment of Xiluodu reservoir was initiated on 4 May 2013 and the water level varied widely between 540 and 600 m (above sea level) throughout the following years. The length of Xiangjiaba reservoir is about 156 km and its width varies between 130 and 1500 m. The impoundment of Xiangjiaba reservoir was initiated on 10 October 2012 and its water level varies between 370 and 380 m throughout the year. The two reservoirs are located in a subtropical valley where perennial mean temperature is about 11.6 ℃ and the average annual rainfall is about 893 mm. The rainfall displays an uneven characteristic, with the seasonal average of 136, 513, 212, 32 mm from spring to winter, respectively. The main features of the four cascading hydroelectric reservoirs are summarized in Table 1. In this paper, period I (1980-2011) will be considered as the pre-impoundment situation and period Ⅱ (after 2012) as the current hydrologic situation.

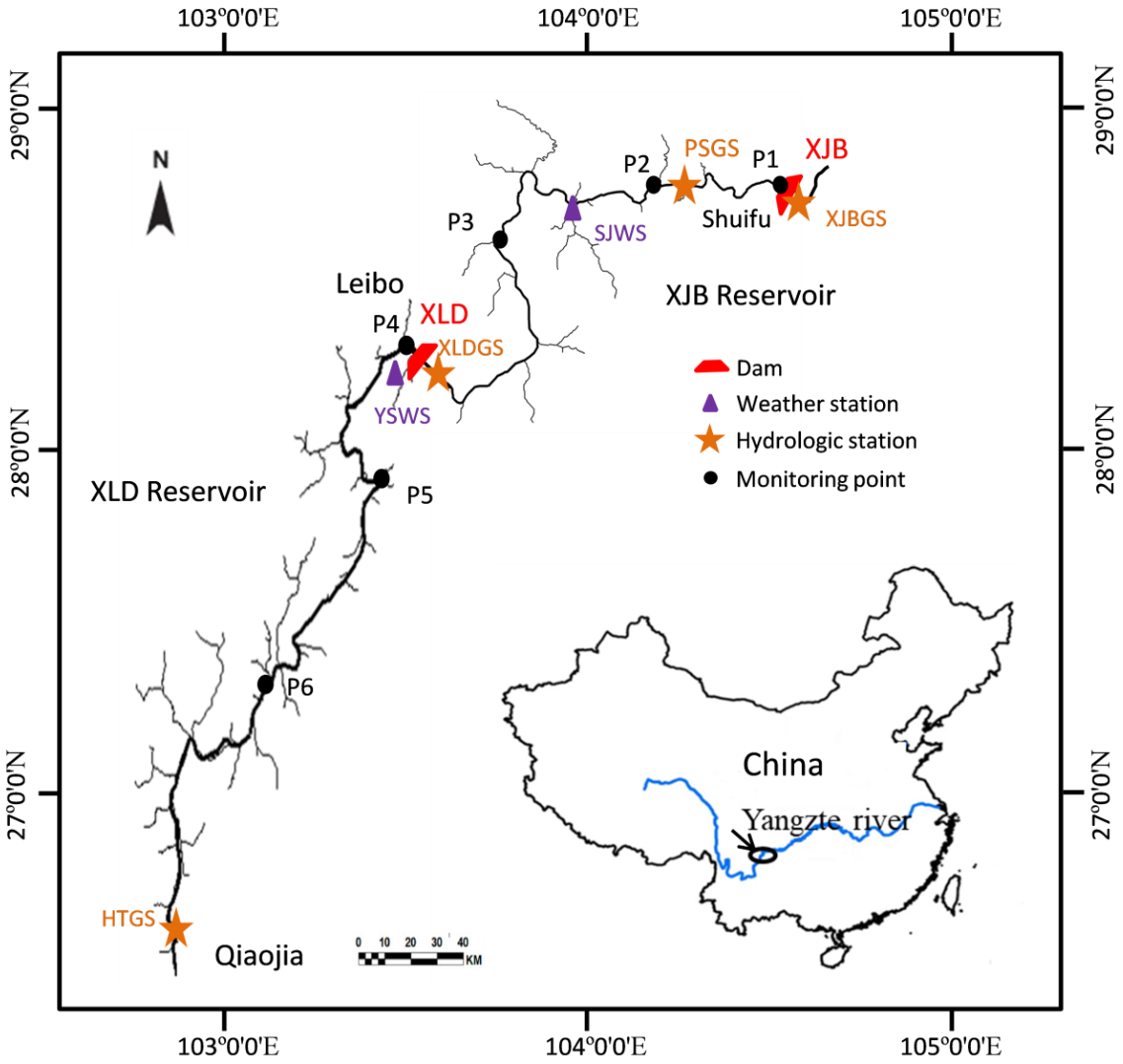

Figure 1. Map of the lower Jinsha River (black solid line, the flow direction is from south to north) with major tributaries (thin black lines). The inset shows the location of the main map within the Yangtze River basin (blue line) in China (not to scale). Symbols mark the location of Xiluodu and Xiangjiaba dam, as well as the location of weather stations (SJWS, YSWS), hydrological stations (XJBGS, PSGS, XLDGS, HTGS) and sampling points for field monitoring (P1-P6).

Table 1. Main features of the cascading hydroelectric reservoirs in the lower reaches of Jinsha River (* denote dams under construction). Dead water level refers to the lowest water level that allows the reservoir to operate under normal operation).

Reservoir	Hydropower capacity (MW)	Dam height (m)	Normal Water level (m a.s.l.)	Dead water level (m a.s.l.)	Storage capacity (10^8 m^3)	Hydraulic residence time (days)	Operation year
Xiangjiaba	7750	162	380	370	52	16	2012
Xiluodu	13860	285.5	600	540	129	37	2013
Baihetan*	16000	289	820	760	179	-	2022
Wudongde*	10200	270	950	920	43	-	2020

2.2. Data

Daily mean values of river discharge from 1980 to 2015 and daily mean water temperature from 2000 to 2015 were available from four different hydrological stations: Huatan gauge station (HTGS, 235 km upstream of Xiluodu dam); Xiluodu gauge station (XLDGS, 2.9 km downstream to of Xiluodu Dam, measured from 2013); Pingshan gaging station (PSGS, 29 km upstream of Xiangjiaba Dam, abandoned after 2012) and Xiangjiaba gaging station (XJBGS, 2.4 km downstream to Xiangjiaba Dam). Basic parameters of reservoir operation including water level, inflow, outflow and outlet locations were provided by the hydropower company. All the hydrological and meteorological data used in this study are summarized in Table S1.

Meteorological data for the hydrodynamic model were available from Suijiang and Yongshan meteorological stations (Fig.1). The data from 1 January 2014 to 31 December 2015 included daily average values of air temperature, wind speed and direction, number of sunshine hours and relative humidity, as well as annual average air temperature and precipitation.

Depth profiles of water temperature for model calibration were measured in 2014 at six sampling sites (P1-P6), which were nearly evenly spaced along both reservoirs (sites P1 to P3 in Xiangjiaba reservoir, sites P4-P6 in Xiluodu reservoir, Fig. 1). Measurements were conducted in both reservoirs on 24-27 April, 15-17 August and 17-19 December 2014. Vertical profiles of water temperature were recorded with 2 m depth increments using a multi-parameter water quality probe (YSI EXO2, USA).

Annual mean precipitation in the Jinsha River basin was estimated from data was provided by China Meteorological Science data sharing Service network (http://www.data.cma.cn/) for 30 meteorological stations. Air temperature at the two reservoirs was estimated from data recorded by three weather stations, located on the upper, middle and lower reaches of the reservoir, respectively (see Table S2 in supplementary information). Parts of the data analysis were conducted for seasonal time scales, which we defined as spring (March-May), summer (June-August), autumn (September-November), and winter (December-February).

2.3. Assessment method

In a riverine system, seasonal water temperature variations can be described by an annual periodic function [19], and alterations of water temperature dynamics after reservoir construction in terms of changes in its amplitude and phase [20]. We use the baseline deviation index, phase offset index and the extreme value amplitude index to evaluate the water temperature change after impoundment of Xiangjiaba and Xiluodu reservoir [36,37].

The baseline deviation index (I_{BD}) is the annual sum of squared differences in monthly mean water temperature before impoundment ($T_{i,b}$, the index i ($1 \le i \le 12$) refers to month) and after impoundment ($T_{i,a}$), normalized by the squared mean deviation of monthly mean temperature from the annual mean temperature before impoundment ($\bar{T}$):

$$I_{BD} = \sum_{i=1}^{12}\left(T_{i,a} - T_{i,b}\right)^2 / \sum_{i=1}^{12}(T_{i.b} - \bar{T})^2 \quad \text{Eq. 1}$$

The phase offset time index (I_{PO}) is defined as the phase difference between the river water temperature and the natural river reference water temperature before the construction of the reservoir. The calculation formula is as follows:

$$I_{PO} = \left(\tan^{-1}\left(\frac{\sum_{i=1}^{12} T_{i,a} \sin \theta_{i,a}}{\sum_{i=1}^{12} T_{i,a} \cos \theta_{i,a}}\right) - \tan^{-1}\left(\frac{\sum_{i=1}^{12} T_{i,b} \sin \theta_{i,b}}{\sum_{i=1}^{12} T_{i,b} \cos \theta_{i,b}}\right)\right) \quad \text{Eq. 2}$$

The $\theta_{i,a}$ and $\theta_{i,b}$ are vector angles of water temperature in month number i after impoundment and before impoundment. With 365 days corresponding to a phase shift of 360°, one month corresponds to a phase shift of 30°).

The extreme fluctuation index (I_{EC}) is the ratio of signed differences of annual extreme values of monthly mean water temperature after ($T_{max,a}$ and $T_{min,a}$) and before ($T_{max,b}$ and $T_{max,b}$) impoundment:

$$I_{EC} = (T_{max,a} - T_{min,a})/(T_{max,b} - T_{\min,b}) \quad \text{Eq. 3}$$

The theoretical mean hydraulic residence time of the reservoirs (HRT) was estimated following [38]:

$$HRT = Volume / Q_{outflow} \quad \text{Eq. 4}$$

Where Volume is the storage capacity of reservoir, and Q outflow is the perennial average discharge in the lower reaches of the Jinsha River.

2.4. Numerical simulation

CE-QUAL-W2 is a two-dimensional (longitudinal and vertical), laterally averaged, hydrodynamic and water quality model [39]. The model has been used to simulate flow velocity, temperature and various water quality parameters in lakes and reservoirs [40,41]. We used the observed temperature profiles measured in 2014 in both reservoirs to calibrate and to validate the model. The initial and boundary conditions, model parameters and results of the model calibration are presented as supplementary information (see Fig. S2 – S6). The model performance in simulating the water temperature stratification was comparable to that achieved in other studies [42-44], indicating that the model parameters were set reasonably and the simulations of thermal regimes was accurate and credible. Using the calibrated model, we simulated the spatial and temporal distribution of water temperature in both reservoirs 2015.

The effect of Xiluodu reservoir on the temperature stratification in Xiangjiaba reservoir in 2015 was additionally analyzed in a hypothetical scenario, without the upstream Xiluodu reservoir. We simulated the water temperature dynamics in Xiangjiaba reservoir with inflow rate and inflow temperature data measured at HTGS, i.e. upstream of Xiluodu reservoir. The inflow conditions were corrected according to the longitudinal water temperature and flow gradient between HTGS station and Xiangjiaba reservoir observed in the long-term hydrological observations during the pre-impoundment period. Daily outflow from Xiangjiaba reservoir was estimated by the storage-capacity curve and known pre-dam daily water levels. Direct measurements were used for the withdrawal height at Xiangjiaba and meteorological conditions during the simulated scenario.

3. Results

3.1. Long-term flow variability and hydrological alteration

3.1.1. Annual mean discharge

Discharge in the Jinsha River showed pronounced inter-annual variations, which were consistent at both gaging station (HTGS and PSGS, Fig. 2). The more than three decades of pre-impoundment observations existed distinct hydro-meteorological dynamics. Between 1980 and 1997, annual mean precipitation and discharge fluctuated from year to year (mean value ± standard deviation: 623 ± 31 mm/year and 4274 ± 487 m^3/s, respectively), but had no significant trend. In 1998, precipitation and discharge were maximal and then decreased gradually with significant linear trends until the

impoundment of Xiangjiaba reservoir in 2012. However, no significant abrupt change for precipitation and discharge was detected in former time series analysis of data from PSGS [45,46]. The increase of precipitation and river discharge conditions in 1998 has been documented as an extreme event (the biggest flood of the Yangtze River in nearly 50 years) in former studies [45]. We consider 1980-2011 as the pre-impoundment period in our analysis the pre-impoundment period and 2012-2016 as the post-impoundment period. The annual mean discharge at the upstream and downstream gaging stations was highly correlated during pre-impoundment period (r^2 = 0.95, *Pearson's* r=0.98, p < 0.05). The few data points from the post-impoundment period did not deviate from the regression curve, indicating that dams operation had no significant influence on annual mean discharge. The annual average discharge was correlated with precipitation during the pre-impoundment period (r^2 = 0.53, Pearson correlation coefficient r=0.73, p < 0.05), but discrete points were biased to one side of the regression curve after impoundment (see figure S1 in supplementary information).

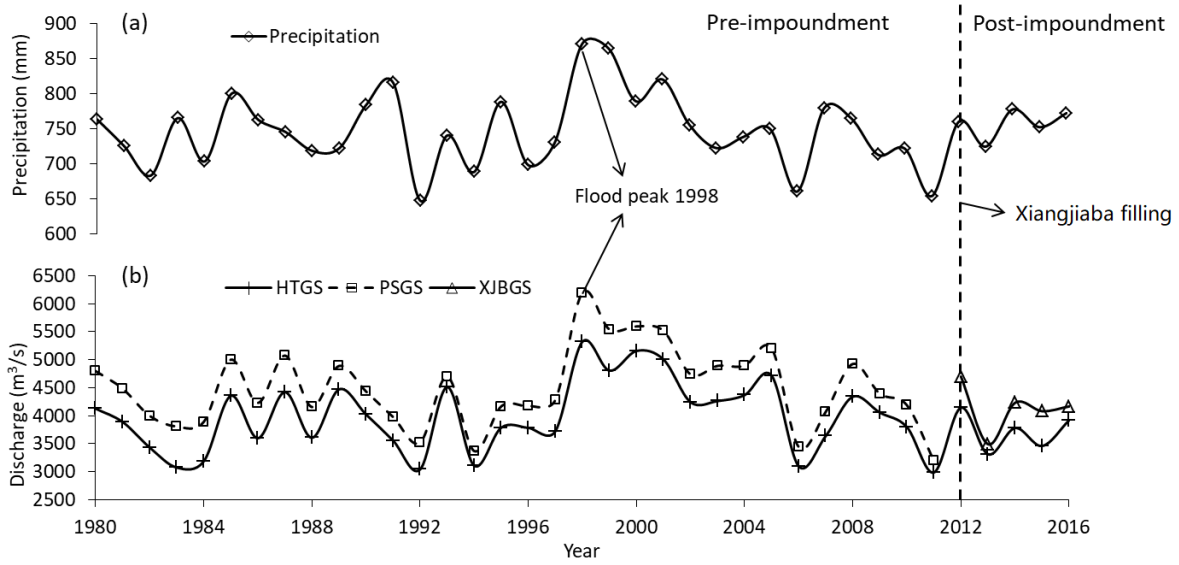

Figure 2. Time series of annual mean precipitation in the Jinsha River basin (a) and annual mean discharge (b) at gauging stations located upstream (HTGS), and downstream (PSGS, XJBGS) of the two studied reservoirs (cf. Fig. 1). The filling of Xiangjiaba reservoir in 2012 (vertical dashed line) divides the time series into the pre- and post-impoundment periods, respectively.

3.1.2. Seasonal discharge distribution

The monthly mean discharge showed pronounced seasonal variations at both gaging stations. During 1980-2011, discharge was typically low with only small inter-annual variations (1601 ± 294 m^3/s) in the dry season (January to April). Highest monthly mean discharge and largest inter-annual discharge variability occurred in July-August (9530 ± 2860 m^3/s). Although the number of observations from the post-impoundment period is rather limited and show large inter-annual variability, they indicate a clear modification of the seasonal discharge distribution (Fig. 3). While the monthly averaged discharge during the dry season (January to April) were up to 69 % higher than that in the pre-impoundment period, the summer discharge (June to September) was exceptionally low and up to 26 % below the pre-impoundment average. Monthly discharge during May and December did not show pronounced deviations from the longer-term average discharge. The seasonal pattern and magnitude of the post-impoundment discharge anomalies were nearly identical in both reservoirs (Fig. 3). This is expected as the inflow of Xiangjiaba reservoir is the release of Xiluodu reservoir and there are no larger tributaries along this section. Discharge alteration was mainly caused by the larger Xiluodu reservoir, which has a storage volume almost 2.5-fold higher than that of Xiangjiaba reservoir.

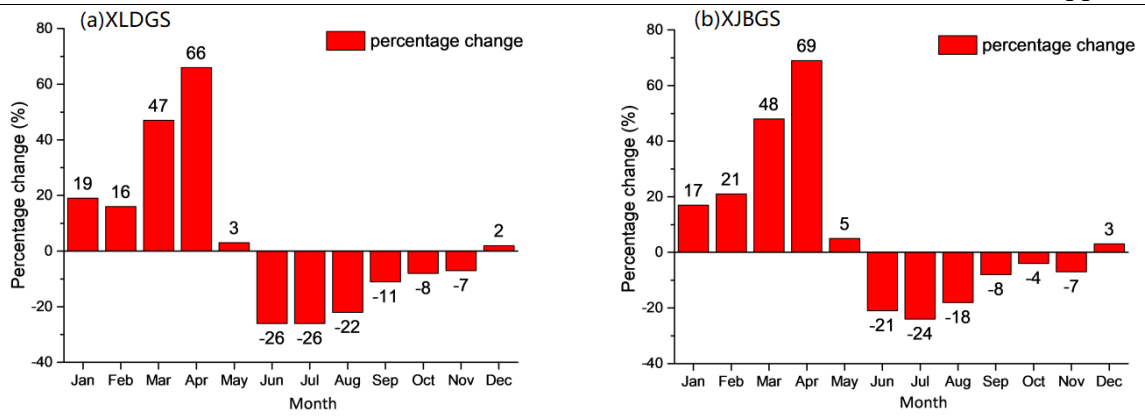

Figure 3. The seasonal distribution of the mean percentage change of discharge at XLDGS (a) and XJBGS (b) relative to the pre-impoundment period. Percentage change = (monthly mean discharge after impoundment-monthly mean discharge in pre-impoundment period) ×100 %/ monthly mean discharge in pre-impoundment period.

3.2. Long-term temperature alterations

3.2.1. Water temperature variation

The water temperature in the Jinsha River showed consistent inter-annual variations at both gaging stations with mean water temperature of 17.7 ± 0.5 ℃ and 18.8 ± 0.4 ℃ at HTGS and PSGS, respectively (Fig. 4a). Temperature was increasing at a rate of 0.06 ℃/yr at HTGS (Person's $r = 0.54$, $p < 0.05$). At the 0.05 level, the temperature trend at PSGS from 1980 to 2015 was not significant, probably because of a slight decrease of mean water temperature after dam construction. Monthly mean water temperature was closely related to air temperature at PSGS (Pearson's $r = 0.98$, $p < 0.05$) during the pre-impoundment period (Fig. 4b), but this consistent relationship broke up into two seasonally different linear relationships during the post-impoundment period (Fig. 4b and 4c).

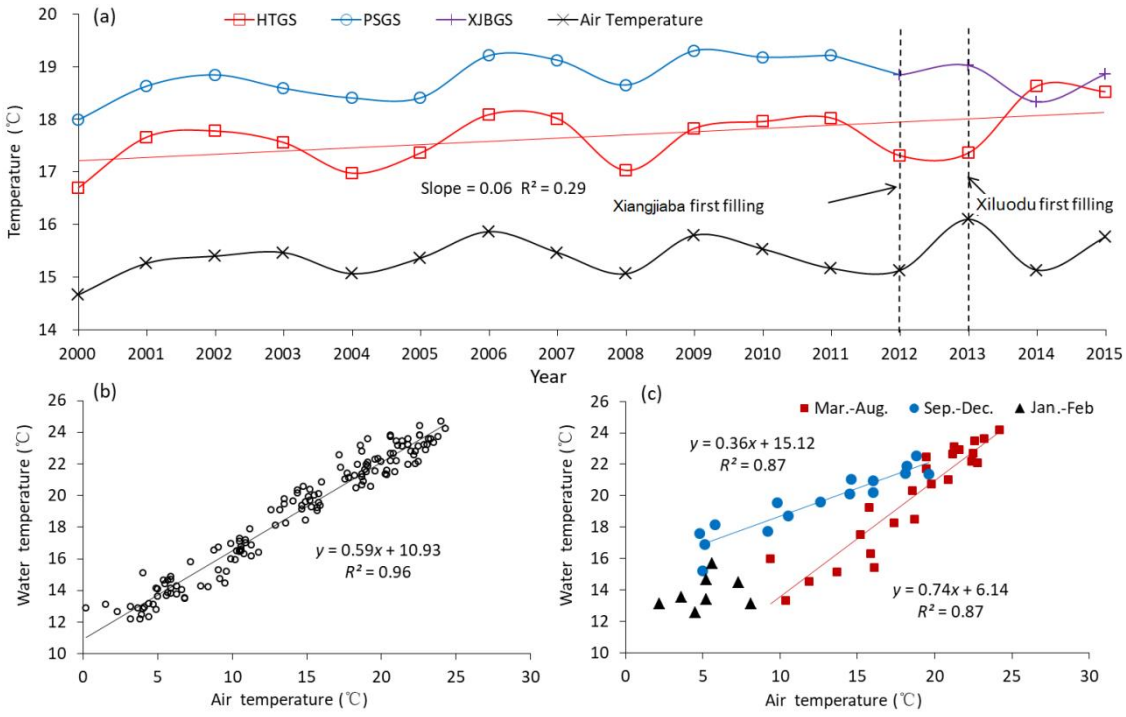

Figure 4. (a) Annual mean water temperature at HTGS, PSGS, XJBGS from 2000 to 2015. Black symbols show annual mean air temperature in the reservoir basin. Solid lines indicate significant linear trends of

mean water temperature at HTGS; (b) Correlation between monthly mean air temperature and water temperature during the pre-impoundment period. The solid line shows a linear regression (according to the equation in the legend); (c) Correlation between monthly mean air temperature and water temperature during the post-impoundment period with different color denoting different seasons (see legend). Solid lines show linear regressions (equations provided in legend).

Filling of Xiluodu reservoir was associated with rapid drop in water temperature in February and March 2014 (Fig. 5), causing the lowest annual minimum temperature within the observation period in 2014 (Fig. 4a). The consistent increase of water temperature between the locations of both dams that was evident in the mean water temperature before 2012 was not observed after the filling of both reservoirs (Fig. 4).

3.2.2. Seasonal temperature variation and alteration indices

Water temperature followed a seasonal cycle with lowest monthly mean temperature in January and highest values in June to August. Before impoundment (2000-2011), inter-annual variations of monthly-mean temperatures were relatively small, mostly within ±1.0 ℃ (Fig. 5a). After impoundment, the observations showed a decrease in the amplitude of seasonal temperature variations (I_{EC} = 0.83-0.92), as well as a delay in the seasonal cycle of the discharge temperature at both dams (Offset-time ＞ 20 d at Xiluodu; Offset-time ＞ 30 d at Xiangjiaba, table 2). Monthly mean water temperature was reduced (maximum: 2.8 ℃) between March and June, and consistently higher (maximum: 3.2 ℃) than the long-term monthly average temperature between October and January (Fig. 5b). In February and July-September, no great change in water temperature was observed.

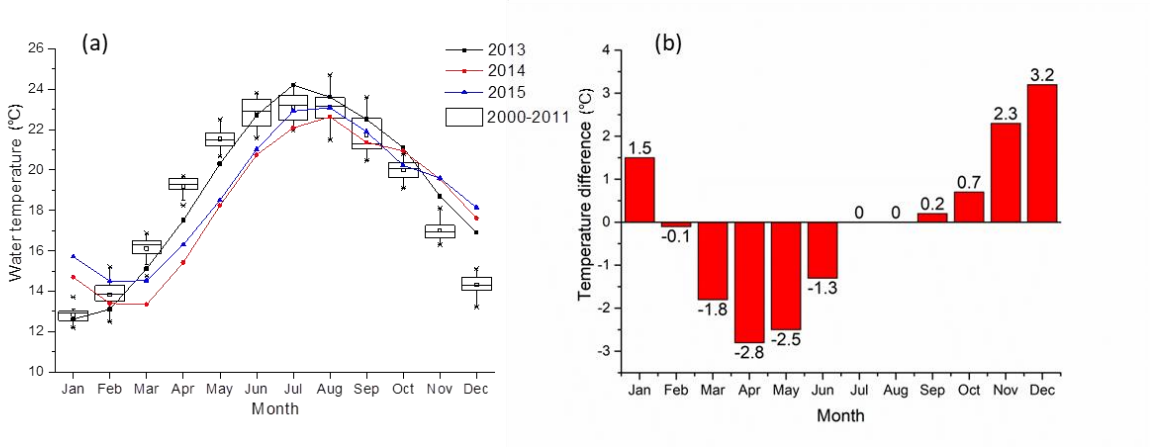

Figure 5. (a) Box plot of monthly mean water temperature between 2000 and 2011 (pre-impoundment period) at PSGS (see caption of Fig. 3 for explanations of the box plot elements). The line plot show measured water temperature at XJBGS in 2013-2015 (post-impoundment). (b) Monthly mean temperature difference between the post- and pre-impoundment periods at XJBGS (monthly average temperature in 2013-2015 minus monthly average temperature from 2000 to 2011).

In 2013, when only Xiangjiaba reservoir was in operation, a low baseline deviation index (I_{BD} = 0.12) indicated little alteration of water temperature (Table 2). The extreme fluctuation index was slightly higher than unity (I_{EC} = 1.13), indicating above average seasonal variation amplitude. Furthermore, the offset-time was about 16 days, which corresponds to the hydraulic residence time of Xiangjiaba reservoir (Table 1). However, after Xiluodu impoundment (2014 and 2015), I_{BD} at XLDGS was almost twofold higher (average 0.21), than during Xiangjiaba single operation in 2013. The offset time was exceeding 20 days already at the outlet of Xiluodu reservoir. In the downstream reservoir (XJBGS), both the baseline deviation and the phase shift index increased further from the values at the upstream reservoir (Table 2). Also the extreme fluctuation index decreased, indicating homogenization of the seasonal temperature cycle. The offset-time at the outlet of Xiangjiaba

reservoir eventually exceeded one month. All indices indicate accumulative effects of Xiluodu and Xiangjiaba reservoirs on river water temperature.

Table 2. Baseline deviation index (IBD, Eq. 1), phase shift index (IPS, Eq. 2), extreme fluctuation index (IEC, Eq. 3) and offset-time for the discharge temperature at both dams. We considered the monthly average water temperature at PSGS from 2000-2011 as the natural water temperature baseline (pre-impoundment period).

Site	Year	I_{BD}	I_{PO} (days)	I_{EC}
XLDGS	2014	0.23	23	0.92
	2015	0.19	20	0.88
XJBGS	2013	0.12	16	1.13
	2014	0.37	34	0.90
	2015	0.33	31	0.83

3.3. Stratification in the reservoirs

3.3.1. Stratification features in Xiluodu and Xiangjiaba reservoirs

The simulated longitudinal and vertical distribution of water temperature in both reservoirs is shown for four different seasons in Fig. 6. Water temperature in Xiluodu reservoir stratified gradually during the low discharge period in spring, when a thermocline occurred below the elevation of the reservoir outlet (power tunnels, see Fig. S2). Surface water warmed up from 13.0 °C in January to 19.5 °C in April. Between April and July, the temperature differences between the epilimnion and hypolimnion slowly increased from 3.6 °C on 17 April to 8.1 °C on 25 July because of further warming of the epilimnion. Epilimnion temperature was highest (23 °C) in June-August when the reservoir was operated at low water level. Flood discharge at the beginning of September, when inflow and outflow rates sharply increased to more than 1×10^4 m^3/s and water was mainly released through the bottom hole (see Fig. S4), the thermocline moved down quickly at a rate of 1.7 m/d, and the hypolimnion shrunk gradually. After October, the inflowing water became colder and formed an underflow, while surface water temperature decreased more slowly. Ultimately, water temperature in the entire reservoir became increasingly homogenous in winter.

In Xiangjiaba reservoir, vertical temperature stratification was less pronounced. The warmer water released from the epilimnion of Xiluodu reservoir in winter, delayed the seasonal cooling of the water at the Xiangjiaba outflow and temperature gradients were mainly in the longitudinal direction. During spring, in contrast, the inflow of Xiangjiaba reservoir was cooler than the river water, causing a delayed warming of the surface water in Xiangjiaba reservoir and weak vertical temperature stratification. The bottom water heated up quickly by vertical mixing, and the temperature differences between surface and bottom decreased from 6.1 ℃ in May to 2.0 ℃ in July when the hypolimnion had almost disappeared. The near-surface temperature close to dam was relatively high due to warming by surface heat fluxes. Vertical temperature gradients disappeared after July and then water temperature gradually decreased from 21 ℃ to 15 ℃ during winter.

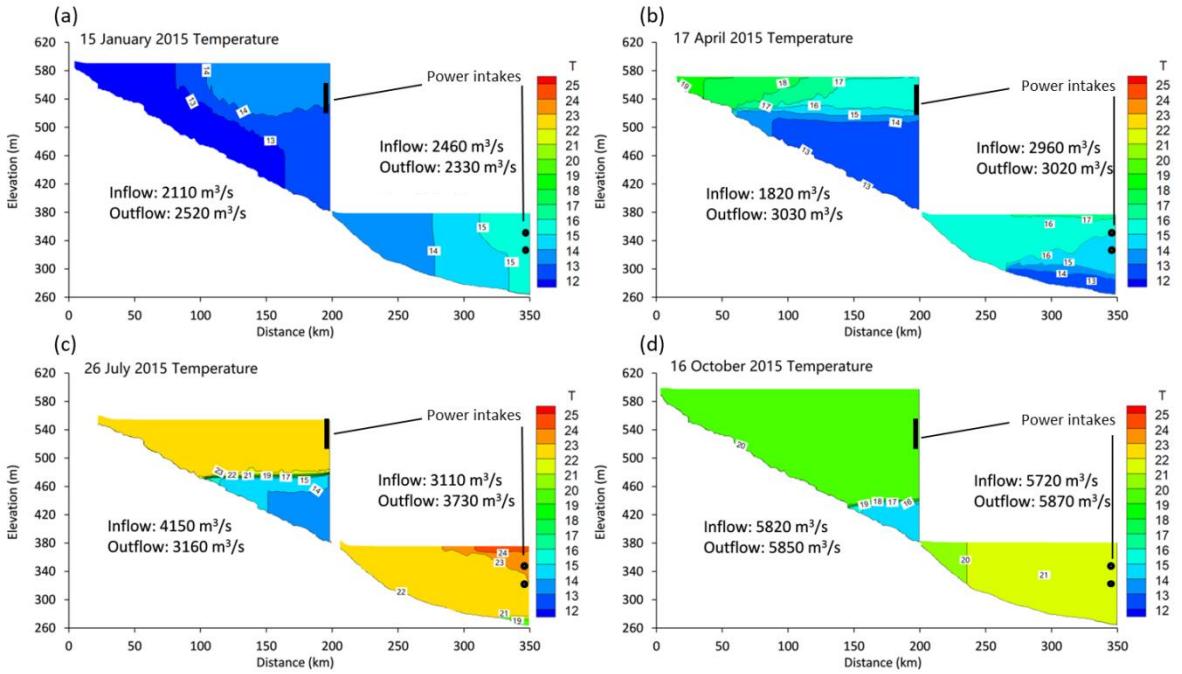

Figure 6. Simulated vertical and longitudinal distribution of water temperature in Xiluodu and Xiangjiaba reservoirs during (a) winter, (b) spring, (c) autumn and (d) winter 2015. The location of the turbine intakes as well as in and outflow rates are indicated by labels.

3.3.2. Influence of upstream reservoir on stratification structure of downstream reservoir

The results presented above suggest that the discharge flow and temperature of the upstream reservoir (Xiluodu) affected the vertical stratification and thermal regimes of the downstream reservoir (Xiangjiaba) by weakening or inhibiting thermal stratification. Without Xiluodu reservoir, the inflow water temperature of Xiangjiaba would have been warmer in spring and summer and lower in autumn and winter, possibly promoting stronger thermal stratification by forming an overflow and an underflow, respectively. In a hypothetic model scenario we simulated the variation of the thermal structure in Xiangjiaba reservoir in 2015 for modified inflow conditions, reflecting the absence of Xiluodu reservoir. Inflow temperatures were estimated from measurements at HTGS using the regression equation (T_{PSGS}=1.0∗T_{HTGS}+1.1℃). The inflow rate Q was estimated using the formula (Q_{HTGS}=1.1 × Q_{PSGS} + 112.1 m³/s), which we derived from the linear trend of the long-term observations (r^2 = 0.99).

The simulations revealed no obvious differences in vertical thermal stratification in the Xiangjiaba reservoir, depending on whether the inflowing water was coming from the Jinsha River or from the upstream located Xiluodu reservoir (Fig. 7). One obvious impact of the upstream reservoir, however, is the delay in the seasonal cycle of water temperature that was verified by field measurement (Table 2). Nevertheless, the simulation confirms the additive effect of both reservoirs for the discharge temperature at Xiangjiaba reservoir (Fig. 8). Without Xiluodu reservoir, water temperature in April and May is warmer, indicating that spring warming was delayed with Xiluodu operation. In July-September, in contrast, there was no obvious difference in water temperature between the three different situations. The amplitude of annual temperature fluctuations without dam (12.5 - 23.3 ℃) were larger than that with Xiangjiaba operation (14.2 - 23.2 ℃) and the joint operation of both reservoirs (14.2 - 23.6 ℃). With only Xiangjiaba reservoir in operation, the delay of the annual temperature cycle (Offset-time) was about 16 days. In the joint operation of both reservoirs, the delay increased to 31-34 days, which is in good agreement with the offset time estimated from time series analysis (Table 2).

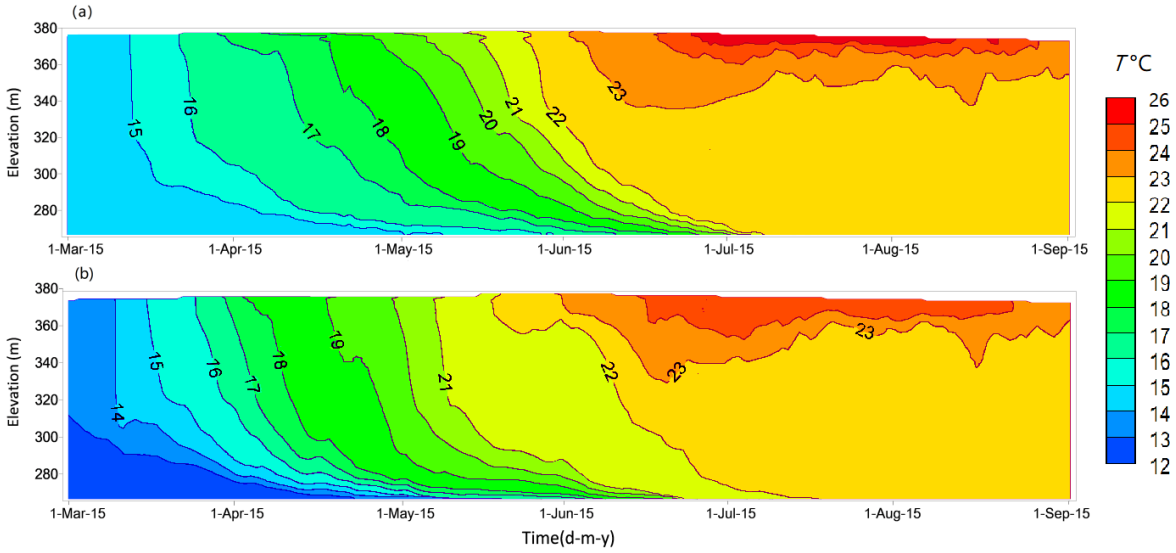

Figure 7. Contour plots of simulated water temperature at a cross-section near to Xiangjiaba dam from March to August in 2015 with Xiluodu reservoir (a) and without Xiluodu operation (b).

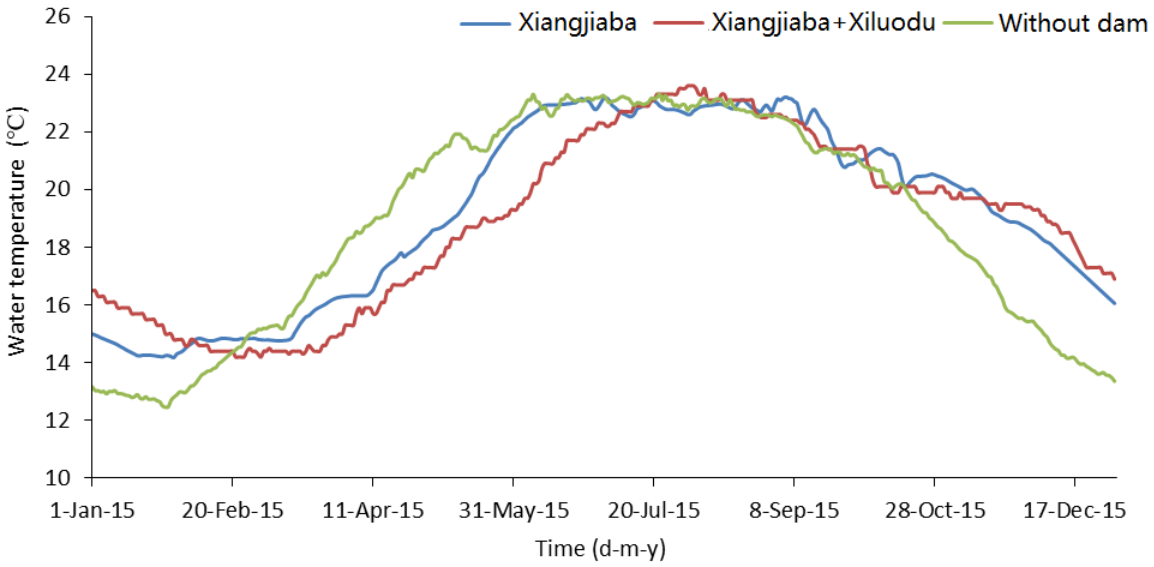

Figure 8. Water temperature of the discharge at Xiangjiaba reservoir in 2015 for different situations (without dam: average water temperature from 2000 to 2011, Xiangjiaba: Xiangjiaba dam with river water temperature inflow; Xiangjiaba+Xiluodu: both dams in operation).

4. Discussion

4.1. Effect of reservoir construction on river discharge dynamics

Construction and operation of Xiluodu and Xiangjiaba reservoir caused changes of the seasonal flow variability, with higher discharge during the dry season (up to 50% increase in January-April) and reduced high discharge during the wet season. Although the decrease was only about 25% of the mean summer discharge, the flow decreased by more than 2000 m^3/s. Comparable homogenization of the seasonal discharge regime has been observed in other reservoirs [4]. The two reservoirs studied here, however, were only four (Xiangjiaba) and three (Xiluodu) years in operation, respectively, and the limited period of observations is certainly too short to derive common quantitative indices describing the degree of alteration in comparison to the complex natural discharge dynamics [47]. Analysis of longer-term flow variability in the Jinsha River, revealed pronounced inter-annual

variability of discharge, which before dam construction was closely correlated to precipitation. In the few years after impoundment, this correlation appeared to be broken, indicating additional effects of the impoundments on longer-term flow variability related to multi-year weather phenomena. In contrast to the annual mean discharge, we found large inter-annual variability of the seasonal discharge distributions after impoundment. For example, exceptional low discharge in June and August in 2015, as well as in August and September in 2016. It remains open, if this variability was related to the initial filling and dam implementation, or if the strong inter-annual discharge variability persists also during regular reservoir operation.

Interestingly, the comparison of the percentage change of the average seasonal discharge distributions at both reservoirs showed, that discharge alteration can mainly be attributed to the larger upstream reservoir (Xiluodu), and remained nearly unchanged during the passage through Xiangjiaba reservoir (weaker water-level fluctuation, Fig. S3). Hence, the discharge in the downstream river will mainly be controlled by Xiluodu reservoir and that the cascading operation of Xiangjiaba and Xiluodu dam were not accumulative in terms of downstream discharge variations.

4.2. Effect of reservoir stratification on river water temperature

Most longer-term studies on the thermal impact of reservoirs on river water temperature showed that the main thermal effects of impoundment and regulation are a raise of mean water temperature, reduction of summer maximum temperature, delay of the annual cycle and reduction in diurnal fluctuation [20,48]. Surprisingly, the effects of Xiluodu and Xiangjiaba dams on annual mean and maximum temperatures in the downstream river were small and within their inter-annual variability before impoundment. The annual minimum temperature, however, has been increasing during the three years after initial filling of Xiluodu reservoir. More pronounced effects have been found for the seasonal temperature cycle. The offset-time of water temperature was in close agreement with the hydraulic residence time in Xiangjiaba reservoir. Contrarily, in the partially stratified Xiluodu reservoir, the delay of the annual cycle (22 days) was only approximately half of its residence time due to limited mixing of the inflowing water with the hypolimnion in the reservoir.

Monthly mean water temperature was found to be smaller (average - 2.4 ℃) in March-May, and warmer (average + 2.3 ℃) in November-January, while during summer the alterations were small, (mostly < 1 °C). This observation is contrary to many other reservoirs where cooler water is released during summer [49,50]. For example, summer water temperature decreased by 3 ℃ after the construction of Hills Creek Dam [51], and even by 5-6 ℃ in the regulated Lyon River [50]. The reason for the lower discharge temperature during in these studies was thermal stratification of the reservoir and water withdrawal from the hypolimnion. Contrasting patterns, i.e. an increase of summer discharge temperature, have been observed in reservoirs where the release depth was located in the epilimnion [52].

Discharge temperature can strongly be affected by thermal stratification in reservoirs [20] with larger alterations of the natural temperature regime caused by thermally stratified reservoirs. In accordance with previous numerical simulations of the thermal structure in Xiluodu reservoir [30], we found seasonal vertical temperature stratification. As analyzed by Xie in greater detail [30], the formation of vertical temperature stratification in Xiluodu is mainly controlled by the temperature of the inflowing water, which supports vertical stratification by forming density currents, i.e. by forming an underflow during winter and a near-surface flow during spring and summer. The strength of the vertical stratification is strongly controlled by the water residence time as well as by the epilimnetic release depth. In Xiangjiaba reservoir, in contrast, a strong thermocline did not develop. In addition to shorter residence time and shallower water depth, the homogenization of the seasonal temperature cycle by the upstream located Xiluodu reservoir was expected to contribute to the absence of stratification in Xiangjiaba reservoir. Similarly, a reduction of thermal stratification along cascading reservoirs due to homogenization of inflow temperature has been found for two reservoirs at the Yalong River [53]. Our scenario simulation for Xiangjiaba reservoir, however, suggests that thermal

stratification was also absent when its inflow temperature was not affected by Xiluodu reservoir, most likely on account of its short residence time and strong vertical mixing.

4.3. Importance of cumulative impacts in cascading reservoirs

In contrast to the accumulative effects of cascading dams on downstream water temperature, the discharge in the Jinsha River way mainly affected by the larger, upstream located reservoir with only small additional changes during the passage of the downstream reservoir. Two additional reservoirs, located further upstream of Xiluodu reservoir, are currently under construction and planned to be put into operation in 2020 and 2022. With discharge being primarily controlled by reservoir operation and management, it remains unclear to what extent the seasonal discharge variations will be affected in the future after completion of the two additional dams.

For the two existing dams, we found accumulative effects for the delay of seasonal water temperature variations. The two additional reservoirs will more than double the existing storage capacity (Table 1) and probably add to the existing alteration of the temperature regime. With dam heights comparable to that of Xiluodu reservoir and larger storage capacity, the new reservoirs can potentially develop thermal stratification. On the other hand, the changing inflow temperature will probably further weaken the stratification in Xiluodu reservoir, which now is strongly affected by density currents formed by the inflowing water.

Comparable observations of alterations of seasonal temperature variations from other cascading reservoirs at large Asian rivers [54-56] demonstrate the increasing importance of cascading reservoirs on water temperature dynamics. Besides water temperature, current research aims at understanding sediment transport and trapping, greenhouse gas emissions and pollutant transport along these systems [22,57]. Despite these efforts, existing strategies for optimization of reservoir operation in terms of minimizing alterations of natural variations and maintaining good ecological state of downstream river reaches, mostly focus on flow regulation [58,59], and do not include temperature. The measurements and simulations presented here emphasize the two-dimensional nature of the temperature dynamics in reservoirs. Thus, at least two-dimensional hydrodynamic models are required to resolve density-driven flows and the longitudinal variations in temperature and vertical stratification along individual and cascading reservoirs. Future research should aim at overcoming the case and site-specific assessments, which are typically associated with such complex simulations, by providing a physical-based framework for assessing and predicting thermal impacts of reservoirs and reservoir cascades based on bulk parameters. In a simplified approach, the two-dimensional nature of temperature stratification could be described in terms of longitudinal and vertical temperature gradients, which develop as a function of the rate of change of inflow temperature, residence time, surface heat fluxes and vertical mixing along the reservoirs. In a system-analytical approach, the interactions of individual reservoirs with up- and downstream located reservoirs and with the atmosphere can be prescribed as annually periodic boundary conditions with amplitude and phase. That approach could potentially be linked to existing frameworks describing the ecological impacts of cascading reservoirs, such as the cascade reservoir continuum concept [60].

Our analysis further revealed the existence of pronounced inter-annual variability of the natural flow and temperature regime in the Jinsha River during the pre-impoundment period. Before impoundment, river discharge was correlated to annual mean precipitation, which varied strongly during the more than 30 years of observation. River water temperature without reservoir operation showed an increasing trend. The observed rate of increase of the mean water temperature during the last ten years before impoundment was with 0.06 °C/year among the highest rates observed globally in aquatic systems [61,62]. These rather rapid climatic changes proceed in addition to reservoir construction and underlined the importance of incorporating also longer-term variability and trends into assessments and process-based analysis of the hydrological, thermal, but also biogeochemical and ecological impacts of cascading reservoirs.

5. Conclusions

Before dam construction, annual mean discharge in the lower reaches of the Jinsha River was mainly controlled by precipitation. After 2012 flow regulation by newly established cascading reservoirs caused significant changes of the seasonal flow distribution, with higher discharge during the dry season (especially in March and April) and reduced high discharge during the wet season. The discharge in the downstream river was mainly controlled by the upstream-located Xiluodu reservoir.

Inflow temperature and outflow depth were dominant factors in controlling the thermal structure in both reservoirs as well as the downstream river water temperature. Xiluodu reservoir stratified gradually in spring, partially caused by the inflow and longitudinal spreading of warmer in the upper mixed layer. Vertical temperature stratification disappeared in autumn after continuous deepening of the thermocline during summer. The homogenization of the seasonal temperature cycle by the upstream located Xiluodu reservoir had no effect on the temporary development of thermal stratification in the downstream-located Xiangjiaba reservoir.

Water temperature effects (homogenization and delay of the seasonal cycle) were additive along the two cascading reservoirs, and will probably be exacerbated in the upcoming years with additional reservoirs being under construction upstream of the two study sites.

Author Contributions: Conceptualization: L.L. and D.L., Investigation: L.L., D.J. and Z.Y., Methodology: L.L. and D.J., Formal analysis: L.L. and A.L., Writing: L.L. All the authors have approved of the submission of this manuscript.

Funding: This study was jointly supported by the Natural Science Foundation of China (grant numbers 91647207 and 51779128), and by the Natural Science and Technology Major Special Program of China (2016YFC05022208).

Acknowledgments: Special thanks to Andreas Lorke for providing instructions and suggestions on this work.

Conflicts of Interest: The authors declare no conflict of interest.

Reference

1. Altinbilek, D. The role of dams in development. *Water Science and Technology* **2002**, *45*, 169-180.
2. Suen, J.P.; Eheart, J.W. Reservoir management to balance ecosystem and human needs: Incorporating the paradigm of the ecological flow regime. *Water resources research* **2006**, *42*, 1-9.
3. Bunn, S.E.; Arthington, A.H. Basic principles and ecological consequences of altered flow regimes for aquatic biodiversity. *Environmental management* **2002**, *30*, 492-507.
4. Poff, N.L.; Olden, J.D.; Merritt, D.M.; Pepin, D.M. Homogenization of regional river dynamics by dams and global biodiversity implications. *Proceedings of the National Academy of Sciences* **2007**, *104*, 5732-5737.
5. Maavara, T.; Parsons, C.T.; Ridenour, C.; Stojanovic, S.; Dürr, H.H.; Powley, H.R.; Van Cappellen, P. Global phosphorus retention by river damming. *Proceedings of the National Academy of Sciences* **2015**, *112*, 15603-15608.
6. Maavara, T.; Lauerwald, R.; Regnier, P.; Van Cappellen, P. Global perturbation of organic carbon cycling by river damming. *Nature communications* **2017**, *8*, 15347.
7. Barros, N.; Cole, J.J.; Tranvik, L.J.; Prairie, Y.T.; Bastviken, D.; Huszar, V.L.; Del Giorgio, P.; Roland, F. Carbon emission from hydroelectric reservoirs linked to reservoir age and latitude. *Nature Geoscience* **2011**, *4*, 593-596.
8. Deemer, B.R.; Harrison, J.A.; Li, S.; Beaulieu, J.J.; DelSontro, T.; Barros, N.; Bezerra-Neto, J.F.; Powers, S.M.; Dos Santos, M.A.; Vonk, J.A. Greenhouse gas emissions from reservoir water surfaces: a new global synthesis. *BioScience* **2016**, *66*, 949-964.
9. Vörösmarty, C.J.; Meybeck, M.; Fekete, B.; Sharma, K.; Green, P.; Syvitski, J.P. Anthropogenic sediment retention: major global impact from registered river impoundments. *Global and planetary change* **2003**, *39*,

169-190.

10. Thornton, K.W.; Kimmel, B.L.; Payne, F.E. *Reservoir limnology: ecological perspectives*; John Wiley & Sons: 1990.
11. Agostinho, A.A.; Pelicice, F.M.; Gomes, L.C. Dams and the fish fauna of the Neotropical region: impacts and management related to diversity and fisheries. *Brazilian journal of biology* **2008**, *68*, 1119-1132.
12. Casamitjana, X.; Serra, T.; Colomer, J.; Baserba, C.; Pérez-Losada, J. Effects of the water withdrawal in the stratification patterns of a reservoir. *Hydrobiologia* **2003**, *504*, 21-28.
13. Huang, T.; Li, X.; Rijnaarts, H.; Grotenhuis, T.; Ma, W.; Sun, X.; Xu, J. Effects of storm runoff on the thermal regime and water quality of a deep, stratified reservoir in a temperate monsoon zone, in Northwest China. *Science of the Total Environment* **2014**, *485*, 820-827.
14. Moreno‐Ostos, E.; Marcé, R.; Ordóñez, J.; Dolz, J.; Armengol, J. Hydraulic management drives heat budgets and temperature trends in a Mediterranean reservoir. *International Review of Hydrobiology* **2008**, *93*, 131-147.
15. Elçi, Ş. Effects of thermal stratification and mixing on reservoir water quality. *Limnology* **2008**, *9*, 135-142.
16. Sharip, Z. Stratification and water quality variations in three large tropical reservoirs. *International Journal of Ecology and Environmental Sciences* **2017**, *43*, 175-184.
17. Maingi, J.K.; Marsh, S.E. Quantifying hydrologic impacts following dam construction along the Tana River, Kenya. *Journal of Arid Environments* **2002**, *50*, 53-79.
18. Jiang, L.; Ban, X.; Wang, X.; Cai, X. Assessment of hydrologic alterations caused by the Three Gorges Dam in the middle and lower reaches of Yangtze River, China. *Water* **2014**, *6*, 1419-1434.
19. Caissie, D. The thermal regime of rivers: a review. *Freshwater biology* **2006**, *51*, 1389-1406.
20. Olden, J.D.; Naiman, R.J. Incorporating thermal regimes into environmental flows assessments: modifying dam operations to restore freshwater ecosystem integrity. *Freshwater Biology* **2010**, *55*, 86-107.
21. Zarfl, C.; Lumsdon, A.E.; Berlekamp, J.; Tydecks, L.; Tockner, K. A global boom in hydropower dam construction. *Aquatic Sciences* **2015**, *77*, 161-170.
22. Ouyang, W.; Hao, F.; Song, K.; Zhang, X. Cascade dam-induced hydrological disturbance and environmental impact in the upper stream of the Yellow River. *Water resources management* **2011**, *25*, 913-927.
23. Song, X.; Zhuang, Y.; Wang, X.; Li, E. Combined Effect of Danjiangkou Reservoir and Cascade Reservoirs on Hydrologic Regime Downstream. *Journal of Hydrologic Engineering* **2018**, *23*, 05018008.
24. Lauri, H.; Moel, H.d.; Ward, P.; Räsänen, T.; Keskinen, M.; Kummu, M. Future changes in Mekong River hydrology: impact of climate change and reservoir operation on discharge. **2012**.
25. Hocking, G.; Straškraba, M. An analysis of the effect of an upstream reservoir by means of a mathematical model of reservoir hydrodynamics. *Water Science and Technology* **1994**, *30*, 91-98.
26. Chen, G.; Fang, X.; Devkota, J. Understanding flow dynamics and density currents in a river-reservoir system under upstream reservoir releases. *Hydrological Sciences Journal* **2016**, *61*, 2411-2426.
27. Yonghui, Y.; Baiping, Z.; Xiaoding, M.; Peng, M. Large-scale hydroelectric projects and mountain development on the upper Yangtze river. *Mountain Research and Development* **2006**, *26*, 109-115.
28. Yin, Z.J.; Chen, J.; Xu, J.J. Application of multiple environmental flow methods to optimize cascade dams operation in the Lower Jinsha River. In Proceedings of Advanced Materials Research; pp. 3057-3064.
29. Duan, W.; Guo, S.; Wang, J.; Liu, D. Impact of cascaded reservoirs group on flow regime in the middle and lower reaches of the Yangtze River. *Water* **2016**, *8*, 218.
30. Xie, Q.; Liu, Z.; Fang, X.; Chen, Y.; Li, C.; MacIntyre, S. Understanding the temperature variations and thermal structure of a subtropical deep river-run reservoir before and after impoundment. *Water* **2017**, *9*, 603.

31. Cheng, F.; Li, W.; Castello, L.; Murphy, B.R.; Xie, S. Potential effects of dam cascade on fish: lessons from the Yangtze River. *Reviews in Fish Biology and Fisheries* **2015**, *25*, 569-585.
32. Ma, Q.; Li, R.; Feng, J.; Lu, J.; Zhou, Q. Cumulative effects of cascade hydropower stations on total dissolved gas supersaturation. *Environmental Science and Pollution Research* **2018**, *25*, 13536-13547.
33. Dai, S.; Lu, X. Sediment load change in the Yangtze River (Changjiang): a review. *Geomorphology* **2014**, *215*, 60-73.
34. Huang, X.-r.; Gao, L.-y.; Yang, P.-p.; Xi, Y.-y. Cumulative impact of dam constructions on streamflow and sediment regime in lower reaches of the Jinsha River, China. *Journal of Mountain Science* **2018**, *15*, 2752-2765.
35. Huang, Y.; Zhang, P.; Liu, D.; Yang, Z.; Ji, D. Nutrient spatial pattern of the upstream, mainstream and tributaries of the Three Gorges Reservoir in China. *Environmental monitoring and assessment* **2014**, *186*, 6833-6847.
36. Song, C.; Zhou, X.; Tang, W. Evaluation indicators for assessing the influence of reservoirs on downstream water temperature. *Advances in Water Science* **2012**, *23*, 419-426(in chinese).
37. Long, L.; Xu, H.; Ji, D.; Cui, Y.; Liu, D.; Song, L. Characteristic of the water temperature lag in Three Gorges Reservoir and its effect on the water temperature structure of tributaries. *Environmental Earth Sciences* **2016**, *75*, 1459.
38. Quinn, F.H. Hydraulic residence times for the Laurentian Great Lakes. *Journal of Great Lakes Research* **1992**, *18*, 22-28.
39. Cole, T.M.; Wells, S.A. CE-QUAL-W2: A two-dimensional, laterally averaged, hydrodynamic and water quality model, version 3.5. **2006**.
40. Kim, D.-K.; Zhang, W.; Watson, S.; Arhonditsis, G.B. A commentary on the modelling of the causal linkages among nutrient loading, harmful algal blooms, and hypoxia patterns in Lake Erie. *Journal of Great Lakes Research* **2014**, *40*, 117-129.
41. Kumar, S.; Godrej, A.; Grizzard, T. Extending Occoquan Reservoir Water Quality Model For Stakeholder Involvement. **2014**.
42. Gelda, R.K.; Owens, E.M.; Effler, S.W. Calibration, verification, and an application of a two-dimensional hydrothermal model [CE-QUAL-W2 (t)] for Cannonsville Reservoir. *Lake and Reservoir Management* **1998**, *14*, 186-196.
43. Kim, Y.; Kim, B. Application of a 2-dimensional water quality model (CE-QUAL-W2) to the turbidity interflow in a deep reservoir (Lake Soyang, Korea). *Lake and Reservoir Management* **2006**, *22*, 213-222.
44. Rangel‐Peraza, J.; Obregon, O.; Nelson, J.; Williams, G.; De Anda, J.; González‐Farías, F.; Miller, J. Modelling approach for characterizing thermal stratification and assessing water quality for a large tropical reservoir. *Lakes & Reservoirs: Research & Management* **2012**, *17*, 119-129.
45. Wang, S.; Zhang, X.; Liu, Z.; Wang, D. Trend analysis of precipitation in the Jinsha River Basin in China. *Journal of Hydrometeorology* **2013**, *14*, 290-303.
46. Li, D.; Lu, X.; Yang, X.; Chen, L.; Lin, L. Sediment load responses to climate variation and cascade reservoirs in the Yangtze River: A case study of the Jinsha River. *Geomorphology* **2018**, *322*, 41-52.
47. Olden, J.D.; Poff, N. Redundancy and the choice of hydrologic indices for characterizing streamflow regimes. *River Research and Applications* **2003**, *19*, 101-121.
48. Webb, B.; Walling, D. Long-term variability in the thermal impact of river impoundment and regulation. *Applied Geography* **1996**, *16*, 211-223.
49. Preece, R.M.; Jones, H.A. The effect of Keepit Dam on the temperature regime of the Namoi River, Australia. *River Research and Applications* **2002**, *18*, 397-414.

50. Jackson, H.; Gibbins, C.; Soulsby, C. Role of discharge and temperature variation in determining invertebrate community structure in a regulated river. *River Research and Applications* **2007**, *23*, 651-669.
51. Angilletta Jr, M.J.; Ashley Steel, E.; Bartz, K.K.; Kingsolver, J.G.; Scheuerell, M.D.; Beckman, B.R.; Crozier, L.G. Big dams and salmon evolution: changes in thermal regimes and their potential evolutionary consequences. *Evolutionary Applications* **2008**, *1*, 286-299.
52. Lessard, J.L.; Hayes, D.B. Effects of elevated water temperature on fish and macroinvertebrate communities below small dams. *River research and applications* **2003**, *19*, 721-732.
53. Deng, Y.; Li, J.; Li, K.; Li, R. Cumulative impact of cascade power stations on water temperature. *Advances in Water Science* **2008**, *19*, 273-297(in chinese).
54. Liu, L.; Chen, K.; Zhang, S. Study on cumu-lative effects of water temperature by cascade hydropower stations built on rivers. *Journal of China Institute of Wa-ter Resources and Hydropower Research* **2007**, *5*, 173-180(in chinese).
55. Hao, H.; Deng, Y.; Li, K.; Li, R.; Li, J. Study on water temperature cumulative effects of diversion type cascade development [J]. *Journal of Sichuan University (Engineering Science Edition)* **2009**, *41*, 29-34.
56. Zhang, S.; Yan, J.; Li, G. Cumulative effects of cascade development project adjustment on water temperature. *Journal of Hydraulic Engineering* **2014**, *45*, 1336-1343(in chinese).
57. Shi, W.; Chen, Q.; Yi, Q.; Yu, J.; Ji, Y.; Hu, L.; Chen, Y. Carbon emission from cascade reservoirs: Spatial heterogeneity and mechanisms. *Environmental science & technology* **2017**, *51*, 12175-12181.
58. Peng, Y.; Ji, C.; Gu, R. A multi-objective optimization model for coordinated regulation of flow and sediment in cascade reservoirs. *Water resources management* **2014**, *28*, 4019-4033.
59. Sabo, J.; Ruhi, A.; Holtgrieve, G.; Elliott, V.; Arias, M.; Ngor, P.B.; Räsänen, T.; Nam, S. Designing river flows to improve food security futures in the Lower Mekong Basin. *Science* **2017**, *358*, eaao1053.
60. Barbosa, F.; Padisák, J.; Espíndola, E.; Borics, G.; Rocha, O. The cascading reservoir continuum concept (CRCC) and its application to the river Tietê-basin, São Paulo State, Brazil. **1999**.
61. O'Reilly, C.M.; Sharma, S.; Gray, D.K.; Hampton, S.E.; Read, J.S.; Rowley, R.J.; Schneider, P.; Lenters, J.D.; McIntyre, P.B.; Kraemer, B.M. Rapid and highly variable warming of lake surface waters around the globe. *Geophysical Research Letters* **2015**, *42*, 10773-10781.
62. Arora, R.; Tockner, K.; Venohr, M. Changing river temperatures in northern Germany: trends and drivers of change. *Hydrological Processes* **2016**, *30*, 3084-3096.

Supplemental information for "Effect of cascading reservoirs on the flow variation and thermal regime in the lower reaches of the Jinsha River"

Data information

All data available to the present study, including station name, locations, measurement time and resolution are summarized in Table S1. From 1980 to 2015, annual mean precipitation and air temperature from 30 meteorological stations in the Jinsha River basin were provided by China Meteorological Science data sharing Service network (http://www.data.cma.cn/) (Table S2). The average annual precipitation in this basin was estimated as the mean values from these 30 stations. Average air temperature was estimated as the mean value measured at three stations (marked by an *) in table S2. These stations are located near the upper, middle and lower reaches of the reservoirs, respectively.

Table S1 Summary of hydrological and meteorological data used in this study (see Fig. 1 for locations of the measurement stations, all data resolution: daily mean)

Station	Description	Data type	Record period
HTGS	Huatan gauging station	Water temperature	2000-2015
	235.1 km upstream of XLD Dam	Flow rate	1980-2015
XLDGS	XLD gauging station	Water temperature	2014-2015
	2.9 km downstream of XLD Dam	Outflow rate	2014-2016
PSGS	Pingshan gauging station	Water temperature	2000-2011
	29.1 km upstream of XJB Dam	Flow rate	1980-2011
XJBGS	XJB gauging station	Water temperature	2012-2015
	2.4 km downstream to XJB Dam	Outflow rate	2012-2016
SJWS	Suijiang city, middle of XJB reservoir	Air temperature, wind speed, precipitation, cloud cover	2014-2015
YSWS	Yongshan city, near to XLD dam	Air temperature, wind speed, precipitation, cloud cover	2014-2015

Table S2 List of the meteorological stations used in the Jinsha Basin

Station ID	Station name	Longitude (8E)	Latitude (8N)
	Jinsha River		
52908	Wudaoliang	93.08	35.22
56004	Tuotuohe	92.43	34.21
56021	Qumalai	95.78	34.13
56029	Yushu	97.01	33.01
56144	Dege	98.57	31.73
56247	Batang	99.01	30
56443	Xiangcheng	99.08	28.93
56543	Xianggelila	99.7	27.83
56487	Meigu	103.31	28.03
56565	Yanyuan	101.52	27.43
56578	Ningnan	102.75	27.07

56651	Lijiang	100.21	26.86
56664	Huaping	101.26	26.63
56675	Huidong	102.58	26.65
56684	Huize*	103.28	26.41
56752	Binchuan	100.57	25.83
56763	Yuanmou	101.87	25.73
56768	Chuxiong	101.53	25.02
56778	Kunming	102.68	25.02
56586	Zhaotong*	103.71	27.35
56596	Weixin	105.01	27.85
56492	Yibin*	104.06	28.08
	Yalong River (main tributary of Jinsha River)		
56034	Qingshuihe	97.13	33.8
56038	Shiqu	98.1	32.98
56146	Ganzi	100	31.62
56167	Daofu	101.12	30.98
56267	Yajiang	101.02	30.03
56462	Jiulong	101.5	29
56474	Mianning	102.02	28.55
56571	Xichang	102.27	27.9

Note: 1.the Yalong River is largest tributary of the Jinsha River.

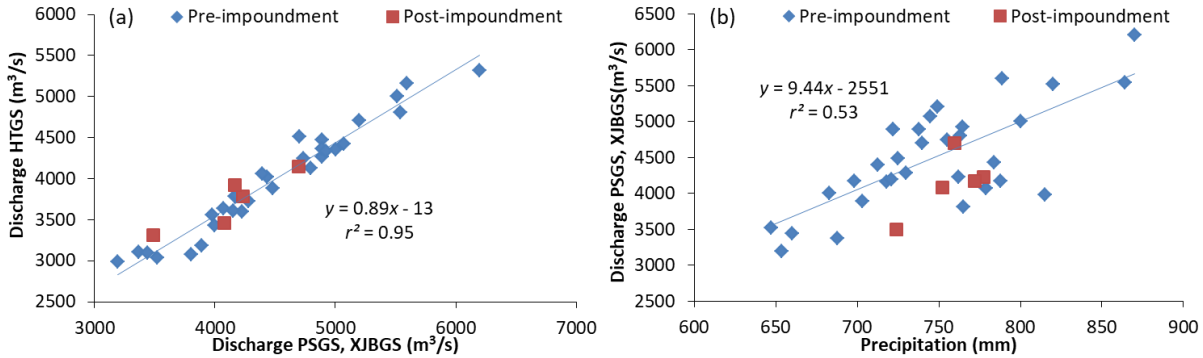

Fig. S1: (a) Discharge measures at PSGS in 1980-2011 and XJBGS in 2012-2016 (x-axis) and HTGS in 1980-2016 (y-axis); b) Correlation between annual mean precipitation in Jinsha Basin and discharge at the downstream gauging station (PSGS, 1980-2011; XJBGS, 2012-2016). Solid blue lines in both panels show linear regression for the pre-impoundment period according to the equations shown as labels.

Model description

Model grid generalization

According to the principle of grid division, the bathymetry of XJB reservoir was formed as single main branch with 149 segments along a longitudinal axis and 118 vertical layers, each 1m deep (Fig. S.2). Each segment is approximately 1 km long. Similarly, the bathymetry of XLD reservoir is composed of 159 longitudinal segments and 121 vertical layers. The length of the longitudinal grid cell varied between 50 and 4000 m, and the vertical

cell size was set to 2 m. The top elevation of the reservoir was 384 m in XJB and 614 m in XLD reservoir. The minimum time-step was 0.5 s and the maximum time-step was 3600 s. Approximately 2-3 hours of runtime was needed by a Pentium PC for the simulation period of 1 year.

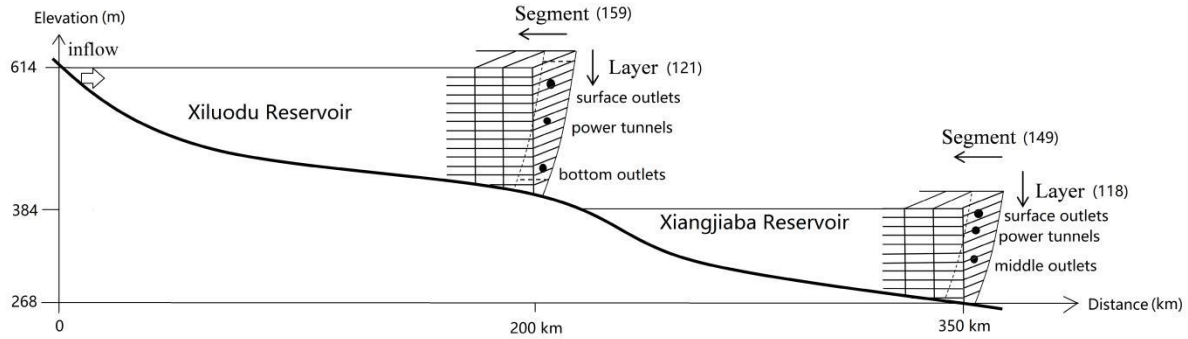

Fig. S2: Grid geometry of the representation of XLD and XJB reservoir in the CE-QUAL-W2 model.

Initial conditions

The initial conditions required in CE-QUAL-W2 model include inflow, outflow, flow velocity, and water temperature. The inflow conditions include upstream flow, water temperature and outflow, are the discharges at the dams. The initial water temperature was set to 15 ℃, and the flow velocity to zero. The sediment temperature is set to 15.5 ℃ that is the local annual mean temperature.

Boundary conditions

Meteorological conditions (wind speed, air temperature) are shown in Fig. S3. Inflow, outflow from different position and water level in both reservoirs from 2014 to 2015 are shown in Fig. S4.

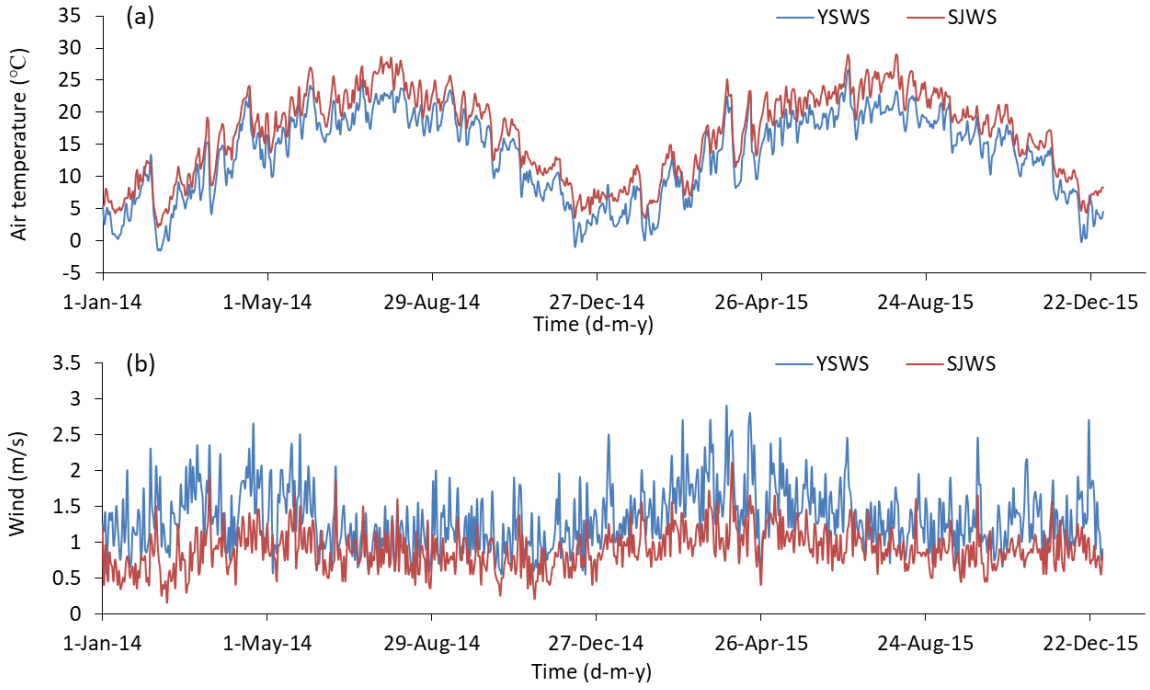

Fig. S3: (a) Daily mean air temperature and (b) wind speed at SJWS and YSWS meteorological station (representative for XLD and XJB reservoir, respectively).

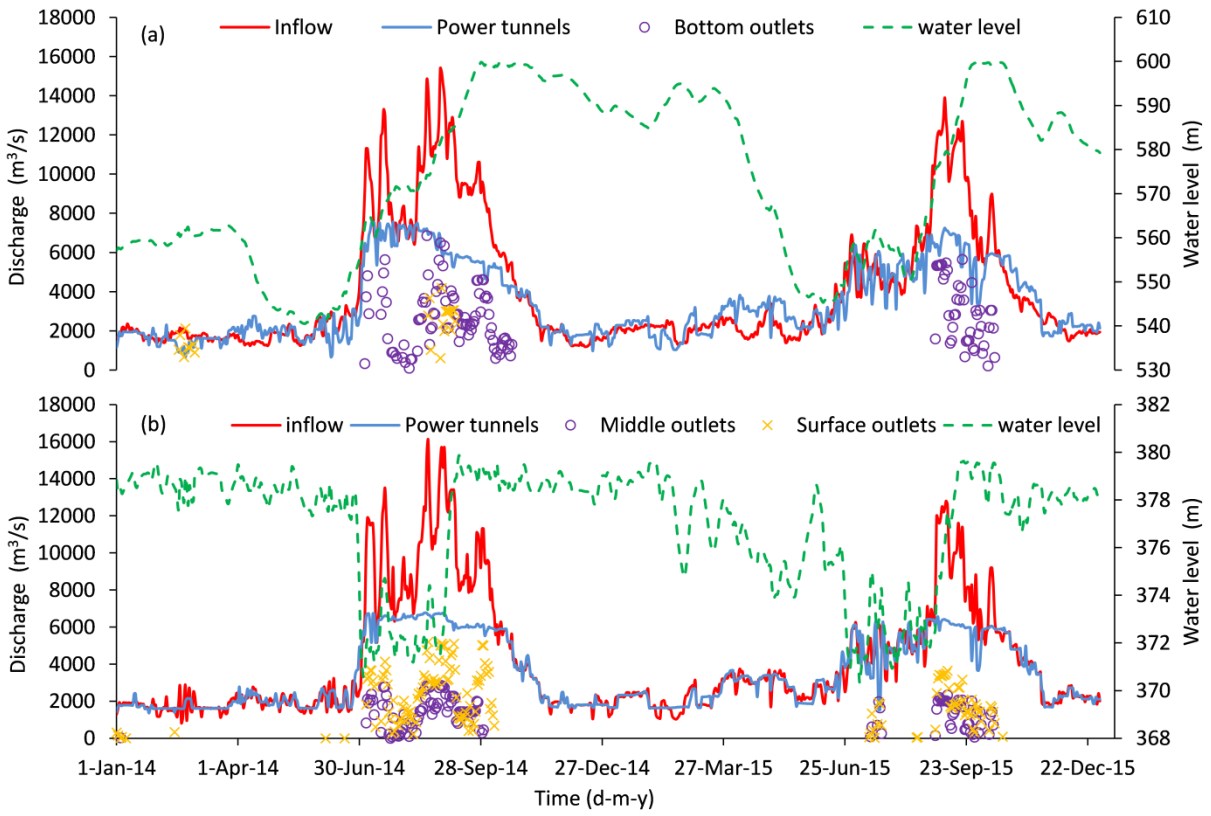

Fig. S4: Measured inflow, outflow, and water level in XLD reservoir (a) and XJB reservoir (b) in 2014-2015. The outflows through the hydroelectric station, bottom hole and spillways as well as water level elevation in front of dam are denoted by different color (see legend)

Calibration

Model performance was evaluated as the mean absolute error (MAE) and the root mean square error (RMSE):

$$\mathrm{MAE} = \frac{\sum|\mathrm{Simulated}-\mathrm{Observed}|}{\text{number of observations}} \qquad \text{Eq. (S.1)}$$

$$\mathrm{RMSE} = \sqrt{\frac{\sum_{i=1}^{n}(\mathrm{Simulated}-\mathrm{Observed})^2}{\text{number of observations}}} \qquad \text{Eq. (S.2)}$$

The water balance during the simulation was validated by comparing predicted elevation with observed elevation (Fig. S5), which had MAE and RMSE of less than 0.1 m. The results show that the bathymetry is correct and the inflow and outflow data are accurate.

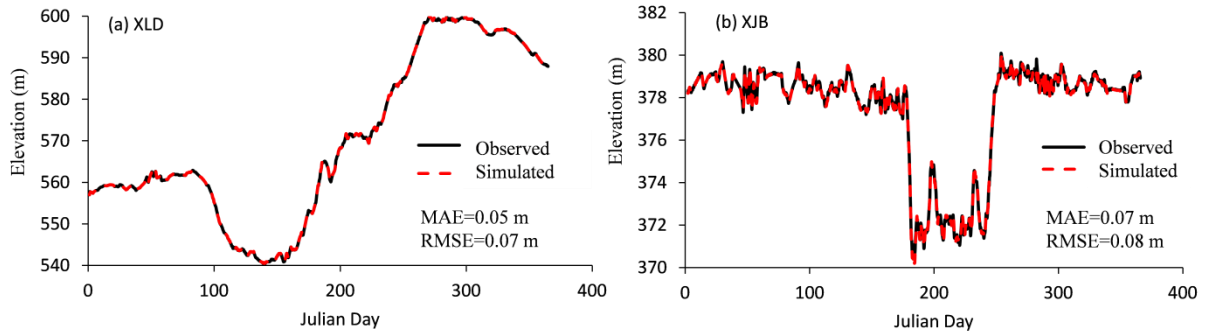

Fig. S5: Observed and simulated water level in front of XLD (a) and XJB (b) dam (MAE: Mean Absolute Error; RMSE: Root Mean Square Error; Start time, 01/01/2014)

Through sensitivity analysis of hydrodynamic model parameters, we found that the most sensitive parameter on temperature is the wind sheltering coefficient (WSC) in XJB reservoir, next dynamic shading (DYNSH) and the light extinction coefficient (EXH2O). In XLD reservoir, temperature predictions were most sensitive to the DYNSH, then the WSC and AZC. The calibrated parameter values for both reservoirs were obtained by repeatedly adjusting the value of the parameters until the best match between predicted and observed temperatures was obtained for (Table S3).

The calibration of the CE-QUAL-W2 model focused on the simulated temperature profiles at six monitoring points at which temperature profiles were measured in 2014 (Fig. S6). These points represent the upper, middle and lower reaches of both reservoirs, respectively. The average MAE of all 9 measured profiles in XLD and XJB reservoirs were 0.36 ℃, 0.52 ℃, respectively. The average RMSE in these two reservoirs were 0.46 ℃, 0.63 ℃, respectively. Comparing the performance of CE-QUAL-W2 model in other reservoirs (Kim and Kim 2006, Smith et al. 2012) (MAE ≥ 0.8 ℃; RMSE ≥ 1.2 ℃), the model performed well in simulating the water temperature stratification. The MAEs of April were higher in initial stratification (Fig.8). In XJB reservoir, as can be seen from Fig.14a, the thermal regime at P1 exhibits two thermoclines in April and disappeared in summer and in winter. In XLD reservoir, Fig.14b illustrates the model's ability to produce the thermocline development in April, the strong thermocline present in August, and the mixing in December. The mean errors in model predictions in the two reservoirs are within 0.5 ℃, most of them are much less, indicating that the model parameters are set reasonably.

Table S3 Main hydraulic coefficients in different reservoirs

Variable name	Description	Values in XJB reservoir	Values in XLD reservoir
[AZC]	Vertical Turbulence Algorithm	THE	W2
[EXH2O]	Water Extinction Coefficients [m^{-1}]	0.35	0.45
[WSC]	Wind Sheltering Coefficient	0.7	0.7
[DYNSH]	Dynamic Shading or Static Shading	0.7	0.9
[TSED]	Sediment Temperature [℃]	17.2	17.2

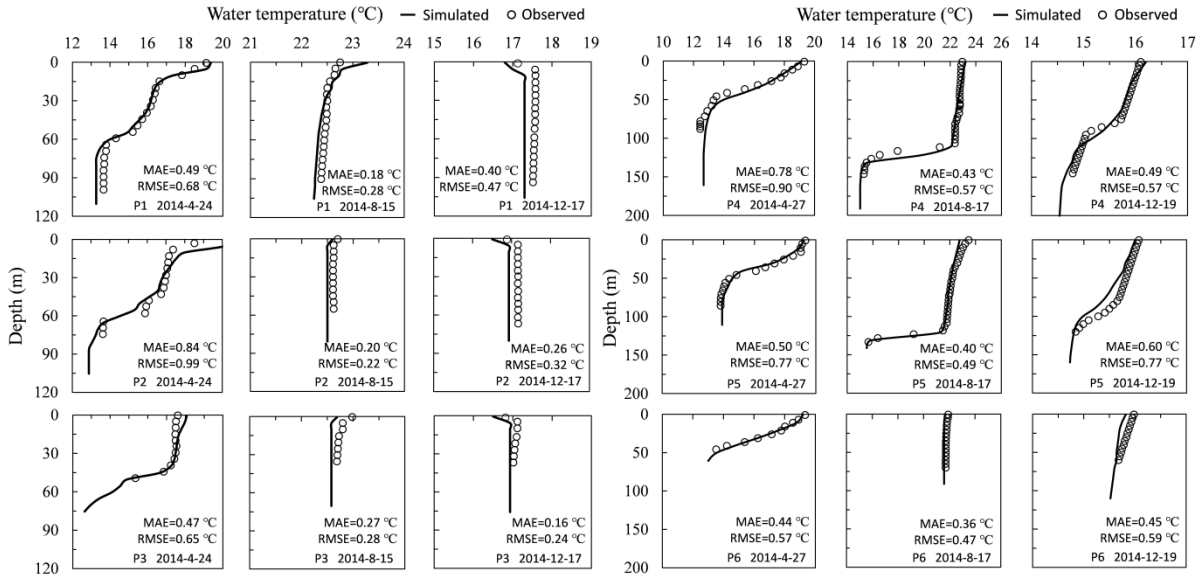

Fig. S6: Simulated and observed vertical temperature profiles in XJB reservoir (left) and XLD reservoir (right) (cf. Fig. 1).

Appendix II

Density Driven Water Circulation in a typical tributary of the Three Gorges Reservoir, China

Lianghong Long [1], Daobin Ji [2*], Zhengjian Yang [2*], Scott A. Wells [4], Jun Ma [3], Defu Liu [3]

[1] *Institute for Environmental Sciences, University of Koblenz-Landau, 76829 Landau, Germany*

[2] *College of Hydraulic & Environmental Engineering, China Three Gorges University, 443002 Yichang, China*

[3] *College of Resources and Environment Sciences, Hubei University of Technology, 430068 Wuhan, China*

[4] *Department of Civil and Environmental Engineering, Portland State University, OR 97207-0751, Portland, USA*

***** Correspondence: dbji01101@ctgu.edu.cn (Daobin Ji);

20141031@hbut.edu.cn (Zhengjian Yang)

Please click the following link to read the publication

https://onlinelibrary.wiley.com/doi/abs/10.1002/rra.3459

https://doi: 10.1002/rra/3459

RESEARCH ARTICLE **WILEY**

Density-Driven Water Circulation in a Typical Tributary of the Three Gorges Reservoir, China

Lianghong Long [1], Daobin Ji [2*], Zhengjian Yang [2*], Jun Ma [3], Scott A. Wells [4], Defu Liu [3], Andreas Lorke [1]

[1] *Institute for Environmental Sciences, University of Koblenz-Landau, 76829 Landau, Germany*
[2] *College of Hydraulic & Environmental Engineering, China Three Gorges University, Yichang, 443002, China*
[3]College of Resources and Environment Sciences, Hubei University of Technology, Wuhan, 430068, China
[4] *Department of Civil and Environmental Engineering, Portland State University, Portland, OR 97207-0751, USA*
∗ Corresponding author at: College of Hydraulic & Environmental Engineering, China Three Gorges University, Yichang, 443002, China
* E-mail addresses: dbji01101@ctgu.edu.cn (Daobin Ji): 20141031@hbut.edu.cn (Zhengjian Yang)

Abstract: A 2-D hydrodynamic model was developed for modeling water circulation from 2008-2011 in a typical tributary of the Three Gorges Reservoir. The model is capable of describing flow behavior and mixing mechanisms for different density current patterns and performs well in computing the velocity, the intrusion layer at the plunge point, and the travel distance of the density current. The effects of 10 flow patterns on thermal stratification, hydrodynamics, and algal bloom risk are discussed and classified in terms of algal growth. Patterns (6) and (10) can effectively prevent algal blooms; patterns (7) and (8) are good for algal blooms. More frequent transformations of flow-driven patterns, as observed in 2010-2011, could create more eddies and mixing and thus reduce bloom risk. Further studies are necessary and recommended for more accurate predictions and assessing the impact of water level fluctuations on transform flow patterns and water quality.

Keywords: Three Gorges Reservoir; Density currents; Thermal stratification; Algal blooms; CE-QUAL-W2

1 Introduction

Hydrodynamic processes significantly affect the water quality and bioproductivity of reservoirs. These processes ultimately provide the conditions for the ecosystem to function (Dubnyak and Timchenko 2000). In estuaries, freshwater inflows produce net seaward transport, whereas tides lead to periodic seaward and landward transport. Hence, different types of flow patterns exist under the interactions of river flow, tidal currents, and basin morphology, affecting the species compositions and distributions of flora and fauna (Mao et al. 2004; Ji et al. 2007). Flow patterns are also evident in reservoirs, and their modes of circulation can be defined by the interaction of reservoir morphometry with inflows. In analyzing hydrodynamic processes, ecological characteristics and water quality dynamics, transport time scales such as residence time are often used to characterize transport processes in a water body. These time scales help to explain how some water quality parameters (such as dissolved oxygen and

chlorophyll-a concentrations) vary (Chen 2007). A 'reservoir' or 'lake' with a long residence time and a stratified water column is more likely to host anoxic conditions at the bottom than a lake with a short residence time and a well-mixed water column. Mixing in lakes, reservoirs, estuaries, coastal and offshore marine waters occurs through several mechanisms, including wind-induced turbulence, convective mixing, and mixing due to inflows/outflows (Martin and McCutcheon 1998; Imboden and Wüest 1995). During a mixing event, nutrients can be mixed to the upper portion of the water column, where they can fuel algal blooms (Lawson and Anderson 2007).

The Three Gorges Reservoir (TGR) is a very large reservoir that was impounded in June 2003. There are forty tributaries comprising a watershed area of more than 100 km^2 (Zhang et al. 2008). Eutrophication and algal blooms appeared in some tributary arms as the reservoir was filled (Fu et al. 2010; Ye et al. 2007). It is known that the tributary bays have much greater thermal stratification than does the mainstream. Since the minimum flow rate of the TGR is higher than 5500 m^3/s, the high flow rate causes strong vertical disturbance and mixing intensity in the TGR mainstream so that vertical differences in water temperature and stratification are reduced (Ji et al. 2013). As a result, the water density profiles of the TGR mainstream and those of tributary bays would be different from the mainstream TGR (Ji et al. 2010a; Yang et al. 2010). Water from the TGR mainstream intrudes into the side arms as a density current (Yang et al. 2010; Ji et al. 2010a).

Since the upstream inflow water temperature is often higher or lower than the water at the ends of the side arms, surface and bottom density currents are induced. Based on the water temperature difference between the mainstream and bay, overflow, upper-interflow, interflow, lower-interflow, and underflow intrusions will occur. Two types of downward density currents caused by upstream inflows and five types of intrusion gravity flows have been identified, which drive complex water circulation and vertical mixing processes in the tributary side arms (Ji et al. 2013). These density currents have a strong influence on the tributary water quality. Ecological simulation models have been used to predict these circulation processes and their resultant impact on water quality (Tufford and McKellar 1999). 2-D models are used broadly in different kinds of water bodies all over the world. The main advantages of 2-D models are that much finer resolution can be achieved in the longitudinal and vertical directions and numerical dispersion can be better controlled than in comparable 3-D models. 2-D models are also computationally less expensive than 3-D models and are better able to provide simulations over longer time scales (e.g., seasons) (Kurup et al. 2000; Davies and Gerritsen 1994).

In this study, a 2-D hydrodynamic model is adopted to (1) model the density currents in Xiangxi River (XXR), a typical tributary arm of the TGR; (2) identify and classify density-driven circulation; (3) characterize the hydrodynamics, temperature distribution and vertical mixing responses of tributary circulation; and (4) discuss the environmental impacts on thermal structure, nutrient distribution and algal bloom risk and provide suggestions for reservoir operations.

2 Study Area

The Three Gorges Dam (TGD) is located in the mainstream of the Yangtze River (China). Construction of the TGD formed a giant subtropical reservoir (Three Gorges Reservoir, TGR) that is one of the largest artificial lakes in the world, with a capacity of 3.93×10^{10} m^3, water level of 175 m ASL, surface area of 1080 km^2 and watershed area of over 1.00×10^6 km^2 (Huang et al. 2006; Xu et al. 2011). The XXR (Yang et al. 2013), the largest tributary in the lower reach of the TGR (32 km from the Three Gorges Dam), can be considered as a representative of most eutrophic side arms of the TGR. It encompasses a watershed area of 3,095 km^2 and has an annual average flow of 47.4 m^3/s. It extends from 110°25′ E to 111°06′ E to 30°57′ N to 31°34′ N (Fig. 1). A deep riverine bay was formed as the lower 24 km were submerged by backwater after the initial filling of the TGR in June 2003 to a water level

of 135 m. The backwater reach extended upstream approximately 40 km when the TGR was filled to a normal water level (175 m).

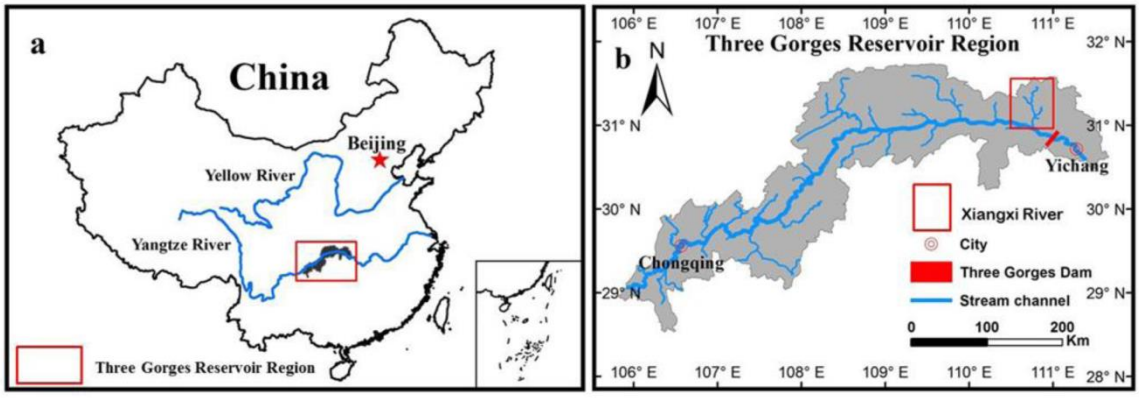

Fig. 1 (a) Location of the Three Gorges Reservoir (TGR) in China; (b) Location of Xiangxi Bay in the TGR, outlined in red

3 Model descriptions

The CE-QUAL-W2 model is a two-dimensional, laterally averaged, hydrodynamic and water quality model. Based on applications for more than 400 different water bodies (rivers, reservoirs, lakes, slough and estuaries) and under a wide variety of conditions, the model can accurately simulate water temperature, hydrodynamics and water quality (Berger and Wells 2008; Bowen and Hieronymus 2003; Martin 1988; Lung and Nice 2007; Chung and Gu 1998; Ma et al. 2015). The CE-QUAL-W2 model was selected for this study because it can well-reproduce the dominant density currents in the side arms of the TGR. Currents induced by density effects are simulated in the model by solving the equation of state, which relates density to the temperature and concentration of dissolved substances.

The XXR has a length-to-width ratio of approximately 400, making it appropriate for the application of the laterally averaged CE-QUAL-W2 model. A computational grid of the XXR was developed based on bathymetric and geometric data for the reservoir. The XXR was represented by 64 longitudinal segments between 500 and 1000 m in length and 109 vertical layers of 1-m thickness. Model widths ranged from 20 to 1300 m. The accuracy of the bathymetry data was confirmed by comparing the observed and simulated storage water elevation curves. The time period from January 1, 2008-December 31, 2011 was chosen as the simulation period. Variable time steps were used in the simulations, which are a fraction of the maximum time step calculated from the numerical stability criterion with an auto-stepping algorithm. The boundary and initial conditions, as well as the model calibration and validation, are shown in the appendix.

4 Results and discussion

4.1 Classifications and analyses of flow patterns in the XXR

Existing monitoring and analysis (Ji et al. 2010a; Yang et al. 2013; Yang et al. 2010) have shown the occurrence of density currents at the confluences of the TGR mainstream and side arms due to the combined effects of differences in temperature and suspended solids in the inflows to the XXR and temperature differences between the XXR and the TGR mainstream. As shown in Fig. 2, two kinds of downward density currents caused by upstream inflows and five kinds of intrusion gravity flows can occur in the side arms of TGR.

Ten major flow patterns were distinguished. Representative longitudinal/vertical profiles of flow patterns with

temperature and flow field with vertical mixing intensity distributions were selected from a four-year modeling period (2008-2011) in the XXR to characterize the density-driven circulations. The ten circulations are sketched in Fig. 2. Representative flow patterns simulated by the model are shown in Fig. 3 (patterns (1)-(5) and Fig. 4 (patterns (6)-(10)).

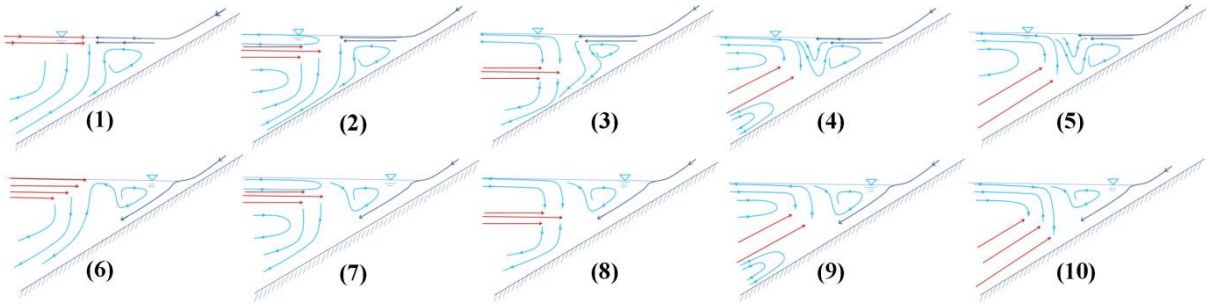

Fig. 2 Schematic graph of ten flow patterns driven by two upstream inflows and five mainstream intrusions

Note: (1) Upstream: Overflow, Mainstream: Overflow; (2) Upstream: Overflow, Mainstream: Upper-Interflow; (3) Upstream: Overflow, Mainstream: Middle-Interflow; (4) Upstream: Overflow, Mainstream: Lower-Interflow; (5) Upstream: Overflow, Mainstream: Underflow; (6) Upstream: Underflow, Mainstream: Overflow; (7) Upstream: Underflow, Mainstream: Upper-Interflow; (8) Upstream: Underflow, Mainstream: Middle-Interflow; (9) Upstream: Underflow, Mainstream: Lower-Interflow; (10) Upstream: Underflow, Mainstream: Underflow.

（1）Upstream: Overflow, Mainstream: Overflow

As Fig. 3(A), (B) shows, water of the TGR mainstream flowed into the XXR through the surface layer, while upstream runoff also entered the surface layer at the end of the XXR. Since momentum is conserved, water below the mainstream intrusion would flow toward the mouth of the XXR, forming a large, clockwise circulation at the lower reach. A small counterclockwise circulation would occur at the end of the XXR. Because the overflows collide, the middle reach often has a longer residence time, with more local eddies and mixing (Fig. 3(B)). However, the location and intensity of mixing depended on the relative magnitudes of the two surface overflows.

（2）Upstream: Overflow, Mainstream: Upper-Interflow

As shown in Fig. 3(C), (D), the TGR mainstream water intruded into the XXR at depths of 3.0-30.0 m and 9.0-38.0 m, respectively. The upstream runoff flowed as surface layer inflow at the end of the XXR. Water below the intrusion layer was forced to flow toward the mouth of the XXR, leading to a large, clockwise circulation, wherein water above the intruding water flowed toward the mouth of the XXR to form a weak, thin, counterclockwise circulation (Fig. 3(C), (D)). When the upstream surface overflow was small enough and located away from the lower counterclockwise circulation, the subsurface water experienced weak vertical mixing such that it warmed quickly (Fig. 3(D)).

（3）Upstream: Overflow, Mainstream: Middle-Interflow

In Fig. 3(E), (F), the upstream runoff still flowed into the surface layer at the end of the XXR, but the TGR mainstream water intruded into the XXR from the middle layer at depths of 14.3-53.3 m and 9.4-46.4 m. The water layer below the intruding water formed a clockwise circulation, and the water layer above the intruding water flowed downward to cause a weak, counterclockwise circulation (Fig. 3(E), (F)). Local eddies and vertical mixing tended to occur in the deep layer, and the surface water was relatively stable.

（4）Upstream: Overflow, Mainstream: Lower-Interflow

As shown in Fig. 3(G), (H), the upstream runoff still flowed through the surface layer of the XXR despite relatively low inflow rates of 23.1 m^3/s and 20.7 m^3/s, and the TGR mainstream water intruded into the XXR from

the middle-lower layer at depths of 27.4-76.4 m and 38.1-83.1 m. The intruding water flowed toward the mouth of the XXR, leading to a counterclockwise circulation (Fig. 3(G), (H)). On Feb. 6, 2009, a large, counterclockwise circulation originated from the mouth of the XXR and rose up to the surface in the middle reach, and then flowed back through the surface (Fig. 3(H)). In this pattern, the counterclockwise circulation could decrease the water residence time in the areas it influenced, even up to the water surface. Strong vertical mixing and large-scale eddies could occur in the upper reach of the XXR, which is unfavorable to water temperature stratification.

（5）Upstream: Overflow, Mainstream: Underflow

In Fig. 3(I), (J), the upstream runoff still flowed into the surface layer at the end of the XXR. The TGR mainstream water intruded into the XXR through the bottom layer. This formed a counterclockwise circulation in the lower reach (Fig. 3(I)). During the development of the mainstream intruding underflow, an eddy formed in front of the underflow (Fig. 3(J)), and a small, counterclockwise circulation formed at the end of the XXR (Fig. 3(J)). In this flow pattern, the downstream underflow increased the lower layer velocity and the upstream overflow surface velocity at the end of the XXR, resulting in more rapid water exchange and mixing (Fig. 3(I), (J)).

（6）Upstream: Underflow, Mainstream: Overflow

The upstream runoff flowed through the bottom of the XXR, and the TGR mainstream water intruded into the XXR through the surface layer at the mouth of the XXR to cause a large, clockwise circulation in the lower reach. In this pattern, both downstream overflow and upstream underflow would increase water velocity, causing more flow movement (Fig. 4(A), (B)). The large-scale eddies and mixing led to rapid breaking of the temperature stratification (Fig. 4(A), (B)).

（7）Upstream: Underflow, Mainstream: Upper-Interflow

As shown in Fig. 4(C), (D), the TGR mainstream water intruded into the XXR at depths of 3.8-29.8 m and 23.0-28.0 m, and the upstream runoff flowed into the XXR as an underflow. Water below the intrusion formed a large, clockwise circulation, and subsurface water flowed slowly toward the mouth of the XXR driven by a thin, counterclockwise circulation (Fig. (D)). A large, clockwise circulation was evident in the deeper layer of the XXR. The upstream underflow merged with the submerged, clockwise circulation in the lower reach, accelerating the movement of water near the bottom (Fig. 4(C), (D)). In this flow pattern, the surface layer was approximately 5 m deep and tended to be stagnant with a longer residence time, which is good for surface stratification (Fig. 4(C), (D)).

（8）Upstream: Underflow, Mainstream: Middle-Interflow

As shown in Fig. 4(E), (F), the upstream runoff flowed along the bottom of the XXR. The TGR mainstream water intruded into the XXR from the middle layer at depths of 21.1-55.1 m and 20.9-54.9 m. Water above the intruding water flowed toward the mouth of the XXR to form a counterclockwise circulation (Fig. 4(E), (F)). The momentum of the TGR mainstream intrusion was more likely to be balanced by upstream underflow, causing a large, clockwise circulation originating from the mouth of the XXR and rising up to the subsurface of the upper reach, enclosing the upstream underflow (Fig. 4(E)). Eddies in the middle reach were created when the TGR mainstream intrusion encountered the upstream underflow (Fig. 4(F)). Similar to pattern (7), surface stratification was observed (Fig. 4(E), (F)).

（9）Upstream: Underflow, Mainstream: Lower-Interflow

The upstream runoff flowed along the bottom of the XXR, and the TGR mainstream water intruded into the XXR from the middle-lower layer at depths of 20.3-68.3 m and 36.9-85.9 m (Fig. 4(G), (H)). Water above the intruding water flowed toward the mouth of the XXR, forming a counterclockwise circulation. In this pattern, a large, counterclockwise circulation originated from the mouth of the XXR, rising to the surface of the upper reach.

As a result, there was no temperature difference in the deep water (Fig. 4(G)). On October 7, 2011, upstream inflows were so large that some of the intrusion water joined the bottom underflow and flowed out of the XXR (Fig. 4(H)). Strong circulation and mixing caused a much shorter water retention time in the XXR.

（10）Upstream: Underflow, Mainstream: Underflow

As shown in Fig. 4(I), (J), the upstream runoff flowed along the bottom of the XXR, and the TGR mainstream water intruded in the XXR near the bottom. The TGR mainstream underflow intruded and caused a counterclockwise circulation within the middle-lower reach. In these cases, upstream underflows would meet the TGR mainstream intrusion water and flow toward the bay (Fig. 4(I), (J)). A local clockwise circulation was generated in the upper reach of the XXR, with more local eddies and mixing, such as on October 24, 2011 (Fig. 4(J)).

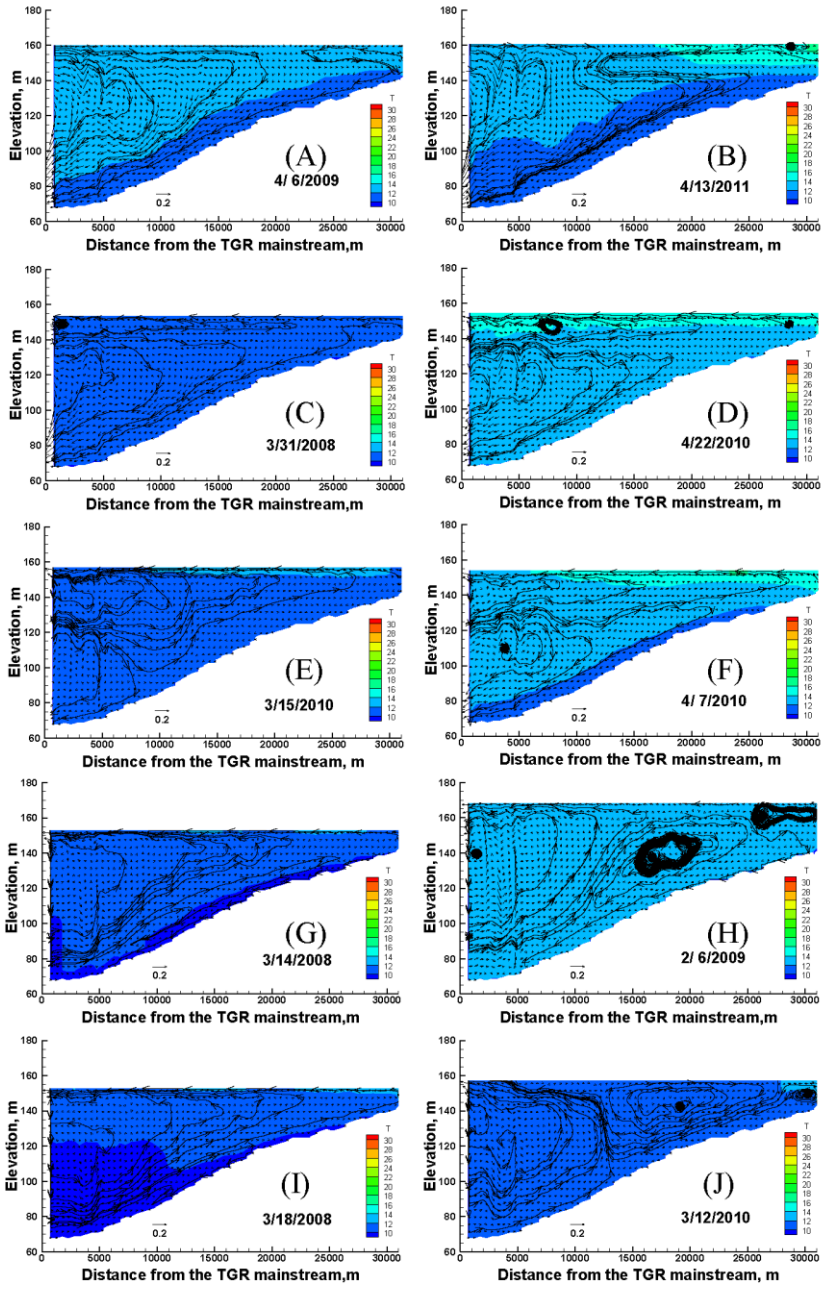

Fig. 3 Representative flow patterns driven by Upstream: Overflow; Mainstream: Overflow**,** Upper-Interflow, Middle-Interflow, Middle-Interflow, Underflow, respectively

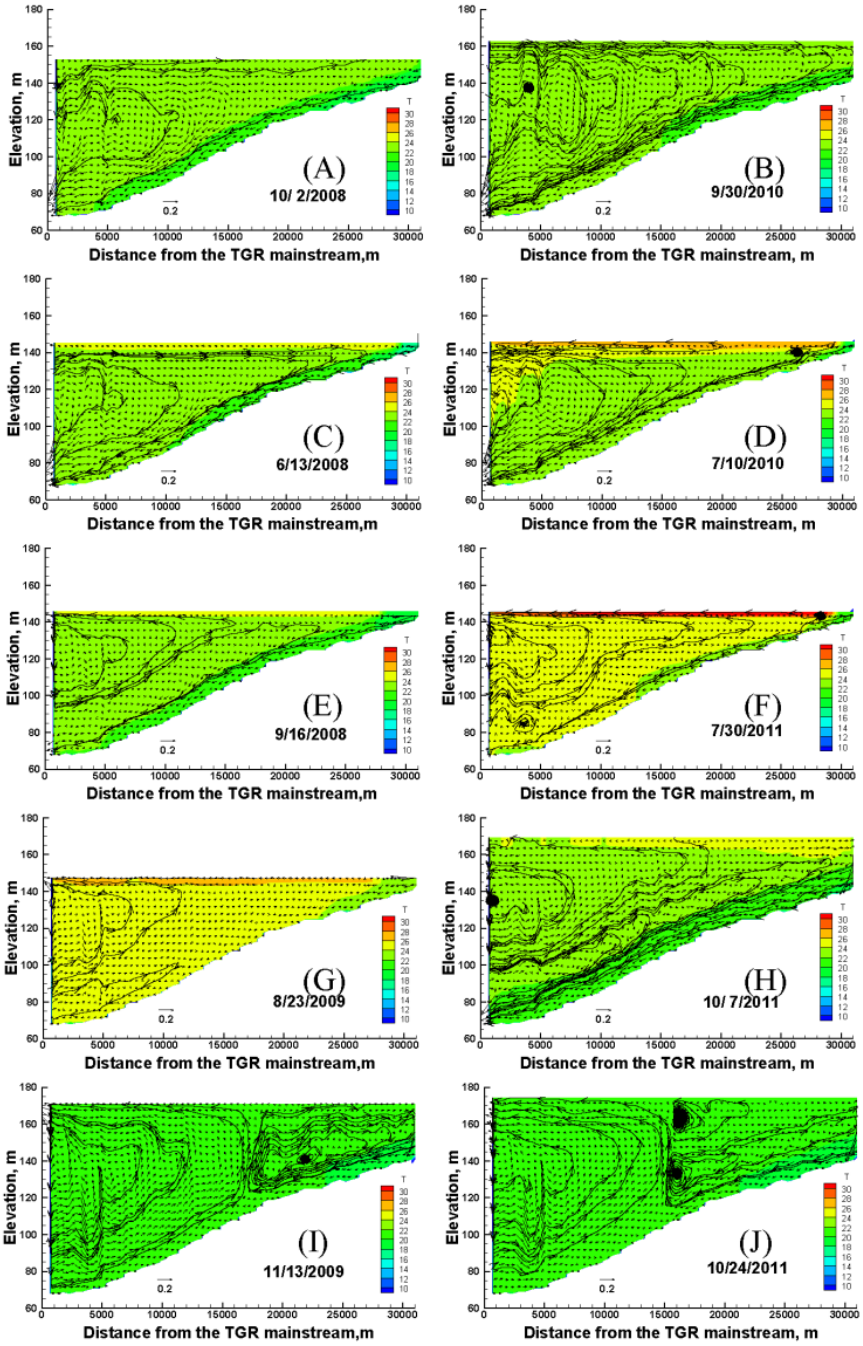

Fig. 4 Representative circulations driven by Upstream: Underflow; Mainstream: Overflow**,** Upper−Interflow, Middle-Interflow, Lower-Interflow, Underflow, respectively

4.2 Categorization of water circulation by algal growth

4.2.1 Water circulation that inhibits algal blooms

During most of the year, as shown in Fig. 5, inflows of the XXR originate from the Shennongjia forest, which has much lower water temperatures than the XXR (Ji et al. 2010a). At the same time, runoff will be stored in the upstream cascade reservoirs to generate electricity, so the colder inflows from the outlets will enter the XXR and plunge to the bottom, forming an underflow. At this point, if the TGR mainstream water intrudes through the surface at the mouth of the XXR (Fig. 4(A), (B), Table 1 pattern (6)), a large, clockwise circulation will occur in

Table 1. Impacts of ten flow patterns on temperature, nutrients, and algal blooms

Pattern		-1	-2	-3	-4	-5	-6	-7	-8	-9	-10
Months witnessed		**1,4**	**1,2-4,6**	**2-4**	**3,8**	**2,3**	**1,4-10,12**	**1-9,11,12**	**1,2,4-12**	**2,3,6-12**	**1-3,7-11**
Temperature	Stratified in the upper reach	√	√	√				√	√		
	Unstratified in the upper reach				√	√	√			√	√
	Stratified in the lower reach		√	√				√	√		
	Unstratified in the lower reach	√			√	√	√			√	√
Nutrient replenishment	to surface of the upper reach	√	√	√	√	√					
	to underwater of the upper reach						√	√	√	√	√
	to surface of the lower reach	√			√	√	√			√	√
	to underwater of the lower reach		√	√	√	√		√	√	√	√
Algal	Increase in the upper reach	√	√	√				√	√	√	
	Decrease in the upper reach				√	√	√				√
	Increase in the lower reach		√	√				√	√		
	Decrease in the lower reach	√			√	√	√			√	√

Note: classification of patterns and schematic diagram are shown in Fig. 2.

the entire XXR. This increases the velocity at the surface and then decreases the water residence time rapidly, with numerous large eddies intensifying the vertical mixing (Fig. 4(A), (B)). As a result, the thermal stratification of the entire XXR would be rapidly broken down by the disturbance, and algal blooms at the surface would be inhibited (Table 1). This pattern was most common at the ends of flood storage periods, which explained why autumn algal blooms disappeared as the water level increased at the end of flood season (Yang et al. 2010; Ji et al. 2010b). On the other hand, if the TGR mainstream water at this time intrudes through the bottom at the mouth of the XXR to form a large, counterclockwise circulation that exchanges the upper layer water, the upper layer water residence time would decrease. If the power of the upstream underflow is lower than that of the mainstream intrusion, the upstream underflows will be lifted to push the upper layer water to the end of the XXR and facilitate a complete exchange (pattern (10)). In this flow pattern, the vertical mixing in most parts of the XXR was very large, weakening the thermal stratification (Fig. 4(I), (J), Table 1). This pattern of inhibiting algal blooms often occurs in the long period after impoundment, which is why thermal stratification in the XXR continued to weaken, due to strong mixing (Yang et al. 2010; Liu et al. 2012).

Additionally, upstream inflows moved through the surface layer at the end of the XXR and progressed downstream, and ultimately merged with the counterclockwise circulation in the upper layer that was caused by the lower-interflow and underflow from the TGR mainstream (patterns (4), (5)). This could also greatly increase surface velocity and shorten the surface water residence time, even triggering eddies that would increase the intensity of surface mixing. The subsurface thermal stratification would then be broken, further inhibiting algal blooms (Table 1).

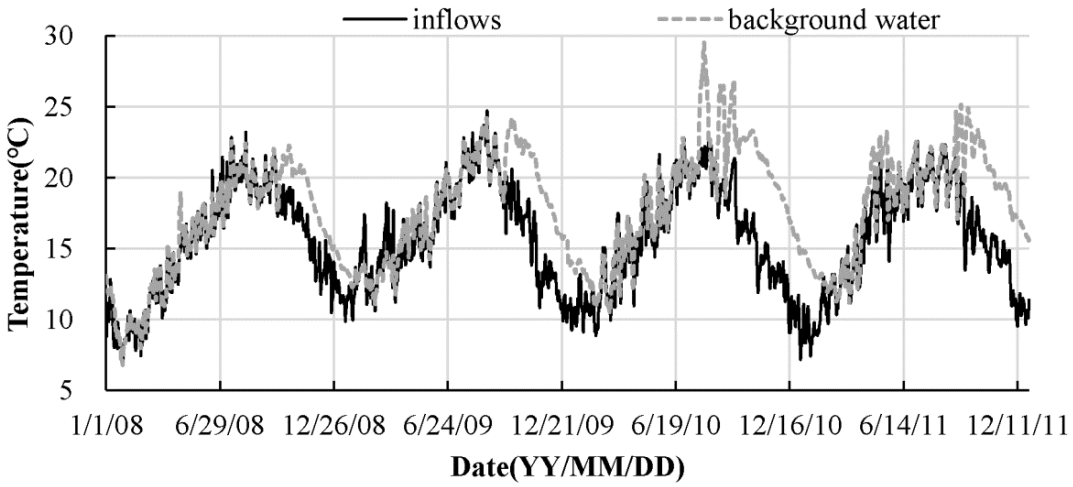

Fig. 5 Temperature of upstream inflows VS water in XXR

4.2.2 Water circulation that promotes algal blooms

In patterns (7) and (8), the intrusion flow created a clockwise circulation with the upstream underflow, causing the formation of eddies between the two density currents and strengthening the vertical mixing. As a result, thermal stratification in the lower depths would be weakened or eliminated (Fig. 4(D), (F)). However, in the surface layers in the middle and lower reaches, even though there is a weak, counterclockwise circulation, the velocities are still relatively small, and surface water commonly could not be mixed or moved quickly. When thermal stratification formed, and a special, vertical temperature profile such as a "double epilimnion-metalimnion" would be witnessed in the lower reaches and a "semi-U" type would form in the upper, shallow reaches (Yang et al. 2012). At the same time, if nutrients were sufficient, these two flow patterns would have the greatest risk of algal blooms, particularly in the upper reaches. From Table 1, the two patterns are prevalent most of the year, which is why algal blooms can occur at any time of year (Fang et al. 2013; Wang et al. 2011; Zhu et al. 2013).

In addition, in patterns (2) and (3), the lower layer water below the intruding water formed a clockwise circulation and the water over the intruding water flowed downward. This occurred in March 2008 and in March-April from 2009 to 2011 (Fig. 6). However, in general, the cascade reservoirs located in the upstream XXR operated with small discharges in the dry season, with an average flow rate of 24.9 m^3/s and a minimum flow rate of only 9.9 m^3/s. The lower inflow rates resulted in a smaller surface velocity in the upper reach of the XXR, as residence time generally increased in the upper reach of the XXR, promoting subsurface thermal stratification (Table 1). Thus, algal bloom risk in the upper reach of the XXR could increase. Fortunately, these water circulations only occurred in March and early April for a short time, when water temperature becomes a factor to be considered.

4.2.3 Water circulation in between

In pattern (9) the intrusion flow created a counterclockwise circulation, creating many violent eddies between the two density currents in the upper reach of the XXR (Fig. 4(G)). However, the magnitudes of eddies and mixing depended on the intensity of the counterclockwise circulation that was caused by the TGR mainstream lower-interflow. If the counterclockwise circulation is strong enough to accelerate upstream vertical mixing, algal blooms would be controlled. However, if this local clockwise circulation is weak, the abundant nutrients and suitable temperature would increase the risk of algal blooms.

In addition, in pattern (1), if the downstream intrusion flow increased, it could greatly increase surface

velocity and shorten surface water residence time, even triggering eddies in the upper reach of the XXR (Fig. 3(A)). Subsurface vertical mixing would then increase, which also prompts algal blooms. If the intrusion water was also a small volume, the slow hydrodynamic process would be good for algal blooms (Fig. 3(B)). However, in general, surface water velocities were always low at this time, and the hydrodynamic effect of density-driven water circulation would not be dominant. The predominant temperature and abundant sunlight would become dominant factors that cannot be ignored in early spring.

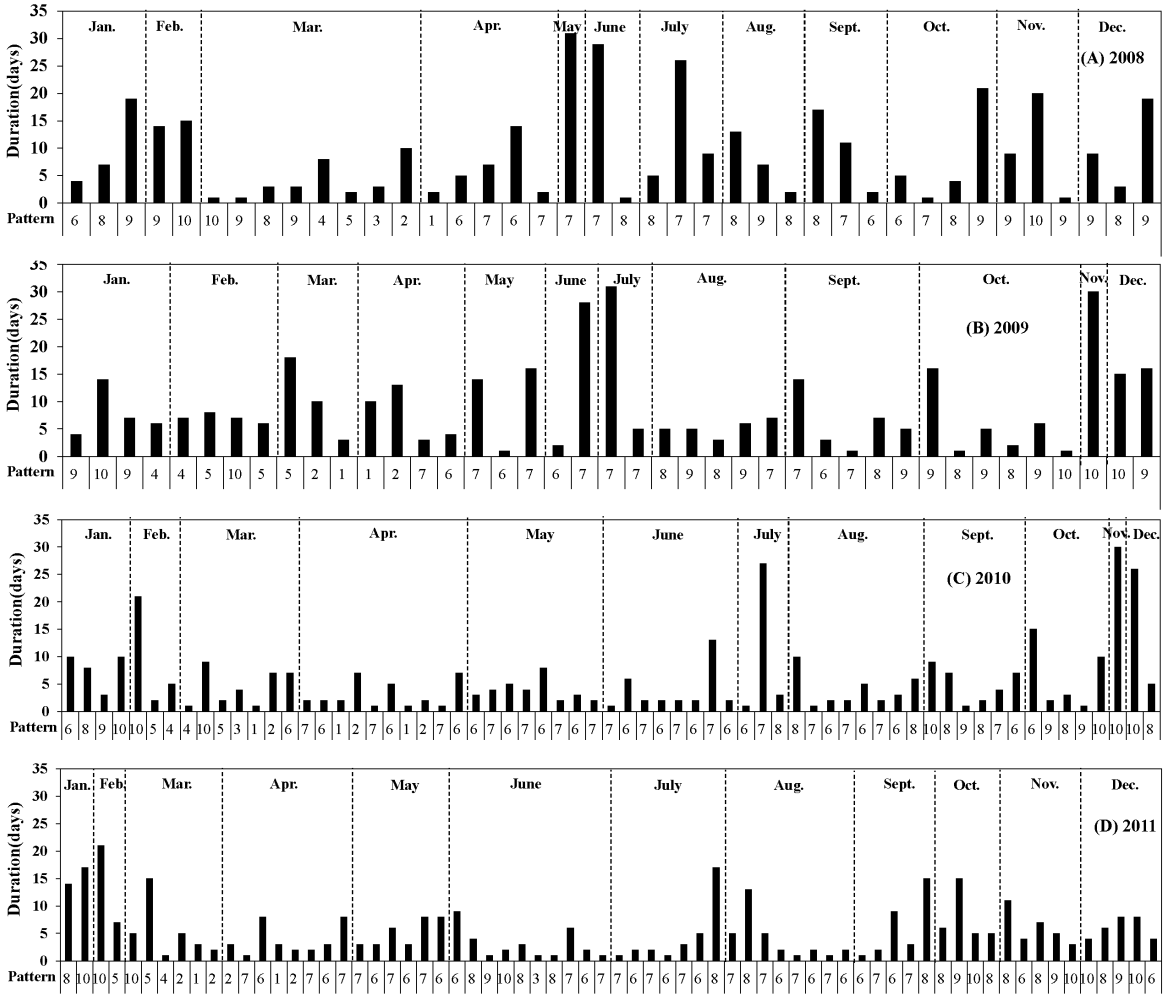

Fig. 6 Emergence and order statistics of the circular patterns in each month from 2008-2011

4.3 Impacts of flow patterns on algal blooms

In Fig. 6, statistics are listed for the flow patterns, which include the order and duration for each month from 2008 to 2011. Mass statistical analyses found that patterns (1)-(5) only occurred in January-April every year when the upstream inflow water temperature was higher or close to that of the water at the end of the XXR, such as in March 2008 and February–April from 2009 to 2011 (Fig. 5). The sum of the duration of the patterns (1)-(5) was only 25, 81, 34, and 42 days in these four years, respectively, and all occurred during low-risk periods of algal bloom. Thus, we focused on the final five circulation patterns and their effect on algal blooms.

In 2008, (Fig. 6(A)), bad patterns (7) and (8) dominated from April 28 to September 28, except for seven-days (pattern (9)) in late August. Patterns (7) and (8) would result in relatively stable thermal stratification in the surface

layer, which might be one of the causes for the 2008 summer blue-green algal blooms. Patterns (7) and (8) also lasted for a long periods from early June to early August in 2009, which provided appropriate flow and thermal stratification conditions for algal blooms. However, there were many more circulation patterns and frequent alternations for each month of 2010 and 2011 (Fig. 6(C), (D)). Patterns (7) and (8) lasted for 40 days from July to August in both 2010 and 2011, but lasted much shorter times in 2008 and 2009.

As previously described, favorable patterns (6) and (10) are capable of forming large-scale flow patterns that cause local turbulence and increase vertical mixing in the bay. This often has a profound impact on hydrodynamic characteristics, nutrient distributions and algal blooms in the side arms of the TGR. As shown in Fig. 7(a), pattern (6) appeared five times in 2008 and four times in 2009. It appeared 19 times in 2010 and 17 times in 2011, showing a significant increase. Similar to pattern (6), pattern (10) appeared seven times in 2010 and eight times in 2011, being more frequent than in 2008 and 2009 when it respectively appeared three times and five times. There was also an increasing trend for the maximum durations of patterns (6) and (10) from 2008 to 2010 (Fig. 7(b)). For pattern (6), it lasted 14 days, 4 days and 15 days, respectively. For pattern (10), it lasted 20 days, 46 days and 66 days, respectively. In 2011, durations of 9 days for pattern (6) and 38 days for pattern (10) were still long enough to cause circulation and vertical mixing to efficiently and profoundly affect the water quality. Ji and Yang (Ji et al. 2010b; Yang et al. 2010) performed extensive field monitoring during the impoundment period after the flood season, and revealed that pattern (6) moved and accelerated the surface water, strengthened the mixing, breaking the temperature stratification, increasing the mixing depth of the algae, and reducing the proportion of euphotic depth versus mixing depth (Z_{eup}/Z_{mix}) that inhibits the rapid growth of phytoplankton. As a whole, flow circulations in the XXR were dynamic and changeable.

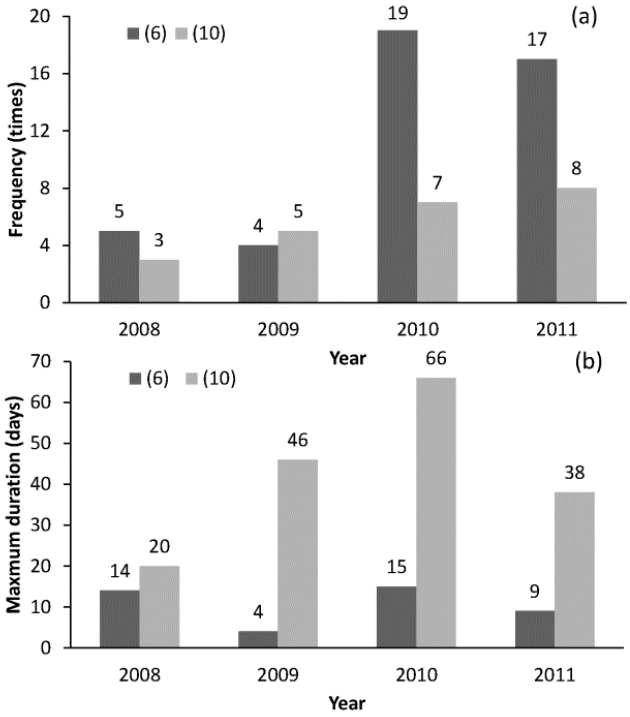

Fig. 7 Frequency and maximum duration of (6) and (10) in 2008-2011, (a) Frequency, (b) Maximum duration

In addition, transformations between patterns in 2010 and 2011 occurred at a higher frequency than in 2008 and 2009. For example, in April 2010 and June 2011, there were frequent transformations of flow patterns (Fig. 6(C), (D)). Different patterns would intrude into the side arms through different layers, with different intensities. A

shift from one pattern to another could strongly disturb the water body and break the thermal stratification. The faster the patterns transformed, the greater and stronger the disturbance and the lower the risk of algal blooms. A reason for the faster transformations of flow patterns since 2010 may be related to frequent fluctuations in water level (Yang et al. 2013). Fig. 8 also shows that more frequent daily fluctuations led to a lower risk and smaller peaks of algal blooms, especially in 2010. The search for deeper reasons requires further research. It can be further speculated that some flow patterns, such as patterns (5), (6) and (10), appear suddenly and have very short durations, but could also have a dramatic impact; as such, they are well worth attention and further study.

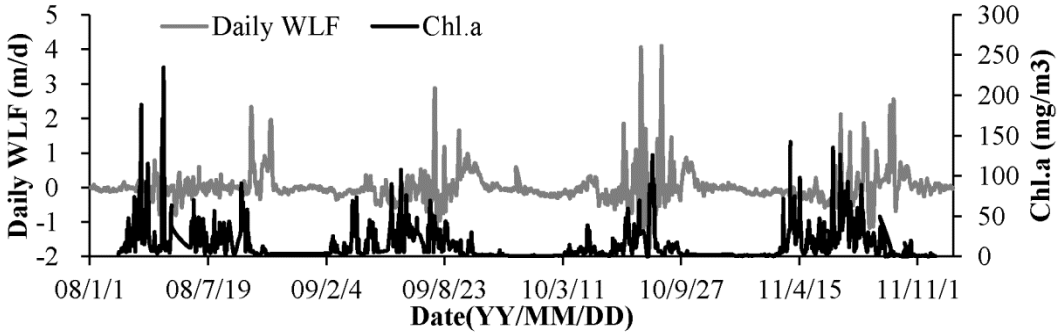

Fig. 8 Dynamics of Chl.a in XXR arm versus Daily WLF process

5 Conclusions

In the ten representative circulations in the XXR, patterns (1)-(5) indicate that upstream inflows through the surface layer and the TGR mainstream water intrude at different layers at the mouth of the XXR, but they only occurred between January and April each year. At most times year, upstream runoff flows into the XXR near the bottom to form an underflow, and then the TGR mainstream water intrudes from different layers at the mouth of the XXR, as characterized by patterns (6)-(10). Advantageous patterns (6) and (10) caused large, clockwise or counterclockwise circulations in the entire bay, accelerating the surface water. The thermal stratification was always broken down rapidly, and thus, algal blooms could be controlled. Patterns (7) or (8) seem to be more common throughout the year. When these patterns occur, the surface layer is often stable with longer residence time and weaker vertical mixing. Thermal stratification is sustained, generating a higher risk of algal blooms.

More frequent transformations of density-driven patterns could facilitate mixing in the tributary, especially for patterns (6) and (10). However, the transformations were more complicated and appear to be irregular, as those representative flow patterns transition from one pattern to another and because water circulation also depended on the strength of the density current. The effects of water circulations on thermal stratification and algal blooms risk were discussed, along with the vertical mixing characteristics of these patterns. Further studies are necessary and recommended for more accurate predictions and for assessing the impact of water level fluctuations on such transformations of flow patterns and water quality. The model in this study is a robust water quality model, but a future water quality model coupled with the TGR mainstream is also needed to evaluate the mutual link among hydrodynamic conditions, water quality, phytoplankton and reservoir operations.

Conflicts of Interest: The authors declare no conflict of interest.

Ethical approval: This article does not contain any studies with human participants or animals performed by any of the authors.

Informed consent: Informed consent was obtained from all individual participants included in the study.

References

Berger, Chris J, and Scott A Wells. 2008. Modeling the effects of macrophytes on hydrodynamics. *Journal of Environmental Engineering* 134 (9):778-788.

Bowen, James D, and Jeffrey W Hieronymus. 2003. A CE-QUAL-W2 model of Neuse Estuary for total maximum daily load development. *Journal of water resources planning and management* 129 (4):283-294.

Chen, XinJian. 2007. A laterally averaged two-dimensional trajectory model for estimating transport time scales in the Alafia River estuary, Florida. *Estuarine, Coastal and Shelf Science* 75 (3):358-370.

Chung, Se-Woong, and Ruochuan Gu. 1998. Two-dimensional simulations of contaminant currents in stratified reservoir. *Journal of Hydraulic Engineering* 124 (7):704-711.

Davies, Alan M, and Herman Gerritsen. 1994. An intercomparison of three-dimensional tidal hydrodynamic models of the Irish Sea. *Tellus A* 46 (2):200-221.

Dubnyak, Sergiy, and Vladimir Timchenko. 2000. Ecological role of hydrodynamic processes in the Dnieper reservoirs. *Ecological Engineering* 16 (1):181-188.

Fang, XiaoFeng., ZhengJian Yang, DaoBin Ji, XuJiao Yao, and DeFu. Liu. 2013. Responses of spring phytoplankton communities to their habitats in the Xiangxi Bay of Three Gorges Reservoir, China. *Acta Ecologica Sinica* 33 (6):308-316.

Fu, BoJie, BingFang Wu, YiHe Lü, ZhiHong Xu, JingHua Cao, Dong Niu, GuiShan Yang, and YueMin Zhou. 2010. Three Gorges Project: Efforts and challenges for the environment. *Progress in Physical Geography*:1-14.

Huang, ZhenLi, YuLiang Li, YongCan Chen, JinXiu Li, ZhiGuo Xing, Min Ye, Ping Lü, ChongMing Li, and XueYi Zhou. 2006. Water quality prediction and water environmental carrying capacity calculation for Three Gorges Reservoir. *China Water Power Press, Beijing(in Chinese with English abstract)*.

Imboden, Dieter M, and Alfred Wüest. 1995. Mixing mechanisms in lakes. In *Physics and chemistry of lakes*, 83-138. Springer.

Ji, DaoBin, YuLing Huang, DeFu Liu, WeiPing Yin, ZhengJian Yang, Jun Ma, and Tao Xie. 2013. Research Progress on the Ocean Estuary and its Enlightenment to the Study of the Tributary in Three Gorges Reservoir. *Applied Mechanics and Materials* 295:2215-2222.

Ji, DaoBin, DeFu Liu, ZhengJian Yang, and ShangBin Xiao. 2010a. Hydrodynamic characteristics of Xiangxi Bay in Three Gorges Reservoir. *Sci China-Phys Mech Astron* 40 (1):101-112 (in Chinese).

Ji, DaoBin, DeFu Liu, ZhengJian Yang, and Wei Yu. 2010b. Adverse slope density flow and its ecological effect on the algae bloom in Xiangxi Bay of TGR during the reservoir impounding at the end of flood season. *Journal of Hydraulic Engineering* 6:691-696(in Chinese).

Ji, ZhenGang, GuangDou Hu, Jian Shen, and YongShan Wan. 2007. Three-dimensional modeling of hydrodynamic processes in the St. Lucie Estuary. *Estuarine, Coastal and Shelf Science* 73 (1):188-200.

Kurup, Rajendra G, David P Hamilton, and Robert L Phillips. 2000. Comparison of two 2-dimensional, laterally averaged hydrodynamic model applications to the Swan River Estuary. *Mathematics and Computers in Simulation* 51 (6):627-638.

Lawson, Rebecca, and Michael A Anderson. 2007. Stratification and mixing in Lake Elsinore, California: An assessment of axial flow pumps for improving water quality in a shallow eutrophic lake. *Water research* 41 (19):4457-4467.

Liu, Liu, DeFu Liu, Devid M. Johnson, ZhongQiang Yi, and YuLing Huang. 2012. Effects of vertical mixing on phytoplankton blooms in Xiangxi Bay of Three Gorges Reservoir: Implications for management. *Water*

research 46 (7):2121-2130.

Lung, WuSeng, and Alex J Nice. 2007. Eutrophication model for the Patuxent estuary: Advances in predictive capabilities. *Journal of Environmental Engineering* 133 (9):917-930.

Ma, Jun, Defu Liu, Scott A. Wells, Hongwu Tang, Daobin Ji, and Zhengjian Yang. 2015. Modeling density currents in a typical tributary of the Three Gorges Reservoir, China. *Ecological Modelling* 296:113-125. doi:10.1016/j.ecolmodel.2014.10.030.

Mao, QingWen, Ping Shi, KeDong Yin, JianPing Gan, and YiQuan Qi. 2004. Tides and tidal currents in the Pearl River Estuary. *Continental Shelf Research* 24 (16):1797-1808.

Martin, James L. 1988. Application of two-dimensional water quality model. *Journal of Environmental Engineering* 114 (2):317-336.

Martin, James L, and Steven C McCutcheon. 1998. *Hydrodynamics and transport for water quality modeling*. CRC Press.

Tufford, Daniel L, and Hank N McKellar. 1999. Spatial and temporal hydrodynamic and water quality modeling analysis of a large reservoir on the South Carolina (USA) coastal plain. *Ecological modelling* 114 (2):137-173.

Wang, L., Q.H. Cai, L. Tan, and L.H. Kong. 2011. Phytoplankton development and ecological status during a cyanobacterial bloom in a tributary bay of the Three Gorges Reservoir, China. *Science of the Total Environment* 409 (19):3820-3828.

Xu, YaoYang, Min Zhang, Lan Wang, LingHui Kong, and QingHua Cai. 2011. Changes in water types under the regulated mode of water level in Three Gorges Reservoir, China. *Quaternary International* 244 (2):272-279.

Yang, ZhengJian, DeFu Liu, DaoBin Ji, and ShangBin Xiao. 2010. Influence of the impounding process of the Three Gorges Reservoir up to water level 172.5 m on water eutrophication in the Xiangxi Bay. *Science China Technological Sciences* 53 (4):1114-1125.

Yang, ZhengJian, DeFu Liu, DaoBin Ji, ShangBin Xiao, YuLing Huang, and Jun Ma. 2013. An eco-environmental friendly operation: An effective method to mitigate the harmful blooms in the tributary bays of Three Gorges Reservoir. *Science China Technological Sciences* 56 (6):1458-1470.

Yang, ZhengJian, DeFu Liu, Jun Ma, YuanYuan Chen, XiaoFeng Fang, and DaoBin Ji. 2012. Effects of special vertical layered water temperatures on algal bloom in Xiangxi Bay of Three Gorges Reservoir. *Engineering Journal of Wuhan University* 45 (1):1-9(in Chinese).

Ye, Lin, XQ Han, YaoYang Xu, and QingHua Cai. 2007. Spatial analysis for spring bloom and nutrient limitation in Xiangxi bay of three Gorges Reservoir. *Environmental monitoring and assessment* 127 (1):135-145.

Zhang, Sheng, CM Li, YC Fu, Yong Zhang, and Jian Zheng. 2008. Trophic states and nutrient output of tributaries bay in Three Gorges Reservoir after impoundment. *Huan jing ke xue* 29 (1):7-12(in Chinese).

Zhu, K.X., Y.H. Bi, and Z.Y. Hu. 2013. Responses of phytoplankton functional groups to the hydrologic regime in the Daning River, a tributary of Three Gorges Reservoir, China. *Science of the Total Environment* 450:169-177.

Appendix III

Tributary oscillations generated by diurnal discharge regulation in Three Gorges Reservoir

Lianghong Long[1,2], Daobin Ji[2], Zhongyong Yang[2], Heqing Cheng[3], Zhengjian Yang[2], Defu Liu[4], Liu Liu[5], Andreas Lorke[1]*

[1] *Institute for Environmental Sciences, University of Koblenz-Landau, 76829 Landau, Germany*

[2] *College of Hydraulic and Environmental Engineering, China Three Gorges University, 443002 Yichang, China*

[3] *State Key Laboratory of Estuarine and Coastal Research East China Normal University, 200062 Shanghai, China*

[4] *Hubei Key Laboratory of River-lake Ecological Restoration and Algal Utilization, Hubei University of Technology,430068 Wuhan, China*

[5] *Department of Experimental Limnology, Leibniz-Institute of Freshwater Ecology and Inland Fisheries, 16775 Stechlin, Germany*

***** Correspondence: lorke@uni-landau.de (Andreas Lorke)

Please click the following link to read the publication

https://iopscience.iop.org/article/10.1088/1748-9326/ab8d80

Journal **Environmental research letters**
https://doi.org/10.1088/1748-9326/ab8d80

Tributary oscillations generated by diurnal discharge regulation in Three Gorges Reservoir

L H Long[1,2], D B Ji[2], Z Y Yang[2], H Q Cheng[3], Z J Yang[2], D F Liu[4], L Liu[5], A Lorke[1*]

[1] Institute for Environmental Sciences, University of Koblenz-Landau, 76829 Landau, Germany

[2] College of Hydraulic and Environmental Engineering, China Three Gorges University, 443002 Yichang, China

[3] State Key Laboratory of Estuarine and Coastal Research East China Normal University, 200062 Shanghai, China

[4] Hubei Key Laboratory of River-lake Ecological Restoration and Algal Utilization, Hubei University of Technology,430068 Wuhan, China

[5] Department of Experimental Limnology, Leibniz-Institute of Freshwater Ecology and Inland Fisheries, 16775 Stechlin, Germany

Email: lorke@uni-landau.de

Key Points: water level fluctuations, Three Gorges Reservoir, reservoir hydrodynamics, discharge regulation

Abstract

Among the major consequences of dam construction and operation are the deterioration of water quality and the increasing frequency of occurrence of harmful algae blooms in reservoirs and their tributaries. Former studies at Three Gorges Reservoir demonstrated that the Yangtze River main stream is the main source of nutrients and pollutants to connected tributary bays. Eutrophication and other water quality problems reported for the tributaries along Three Gorges Reservoir are likely a consequence of density-driven exchange flows. Past work has focused mainly on the influence of seasonal and daily flow regulation on exchange flows, less attention has been paid to hydrodynamic processes resulting from sub-daily discharge dynamics. High-frequency measurements of flow velocity and water level in a eutrophic tributary (Xiangxi River) of Three Gorges Reservoir revealed the persistent nature of bidirectional density currents within the bay. Superimposed on this mean flow, we observed ubiquitous flow oscillations with a period of approximately 2 h. The flow variations were associated with periodic water level fluctuations with increasing amplitude for increasing distance from the river mouth (up to ± 0.1 m at a distance of 27.4 km from the river mouth). They were caused by a standing wave in the tributary bay, which was generated by rapid increase or decrease in discharge following peak-shaving operation modes at Three Gorges Dam. The high-frequency wave made up the largest contribution to the temporal variance of flow velocity in the tributary bay and represents a so far overlooked hydrodynamic feature of tributaries bays in large reservoirs.

1 Introduction

Physical, chemical and biological characteristics of aquatic ecosystems are strongly affected by water level fluctuations (WLF) [1, 2]. Long-term, e.g. seasonal or multi-year WLF are the result of a variable water balance and often controlled by meteorological and hydrological processes. Short-term WLF, with periods in the order of seconds to hours can be generated by hydrodynamic processes (e.g., standing and propagating surface waves) [3]. Particularly in reservoirs, WLF are, to a large extent, subject to daily discharge regulations [4] and shiplock operation [5].

Three Gorges Reservoir (TGR) is one of the largest reservoirs in the world and among the most controversial hydraulic engineering projects in China [6]. High environmental costs have caught the attention of researchers from the globe [7, 8]. Among the major consequences of reservoir construction and operation is the deterioration of water quality in more than 38 tributaries and the continuously increasing frequency of occurrence of harmful algae blooms in tributaries [6]. The main source of nutrients and other pollutants in tributary bays is the Yangtze River, which can flow into the bays as a density current [9]. The type of bidirectional water exchange at the river mouth affects nutrient and pollutant dynamics [10], algal blooms [11, 12], water quality [13, 14], phytoplankton composition [15] and sediment deposition [16] in the tributary bays. WLF of TGR can enhance the water exchange between the bays and the main reservoir and reservoir operation rules have been proposed to improve water quality in tributaries by controlling WLF by short-term (daily) discharge regulation at the dam [17, 18]. Despite the extensive number of measurements and simulations that have been conducted in TGR and its tributaries, direct observations of exchange flows at the river confluences are sparse and restricted to daily resolution. The response of the density currents to high frequency (sub-daily) WLF and the potential success of related mitigation measures remain rather speculative.

The objective of this study is to investigate the effect of short-term WLFs caused by discharge regulation of TGR on the variability of flow velocity and density-driven flows in its tributaries. For this purpose, we conducted high-frequency measurements of flow velocity and water level in the eutrophic Xiangxi Bay (XXB) in combination with the water level and discharge observations. The results will provide new perspective for understanding of hydrodynamic processes and water quality management in large reservoirs.

2 Materials and Methods

2.1 Study area

Three Gorges Dam is located in the middle course of the Yangtze River (China). The Xiangxi River (XXR) is the largest tributary of TGR which is in close proximity to the dam (Fig. 1). The river has a watershed area of 3095 km^2, a length of 94 km and a mean annual discharge of 47.4 $m^3\ s^{-1}$. Xiangxi Bay (XXB) formed after the initial filling of TGR in June 2003 and extends up to 40 km from the river mouth when the reservoir is filled to its maximum water level of 175 m.a.s.l. (meter above sea level).

2.2 Data and measurements

Absolute water level measurements (in m.a.s.l.) from six gauging stations along TGR (Fig. 1) and discharge data were provided by China Three Gorges Corporation. The data included time series of sea-level referenced water levels with a resolution of 5 min and discharge at a resolution of 1 h for the period of January to November 2018. The relative water level and vertical profiles of flow velocity were measured in the middle and upper section of XXB (17.5 and 27.4 km upstream of the river mouth) from September 16 to October 12, 2018. Two Acoustic Doppler Current Profilers (ADCP, Teledyne RDI Sentinel 600 kHz and 1200 kHz) were deployed at the bottom of the river (~0.5 m above the riverbed). The ADCPs were configured to measure vertical profiles of flow velocity with a vertical resolution (bin size) of 0.5 m and a temporal resolution of 15 min. Hydrostatic pressure recorded by both instruments was converted to water depth (relative water level) using water density at in-situ temperature. Horizontal current velocities were measured in earth coordinates and rotated into longitudinal (along the river channel) and transversal velocity components by rotation into the respective mean (depth and temporarily averaged) flow direction at the sampling sites. To analyze daily and sub-daily fluctuations of water level, water depth and flow velocity, the respective time series were high-pass filtered with cut-off frequencies corresponding to periods of 36 h

(7.7 10^{-6} Hz) and 4 h (7.7 10^{-6} Hz). The frequency distribution of variance in water level and velocity fluctuations was analyzed in terms of power spectral density, which was calculated using Welch's method [19].

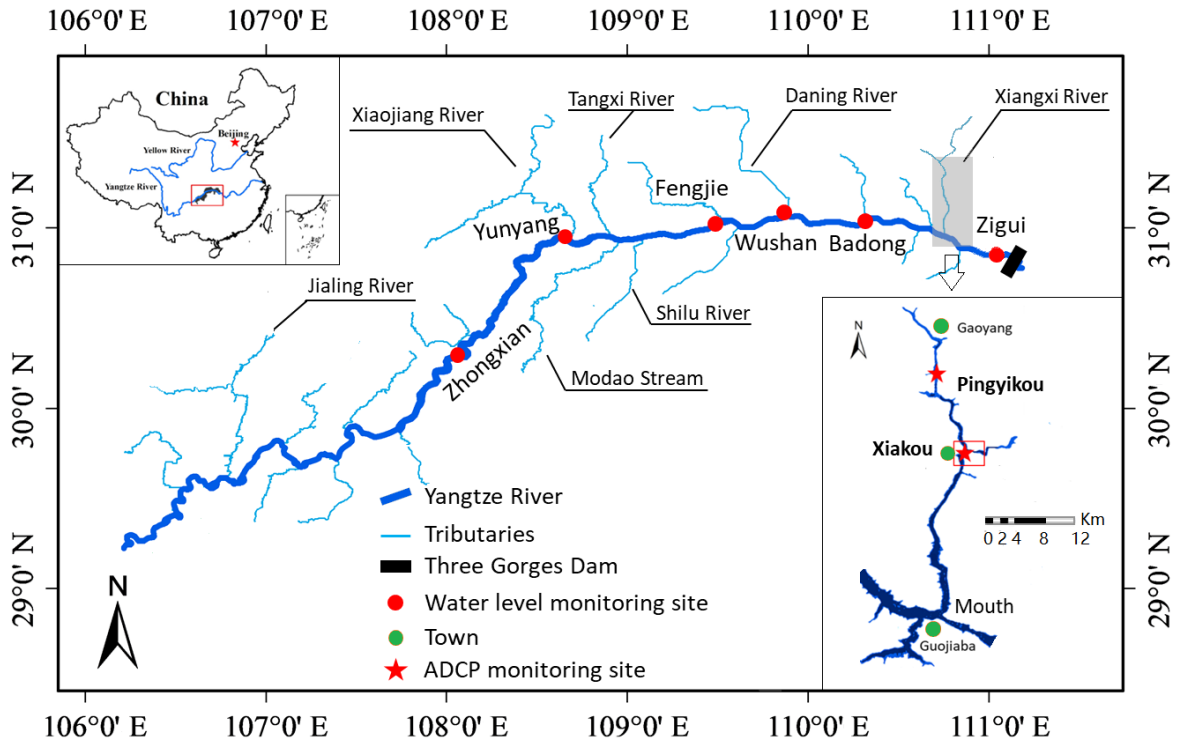

Figure 1. Map of Three Gorges Reservoir at the Yangtze River with major tributaries. The location of Three Gorges Reservoir is marked by red box in the overview map shown in the top left corner. Gauging stations used in this study are marked by red circles. The inset map in the lower right corner shows the tributary bay of the Xiangxi River at greater detail. The sampling sites for water level fluctuations and flow velocity (ADCP – Acoustic Doppler Current Profile) are marked by red star-shaped symbols.

2.3 Theoretical modes of bay oscillation

We compare basin-scale water level fluctuations in XXB with the fundamental period of standing waves in a semi-closed basin. With an open boundary at the mouth of the tributary, the fundamental period corresponds to the Helmholtz mode, with a node (minimum wave amplitude) at the mouth and an antinode (maximum wave amplitude) at the upstream end of the tributary bay. The oscillation period (T_0) of the Helmholtz mode depends on basin length (L) and water depth (H) as:

$$T_0 = \alpha\left[2L/(\mathrm{g}\,H)^{1/2}\right] \quad (1)$$

with g denoting gravitational acceleration [20]. The factor α depends on basin geometry and is equal to two for rectangular basin of uniform depth and width. For linearly decreasing water depth from H at the open mouth to zero at the upstream end of XXB, we used a value of α=2.618 [20].

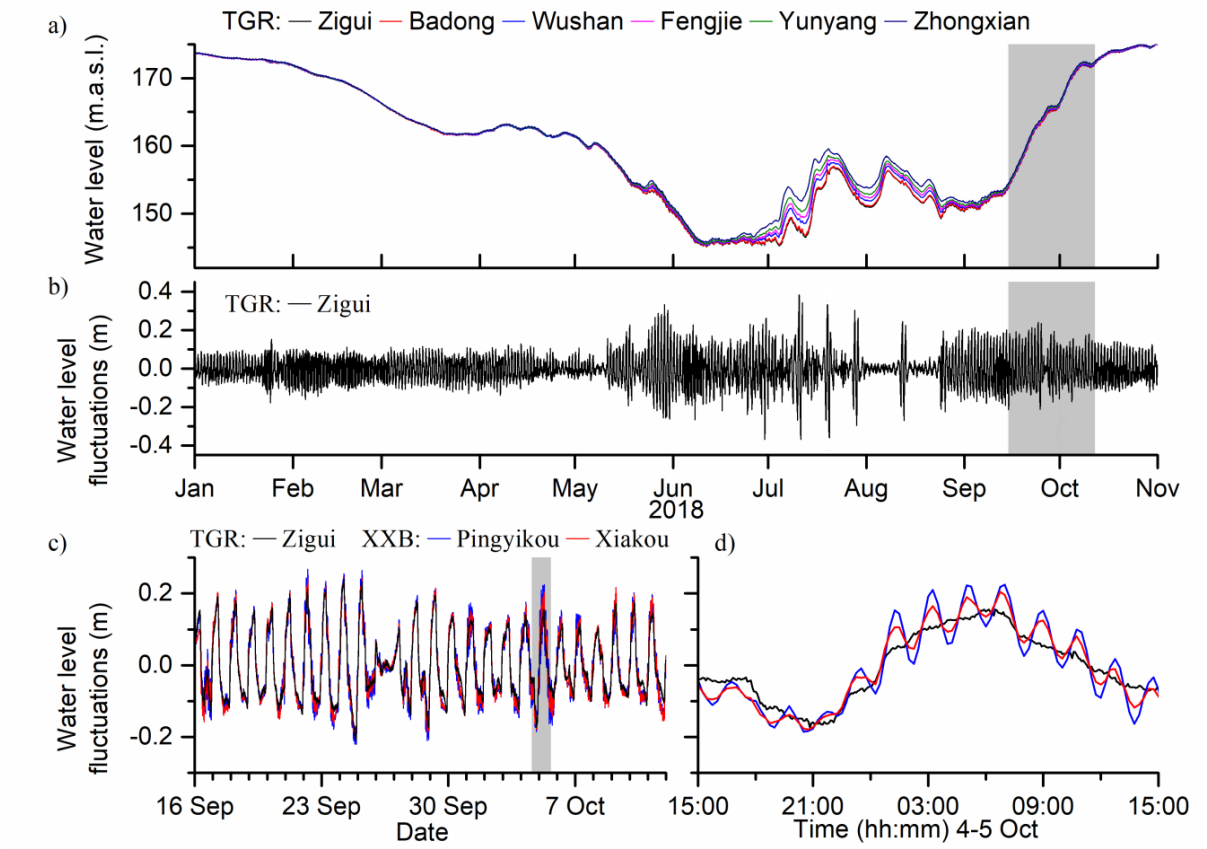

Figure 2. Water level and water level fluctuations: a) Seasonal water level at six gauging stations along Three Gorges Reservoir (TGR, see map in Fig. 1). The stations are located 2.3 km (Zigui) to 369.5 km (Zhongxian) upstream of Three Gorges Dam. b) Seasonal dynamics of daily water level fluctuations (high-passed filtered water level fluctuations with periods <36 h) at Zigui. Grey background color marks the sampling period in Xiangxi Bay (XXB). c) Daily water level fluctuations in TGR (Zigui) and in XXB (Xiakou and Pingyikou). d) As c), but zoom-in on period 4-5 October (grey box in panel c).

3 Results

3.1 Water level fluctuations

The amplitude of seasonal water level variation in TGR was about 30 m, with low water level from June to September (Fig. 2a). With differences in water level smaller than 0.1 m along the up to 360 km distance between the gauging stations, the water level slope was negligible during high water levels, but increased slightly up to 0.02 ‰ during summer. The high-pass filtered water level time series revealed daily WLF of varying amplitude and pattern throughout most time of the year (Fig. 2b). The daily dynamics closely followed variations in discharge at Three Gorges Dam (Fig. S1) and are the result of the seasonally varying daily pattern in hydropower generation (examples for the different modes of daily dynamics of water level and discharge are shown in Fig. S1). The rapid changes in discharge resulted in transient WLFs, i.e., depressions or elevations in front of the dam, which propagated upstream with decreasing amplitudes. Cross-correlation analysis of WLF at the different gauging stations showed a linear increase in time lag with the increasing distance from the dam, suggesting a nearly constant speed of propagation of the daily WLFs (20 m s^{-1}) (Fig. S2). This speed corresponds to the phase speed (c) of a linear shallow-water gravity wave at a water depth (H) of 37 m ($c = (gH)^{1/2}$, with g denoting gravitational acceleration). The estimated depth can be considered as the equivalent water depth of a rectangular channel, while the seasonal-mean water depth at the main river channel varies strongly (21 - 115 m, Table S1). Within the one month measurement period in XXB, the water level increased from 154 to 172 m.a.s.l., (Fig. S1). The water depth at the two sites where ADCPs were deployed increased from 30 to 48 m, and from 12

to 30 m, respectively. Daily WLFs with amplitudes between 0.1 - 0.2 m were observed throughout the entire sampling period (Fig. 2c). In XXB, daily WLFs occurred nearly synchronously and of similar amplitude as in TGR. A more detailed view (Fig.2 d), however, identified high-frequency fluctuations (with a period ~2 h), which were superimposed on the daily WLFs in XXB, but are absent in TGR (Fig. 2d). These oscillations were nearly ubiquitously present throughout the sampling period. The amplitudes were consistently higher (up to 0.1 m) at the more upstream located sampling site (Pingyikou), compared to mid-section site (Xiakou). This observation is further evident in the power spectra of WLFs, which show a peak in spectral variance around a period of ~2 h at the both sampling sites in XXB (see Fig. S3), which is absent the spectra from TGR.

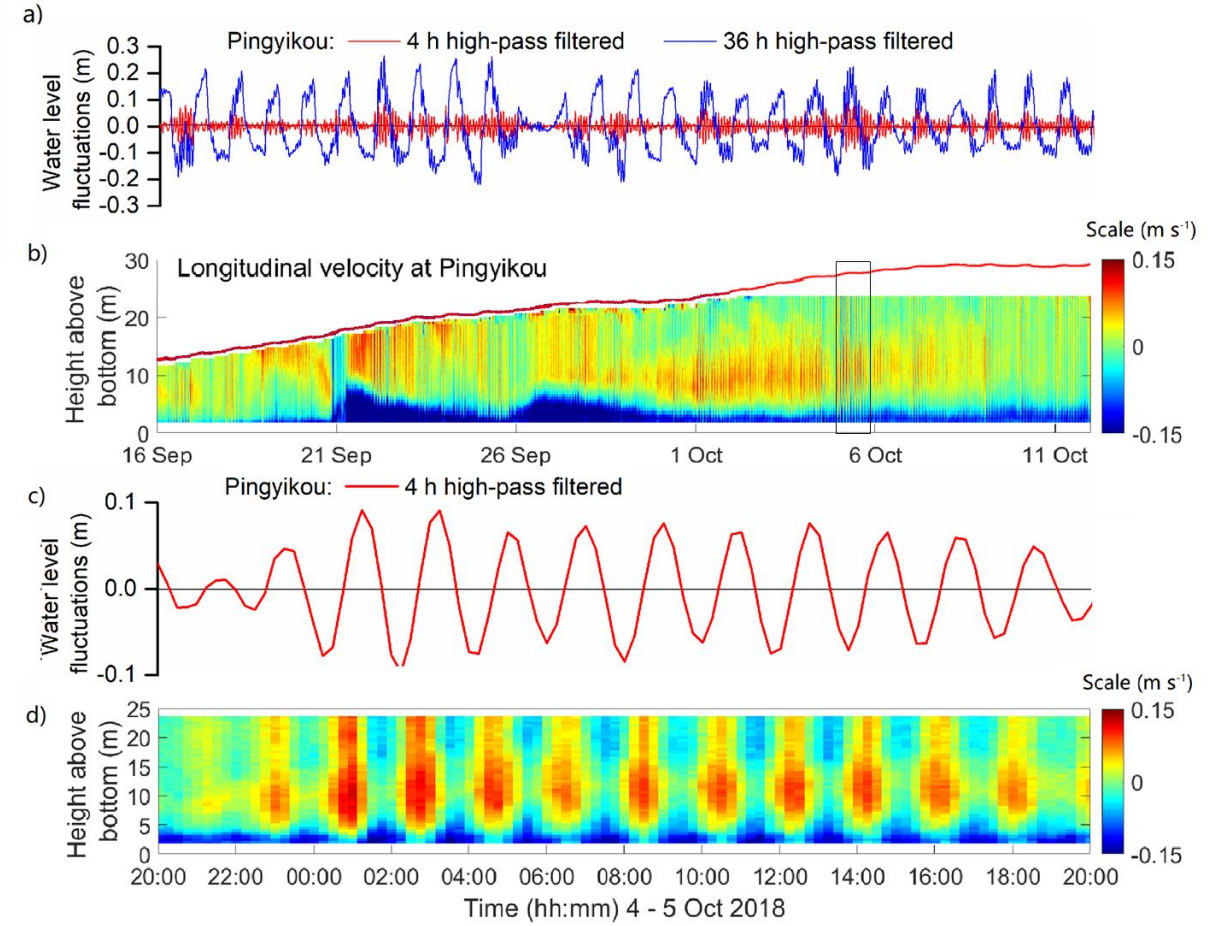

Figure 3. a) Water level fluctuations (4 h and 36 h high-pass filtered) and b) longitudinal flow velocity in Xiangxi Bay (XXB) at Pingyikou. Positive flow velocity corresponds to upstream flow (from TGR into XXB); negative velocity is in the direction of river flow. The red line in b) shows water depth (the measurement range of the current profiler was limited to 24 m). Black selectrect color marks the zoomed time period of panel c and d. c) and d) show a close-up to a 24 h period in a) and b), respectively.

3.2 Flow velocity in Xiangxi Bay

The temporal dynamics of flow velocity in XXB was similar at both monitoring sites and is exemplified for the upper course (Pingyikou) in Fig. 3 (data from Xiakou are presented in Fig. S4). A two-layered flow structure was clearly visible at both sites, indicative of opposing density currents of river inflow along the bottom (underflow) and water flowing into XXB from TGR at mid depth and near the surface (interflow or overflow) (Fig. 3b). The river inflow occurred within a maximal 6 m (Pingyikou) to 10 m (Xiakou) thick layer along the bottom of the bay. In this bottom layer, the average longitudinal flow velocities were negative and maximal near the bottom (-0.11 ± 0.05 m s^{-1} at Pingyikou and -0.12 ± 0.06 m s^{-1} at Xiakou; vertical profiles of mean flow velocities are shown in Fig. S5a). Above the inflowing water, the mean flow was directed upstream, (positive longitudinal velocity) with maximum magnitudes at 10.5 m above the bed at Pingyikou (0.03 ± 0.03 m s^{-1}) and

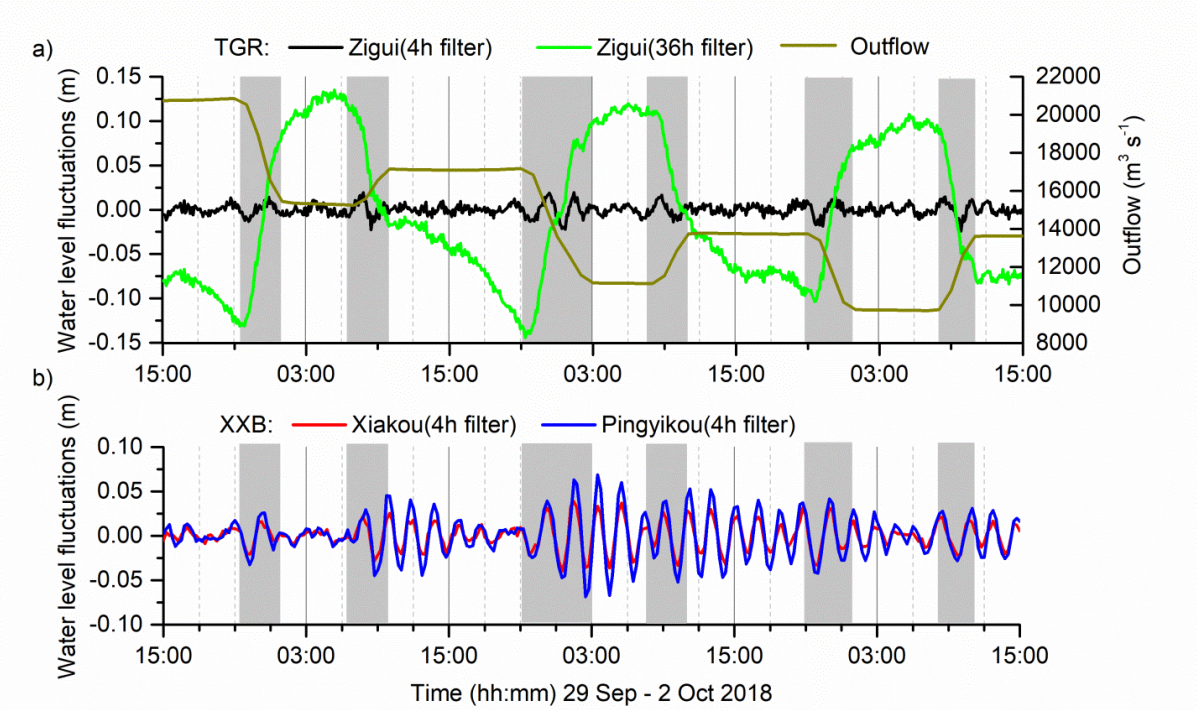

Figure 4. Illustration of the generation mechanism of bay waves in Xiangxi Bay (XXB): a) Water level fluctuations in Three Gorges Reservoir (TGR, Zigui gauging station) are shown as high-pass filtered time series with cut-off periods of 36 h to emphasize daily fluctuations (green line) and 4 h (high-frequency fluctuations, black line). Discharge at Three Gorges Dam is shown by the olive line (grey bars mark periods of discharge regulation). b) High-pass filtered (<4 h periods) water level fluctuations at both monitoring sites in XXB (Xiakou: red line, Pingyikou: blue line). Note that the applied high-pass filter has a finite response to a step change. Therefore, it appears in a) that the water levels start to decrease before the actual change in discharge. This is an artifact of the filter.

at 17.6 m above the bed (0.04 ± 0.03 m s-1) at Xiakou. Currents in both layers show synoptic variability, e.g. intensification of river inflow at the end of September and a change of the inflow from TGR from overflow to interflow occurring around the same period (Fig. 3b). This longer-term variability is most likely related to precipitation and the continuously increasing of water level in TGR. No notable variability in flow was observed at a daily time scale, i.e. in response to daily WLFs (Fig. 3 a and b).

The high-frequency WLFs (2 h period), however, were accompanied by strong periodic flows with amplitudes up to ± 0.05 m s^{-1} (Fig. 3c and d). These periodic flows were superimposed on the density currents and caused periodic variations of the thickness of the river underflow as well as frequent reversals of flow direction in the upper layer. In accordance with the amplitudes of WLFs, also the magnitudes of flow velocity were consistently larger at Pingyikou, compared to Xiakou. Analysis of high-pass filtered longitudinal flow velocities (<4 h periods) revealed that the wave amplitude and phase were constant over the entire water depth at both sites (Fig. S4c). Spectral analysis of velocity variance shows a significant contribution of the high-frequency wave to flow velocity variance at all depths. Variance-preserving spectra of velocity revealed that the majority of velocity variance was associated with the 2 h wave period at the both sampling sites in XXB (Fig. S5b).

3.3 Nature and generation mechanism of the bay oscillation

The detailed diurnal dynamics of water level and discharge of TGR leading to the generation of the bay oscillation in XXB is illustrated in Fig. 4:

A rapid decrease or increase in discharge from TGR leads to a transient pile-up or depression of water level in front of the dam. These water level disturbances are only 1-2 cm in height at the dam (cf. water level fluctuation in Zigui filtered at 4 h in Fig. 4a) and propagate as a surge in the upstream direction of TGR and XXB. The period (better duration, because it is not periodic) of this surge is ~2 h. During the initiation of the wave by changing discharge at the dam, the amplitudes of the high-frequency WLFs in XXB are comparable, or only slightly higher than those in TGR. However, during the following wave cycles, amplitudes are strongly amplified in XXB, while no further WLF

occur in TGR. By the time the surge has propagated to the upstream end of XXB (0.35 – 0.37 h), the water level at the river mouth has continued to change by typically ±5 cm, which adds to the wave amplitude and results in growing wave amplitudes during the period of discharge change. Persistent high-frequency bay oscillations of variable amplitudes are generated by both increasing as well as decreasing in discharge from TGR. Interfering waves generated by subsequent discharge variations lead to amplification or extinction (Fig. 4).

The uniform vertical distribution of wave-induced flow velocity (Fig. 3d) suggests that the 2 h oscillation in XXB represents a surface wave, rather than an internal wave. The latter would be supported by vertical density stratification and characterized by opposing flows in different layers of the water column. With a basin length L = 34-40 km and depth H = 72-90 m, as it was observed during the year 2018 (see Table S1), the fundamental period of a basin-scale surface wave (Eq. 1) varies between 1.84 and 1.94 h, which is in close agreement with observed periods (1.85 - 1.95 h). Consistent with our observations, the amplitude of the bay wave depends on location and increases with increasing distance from the river mouth (Fig. 2d and 4b). For this oscillation, the theoretical ratio of wave heights at the two measurement locations had a nearly constant value of 1.19 (Fig. S6). The observed ratio (1.48) is higher, which can be attributed to changes of channel width and depth.

4 Discussion and Conclusions

High-frequency observations of WLF and flow velocity in a large tributary bay of TGR revealed the ubiquitous presence of a bay oscillation. A standing wave of fundamental mode (Helmholtz mode) with a period of 2 h is generated by rapid discharge regulation at Three Gorges Dam. Although the wave-induced WLFs at the sampling sites were considerably smaller than daily WLFs due to discharge regulation, its projected maximum amplitude at the end of the impoundment is expected to be of comparable magnitude. Bay and harbor oscillations have been extensively studied in coastal and lake environments, where they can be generated by wind or tides [21, 22]. To our knowledge, such waves have not been observed in reservoirs in response to discharge regulation.

The observed wave period in XXB agreed well with a theoretical prediction based on basin geometry and water depth (Eq. 1, [20]). The oscillation amplitude can be expected to depend on the type and intensity of the initial perturbation [23]. For periodic forcing, forced oscillations are produced with amplitudes depending on friction and the proximity of the forcing frequency to the natural frequency of the system [21]. The forcing frequency in XXB is related to the duration of a transient water level change in TGR, and is only indirectly related to the periodicity of daily discharge regulation. Wave excitation can be expected to occur also for different daily patterns of discharge regulation at other seasons (Fig. S1) and in other tributaries. Our findings showed that the wave amplitude is mostly controlled by superposition and inference of waves generated during sequential changes in discharge. The resulting temporal dynamics of wave amplitudes is highly variable and make predictions of wave amplitudes at other seasons and in other tributaries having different resonance frequencies, rather difficult.

As an important finding, our measurements revealed that the bay oscillation had a strong effect on the temporal dynamics and vertical distribution of flow velocity in the tributary. Despite the comparably small contribution to WLFs, the 2 h bay oscillations made up the largest contribution of velocity variance in the bay. The wave caused a frequent reversal of the density current transporting water from TGR into the bay and resulted in a pulsating inflow of the river along the bed. Because vertical mixing is mainly driven by shear production of turbulent kinetic energy at the velocity gradient at the edge of the density-driven intrusion [24], the wave can be expected to provide an important control on the exchange of momentum, heat and solutes between both water masses [18]. Former studies emphasized the importance of the exchange flows for water quality in XXB by demonstrating that the Yangtze River main stream appeared to be the major contributor of dissolved and particulate water constituents [25], including heavy metals [10] and nutrients [11]. Eutrophication and other water quality problems reported for the tributaries along TGR are likely a consequence of this exchange. In fact, the upstream section of XXB, where we found the largest wave amplitudes and wave-induced velocity variations, has been identified as the hot zone where plankton blooms favorably develop [26].

Given the dominant control of the wave-induced currents on velocity and velocity shear in XXB, it appears surprising that the bay oscillations have been overlooked in the extensive research that had been conducted at this particular tributary. While field observations have been limited to discrete (daily) velocity measurements [27, 28], water level and discharge were mostly specified as daily varying boundary conditions in most numerical models [9, 26]. These studies captured the characteristics of density current in tributaries, but did not resolve the high-frequency bay oscillations. The detailed dynamics of

exchange flows in a tributary of TGR in response to reservoir discharge regulation has been analyzed by *Sha et al.,* [18] using a one-dimensional hydrodynamic model. They suggested that rapid changes in discharge at Three Gorges Dam can result in a tidal-like flushing of the tributaries. High-frequency bay oscillations that are excited by rapid increase or decrease in discharge, however, were not reported in that study, indicating the importance for improving hydrodynamic models.

Numerous studies over the last decade have suggested that WLFs in TGR can be used to control the exchange flow between the main stream and the tributaries and to improve water quality in the tributaries bays [17, 29]. However, these studies are based on simulations and observations, which resolved seasonal or daily time-scales of discharge variations. Our findings suggest that high-frequency bay oscillations need to be considered in the development of multi-objective ecological scheduling strategies for optimizing power generation, as well as upstream and downstream flows [30]. Adaptive discharge regulation, which is synchronized with the phase of previously excited bay oscillations, may provide an efficient means for controlling vertical mixing in tributaries for improving water quality and combating harmful algae blooms.

Acknowledgments

This work was financially supported by the Natural Science Foundation of China (grant No. 91647207, 51779128) and by the Natural Science and Technology Major Special Program of China (2016YFC05022208). The Hubei province Chutian Scholar program (granted to AL) provided additional financial support for the field measurements. We thank China Three Gorges Corporation for providing water level and discharge data. The authors are grateful to Bertram Böhrer and two anonymous referees for constructive comments and suggestions. All raw data and process are available at this website (http://doi.org/10.5281/zenodo.3458279).

Author contributions

A Lorke, D B Ji and D F Liu conceived the study and obtained funding; M J B extracted data and tested scaling relationships; H Q Chen and Z Y Yang provided field monitoring instruments and support; A Lorke, L H Long and L Liu contributed to data interpretation; L H Long wrote the first draft of manuscript. A Lorke and L Liu contributed to writing.

Author information

The authors declare no competing financial interests. Correspondence should be addressed to A Lorke at lorke@uni-landau.de.

Data availability statement

The data that support the findings of this study are openly available at doi.org/10.5281/zenodo.3458279

References

[1] Coops H et al 2003 The role of water-level fluctuations in shallow lake ecosystems–workshop conclusions *Hydrobiologia* **506** 23-7

[2] Wantzen K M et al 2008 Ecological effects of water-level fluctuations in lakes: an urgent issue *Hydrobiologia* **613** 1–4

[3] Hofmann H et al 2008 Temporal scales of water-level fluctuations in lakes and their ecological implications *Hydrobiologia* **613** 85–96

[4] Friedl G et al 2002 Disrupting biogeochemical cycles - Consequences of damming *Aquat. Sci.* **64** 55-65

[5] Maeck A et al 2014 Ship-lock induced surges in an impounded river and their impact on sub-daily flow velocity variation *River Res. Appl.* **30** 494–507

[6] Xu X et al 2013 Environmental impact assessments of the Three Gorges Project in China: Issues and interventions *Earth-Sci. Reviews* **124** 115-25

[7] Stone R 2008 Three Gorges Dam: into the unknown *Science* **321** 628-32

[8] Fu B et al 2010 Three Gorges Project: efforts and challenges for the environment *Prog. Phys. Geogr.* **34** 741-54

[9] Ma J et al 2015 Modeling density currents in a typical tributary of the Three Gorges Reservoir, China *Ecol. Model.* **296** 113-25

[10] Holbach A et al 2014Three Gorges Reservoir: density pump amplification of pollutant transport into tributaries *Environ. Sci. Technol.* **48** 7798-806

[11] Yang Z et al 2018 Hydrodynamic mechanisms underlying periodic algal blooms in the tributary bay of a subtropical reservoir *Ecol. Eng.* **120** 6-13

[12] Ji D et al 2017 Impacts of water level rise on algal bloom prevention in the tributary of Three Gorges Reservoir, China *Ecol. Eng.* **98** 70-81

[13] Zhao P et al 2013 Assessing water quality of Three Gorges Reservoir, China, over a five-year period from 2006 to 2011 *Water Res. Manage.* **27** 4545-58

[14] Xia J et al 2018 Tempo-Spatial Analysis of Water Quality in the Three Gorges Reservoir,

China, after its 175-m Experimental Impoundment *Water Res. Manage.* **32** 2937-54
[15] Wang L et al 2011 Phytoplankton development and ecological status during a cyanobacterial bloom in a tributary bay of the Three Gorges Reservoir, China *Sci. Total Environ.* **409** 3820-28
[16] Hu B et al 2009 Sedimentation in the Three Gorges Dam and the future trend of Changjiang (Yangtze River) sediment flux to the sea *Hydro. Earth Syst. Sci.* **13** 2253-64
[17] Liu L et al 2012 Effects of vertical mixing on phytoplankton blooms in Xiangxi Bay of Three Gorges Reservoir: implications for management *Water Res.* **46** 2121-30
[18] Sha Y et al 2015 Artificial tide generation and its effects on the water environment in the backwater of Three Gorges Reservoir *J. Hydrol.* **528** 230-7
[19] Emery W J and U O Colorado 2014 Data analysis methods in physical oceanography (3rd Edition Elsevier)
[20] Wilson B W 1972 Seiches, in Advances in hydroscience (Elsevier) pp 1-94
[21] Rabinovich A B 2010 Seiches and harbor oscillations, in Handbook of Coastal and Ocean Engineering（World Scientific) pp 193-236
[22] Csanady G 1975 Hydrodynamics of large lakes *Annu. Rev. Fluid Mech.* **7** 357-86
[23] Bukreev V I 2013 Seiche oscillations in a rectangular channel with an abrupt expansion of the cross section *J. Applied Mech. Tech. Phys.* **54** 531-40
[24] Ellison T H et al 1959 Turbulent entrainment in stratified flows. *J. Fluid Mech.* **6** 423-48
[25] Holbach A et al 2015 Environmental water body characteristics in a major tributary backwater of the unique and strongly seasonal Three Gorges Reservoir, China *Environ. Sci.: Proc. Impacts* **17** 1641-53
[26] Mao J et al 2015 Spatial–temporal hydrodynamic and algal bloom modelling analysis of a reservoir tributary embayment. *J. Hydro-environ. Res.* **9** 200-15
[27] Yang Z et al 2010 Influence of the impounding process of the Three Gorges Reservoir up to water level 172.5 m on water eutrophication in the Xiangxi Bay *Sci. China Technol. Sci.* **53** 1114-25
[28] Zheng T et al 2011 Impacts of water release operations on algal blooms in a tributary bay of Three Gorges Reservoir *Sci. China Technol. Sci.* **54** 1588-98
[29] Wang L et al 2011Weekly dynamics of phytoplankton functional groups under high water level fluctuations in a subtropical reservoir-bay *Aquat. Ecol.* **45** 197-212
[30] Yu Y et al 2017 Assessment of multi-objective reservoir operation in the middle and lower Yangtze River based on a flow regime influenced by the Three Gorges Project *Ecol. Inform.* **38** 115-25

Supporting Information for "Tributary bay oscillations generated by diurnal discharge regulation in Three Gorges Reservoir"

L.H. Long[1], D.B. Ji[2], Z.Y. Yang[2], H.Q. Cheng[3], Z.J Yang[2], D.F. Liu[4], L. Liu[5], A. Lorke[1*]

[1]Institute for Environmental Sciences, University of Koblenz-Landau, Fortstrasse 7, 76829, Landau, Germany

[2]College of Hydraulic and Environmental Engineering, China Three Gorges University, 443002 Yichang City, Hubei Province, China

[3]State Key Laboratory of Estuarine and Coastal Research East China Normal University Shanghai, China

[4]Hubei Key Laboratory of River-lake Ecological Restoration and Algal Utilization, Hubei University of Technology,430068 Wuhan City, Hubei Province, China

[5]Department of Experimental Limnology, Leibniz-Institute of Freshwater Ecology and Inland Fisheries, 16775 Stechlin, Germany

Contents of this file

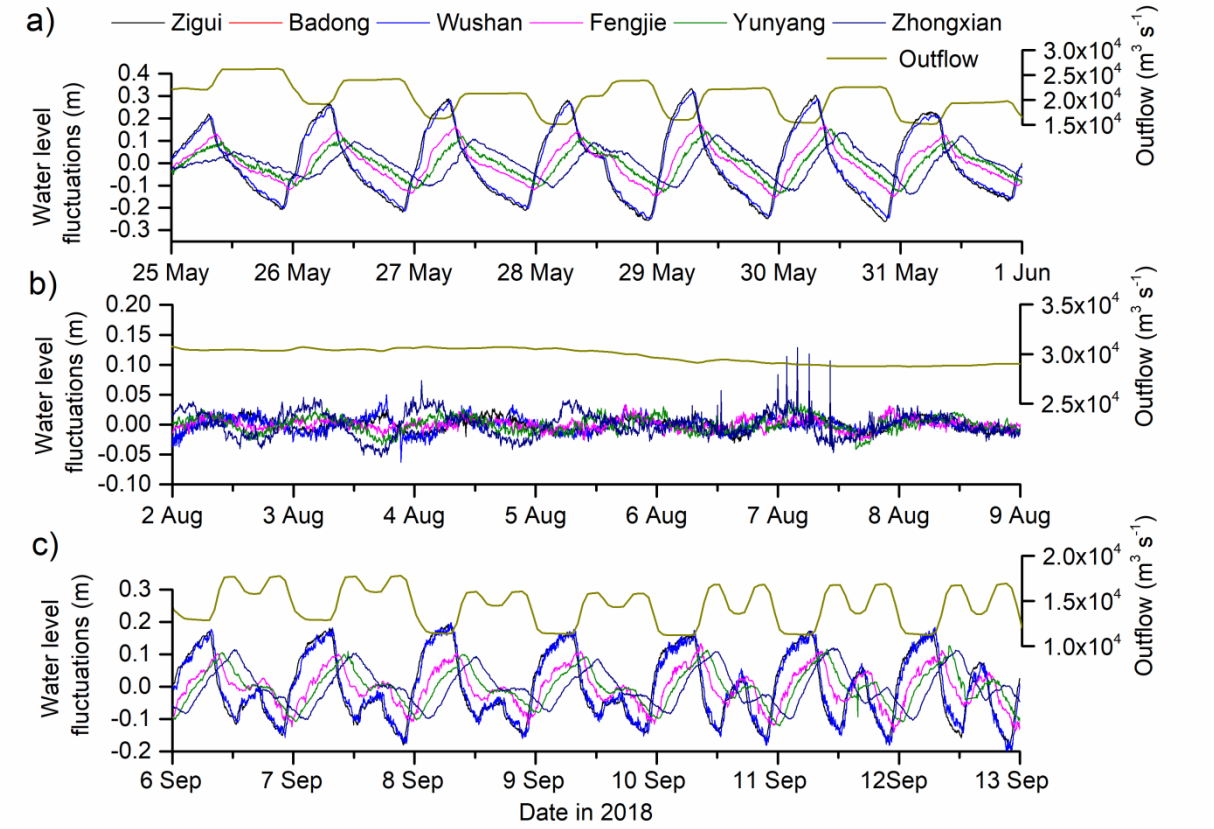

Figure S1. Examples of daily variation of outflow at Three Gorges Dam and high-pass filtered (< 36 h) water level fluctuations at six gauging stations along the reservoir at different seasons (see legend and Fig. 1 for location of the gauging sites). a) A sharp decline and rise of outflow occurred at midnight and early morning, respectively with one cycle in 24 h. b) No significant change in 24 hours. c) Discharge was varied with two cycles in 24 hours.

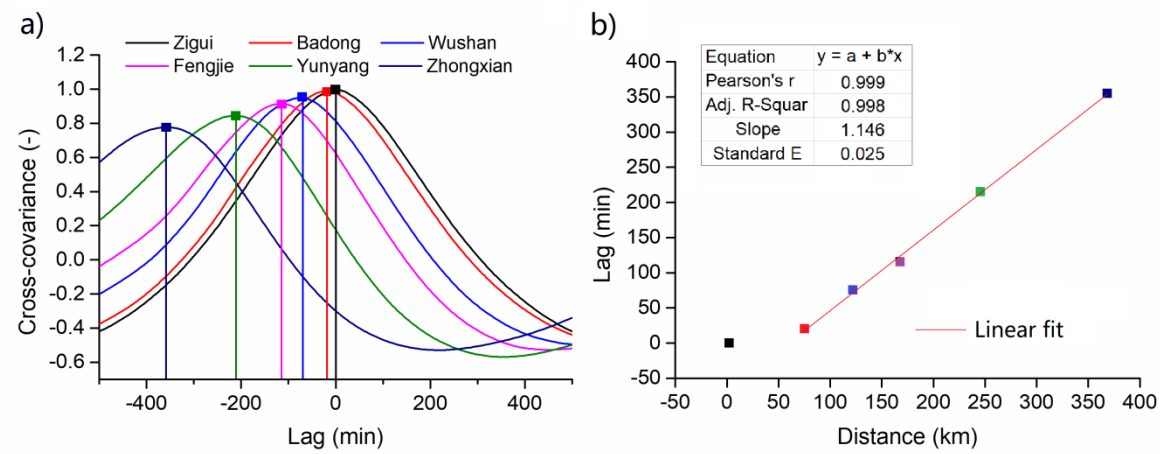

Figure S2. (a) Cross-covariance of high-pass filtered (<36 h hour period) water level variations between the near-dam station (Zigui) and the upstream located gauging stations versus lag time (see Fig. 1 for a map of the stations). Symbols and vertical lines mark the respective maxima. The covariance is scaled such that the auto-covariance of water level fluctuations at Zigui is equal to 1 at zero lag. (b) lag time corresponding to the covariance maxima of the high-pass filtered water level fluctuations along TGR (see left panel) versus distance of the respective gauging station from the dam (see Table S1). Except for the first gauging station (Zigui, 2.3 km upstream of the dam), the lag time increases linearly with distance, suggesting a nearly constant speed of propagation of the diurnal water-level fluctuations (see regression line and statistics in the legend). The slope is 1.15 km min^{-1} corresponding to a speed of 20 m s^{-1}. The speed corresponds to the phase speed of a linear

shallow-water gravity wave ($c = \sqrt{gH}$, with H being mean water depth and g gravitational acceleration) with a water depth of 37 m. The correlation analysis was performed for the entire time series (2018).

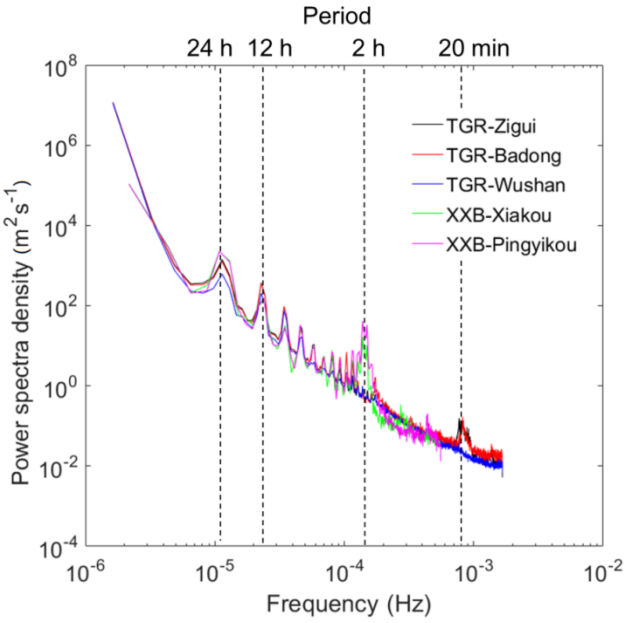

Figure S3. Power spectral density of water level fluctuations at the near-dam stations (Zigui, Badong and Wushan) in Three Gorges Reservoir (TGR) and at the two monitoring sites (Xiakou and Pingyikou) in Xiangxi Bay (XXB). The TGR spectra show a pronounced peak at 24 h (on-and-off of the turbines at TGD for power production) and at its harmonics. The occurrence of harmonics is related to the non-sinusoidal character of the 24 h regulation period and is an artifact of the Fourier-transform based power spectra. Spectra from XXB show a pronounced peak at a period of 2 h, which is related to the bay oscillation. No spectral peak was observed in TGR at this period. In addition, the spectra at Zigui and Badong show a peak at a frequency corresponding to 20 min. The nature of this oscillation is unclear.

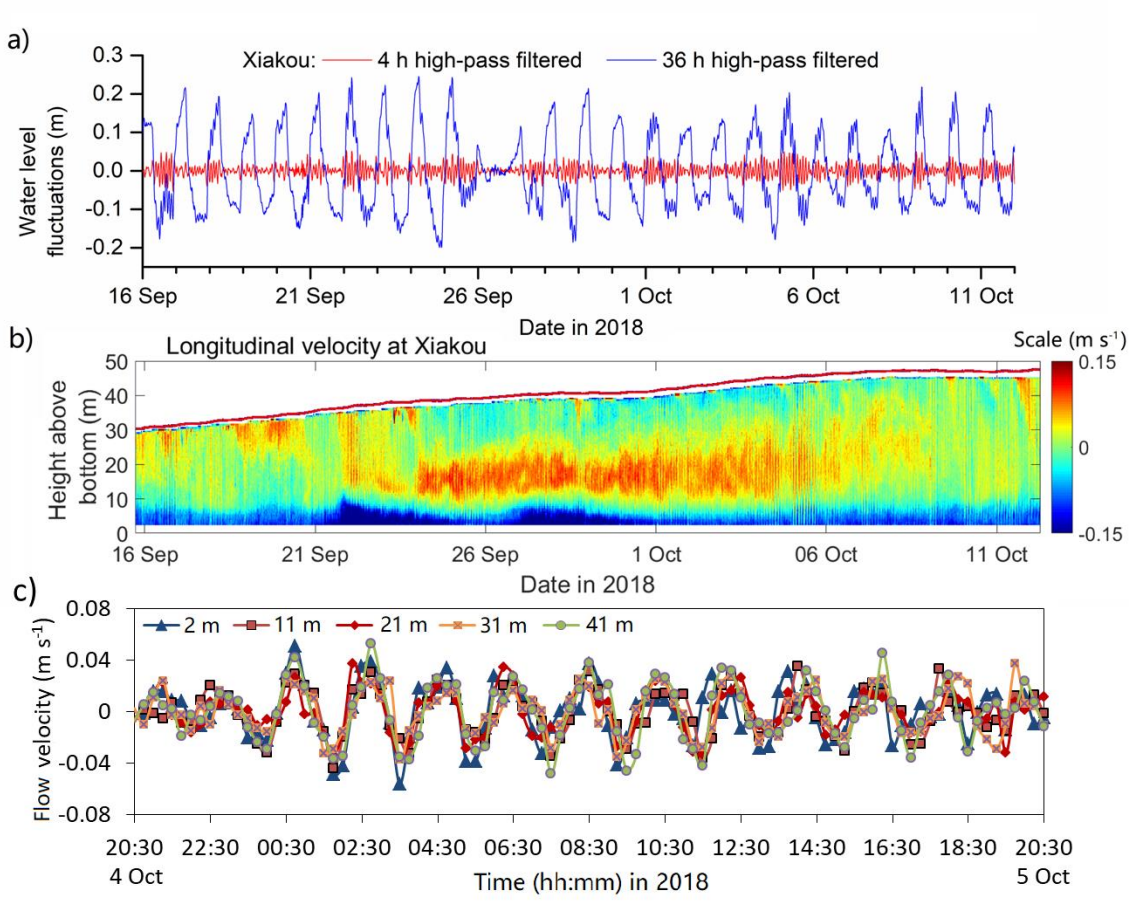

Figure S4. (a) Water level fluctuations (4 h and 36 h high-pass filtered) and b) longitudinal flow velocity in XXB at Xiakou from 16 October to 12 October in 2018. Positive flow velocity corresponds to upstream flow (from TGR into XXB); negative velocity is in the direction of river flow. The red line in b) shows water depth. c)

High-passed filtered longitudinal flow velocity (< 4 h periods) at different water depths observed during 4-5 October 2018.

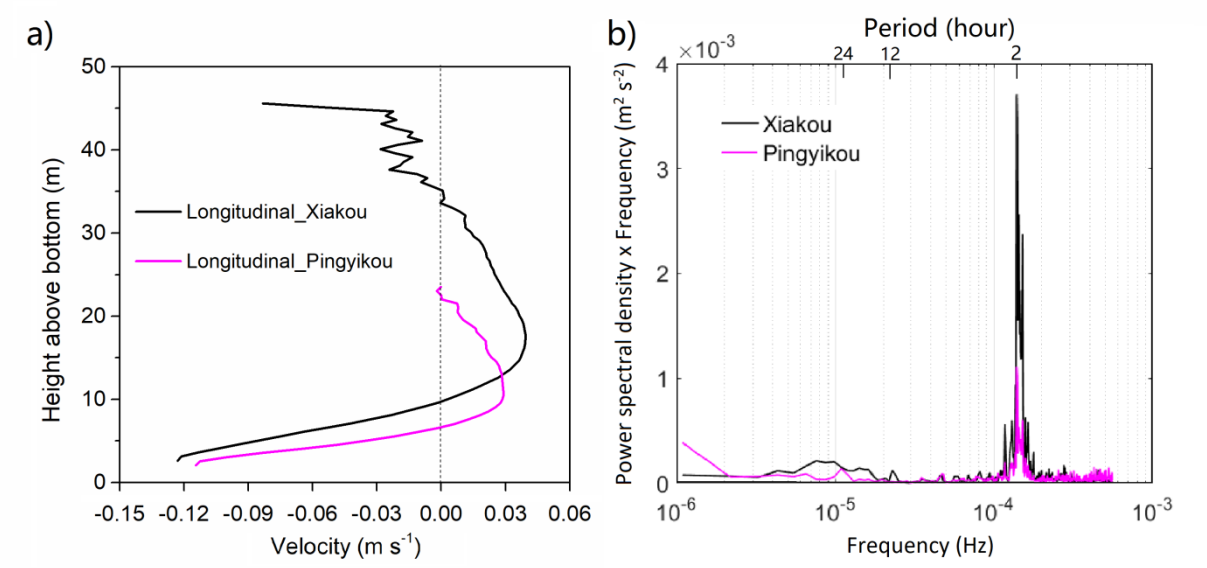

Figure S5. a) Vertical profiles of the mean longitudinal flow velocity at both monitoring sites in Xiangxi Bay (XXB). The velocities were averaged over the entire deployment period (16 Sep to 12 Oct 2018). b) Variance-preserving power spectra of longitudinal velocity fluctuations in XXB. The spectra were estimated at the depth of the velocity maximum, respectively.

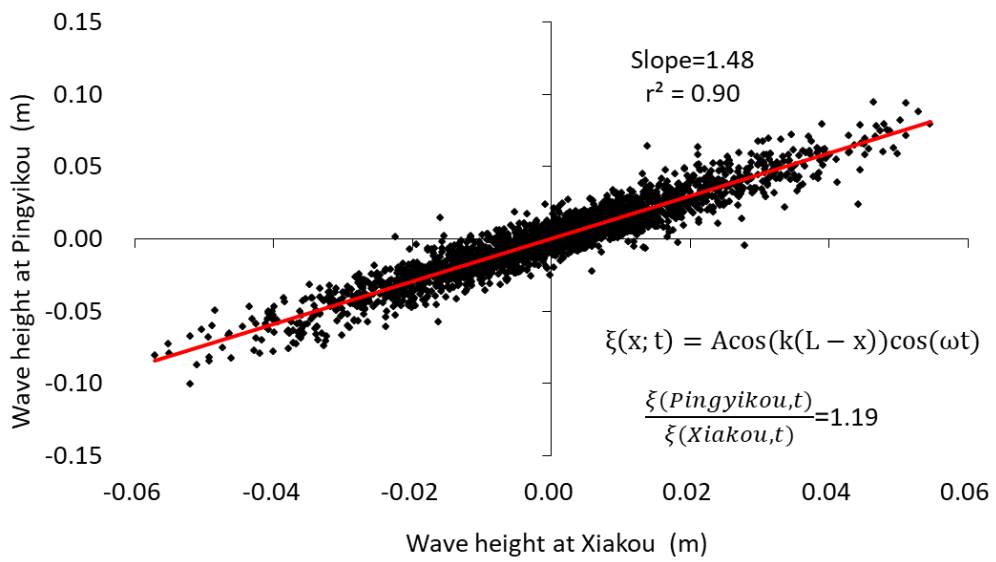

Figure S6. Comparison of measured wave height (high-pass filtered water level fluctuations with periods <4 h) at both monitoring sites in Xiangxi Bay (Xiakou and Pingyikou). The red line shows a linear regression of the measurements (slope 1.48 ± 0.01, r^2=0.90). Standing wave heights in a closed, long and narrow nonrotating rectangular basin of length, L, and uniform depth, H, have a simple trigonometric form:$\xi(x;t) = A\cos(k(L-x))\cos(\omega t)$, where ζ is the sea level elevation, A is the wave amplitude, x is the along-basin coordinate, t is time, $k = 2\pi/\lambda$ is the wave number, $\omega = 2\pi/T$ is the radial frequency corresponding to the wave period T, λ is the wavelength of the wave (four times the bay length). By assuming that at any given time and location, A, ω and λ are constant, the ratio of wave heights at Pingyikou (x = 27.4 km) and at Xiakou (x = 17.5 km) would be 1.19.

Table S1. Location and characteristics of the monitoring sites in Xiangxi Bay (XXB) and in Three Gorges Reservoir (TGR). The range of variation and mean values (in parentheses) of water depths are provided for the observation period (XXB 16/09/2018-12/10/2018, water level range of 154-172 m.a.s.l, corresponding to a total length of XXB of 34-40 km; in TGR: 01/01/2018 – 31/12/2018, water level range of 145-175 m.a.s.l.). The distance in XXB refers to the along-channel distance from the river mouth. In TGR, distance refers to the along-channel distance from Three Gorges Dam.

Name	Site	Location		Distance (km)	Depth (m)
Xiangxi Bay (XXB)	Mouth	30°57'53.7"N	110°45'34.1"E	0	72-90 (81)
	Xiakou	31°07'09.2"N	110°46'56.7"E	17.5	30-48 (39)
	Pingyikou	31°10'59.0"N	110°45'13.9"E	27.4	12-30 (21)
Three Gorges Reservoir (TGR)	Zigui	30°52'00.4"N	110°58'15.3"E	2.3	85-115 (115)
	Badong	31°03'07.5"N	110°19'56.3"E	75.4	83-113 (98)
	Wushan	31°04'02.1"N	109°52'40.0"E	122.1	80-110 (95)
	Fengjie	31°00'46.4"N	109°28'08.5"E	167.8	72-102 (87)
	Yunyang	30°55'39.8"N	108°41'14.9"E	245.7	58-88 (73)
	Zhongxian	30°17'17.5"N	108°02'20.2"E	368.5	31-61 (46)

Appendix IV

Recent changes of the thermal structure in Three Gorges Reservoir and its ecological impacts on tributary bays

Lianghong Long[1,2], Zhengjian Yang[2*], Liu Liu[3], Daobin Ji[2], Defu Liu[4], Andreas Lorke[1*]

[1] *Institute for Environmental Sciences, University of Koblenz-Landau, 76829 Landau, Germany*

[2] *Hubei Field Observation and Scientific Research Stations for Water Ecosystem in Three Gorges Reservoir, China Three Gorges University, 443002 Yichang, China*

[3] *Department of Experimental Limnology, Leibniz-Institute of Freshwater Ecology and Inland Fisheries, 16775 Stechlin, Germany*

[4] *Hubei Key Laboratory of River-lake Ecological Restoration and Algal Utilization, Hubei University of Technology, 430068 Wuhan, China*

*Correspondence:yangzi1985@ctgu.edu.cn (ZhengJian Yang);

lorke@uni-landau.de (Andreas Lorke)

Submitted to Science of Total Environment

Recent changes of the thermal structure in Three Gorges Reservoir and its ecological impacts on tributary bays

Lianghong Long[1,2], Zhengjian Yang[2*], Liu Liu[3], Daobin Ji[1], Defu Liu[4], Andreas Lorke[1*]

[1] Institute for Environmental Sciences, University of Koblenz-Landau, 76829 Landau, Germany

[2] Hubei Field Observation and Scientific Research Stations for Water Ecosystem in Three Gorges Reservoir, China Three Gorges University, 443002 Yichang, China

[3] Department of Experimental Limnology, Leibniz-Institute of Freshwater Ecology and Inland Fisheries, 16775 Stechlin, Germany

[4] Hubei Key Laboratory of River-lake Ecological Restoration and Algal Utilization, Hubei University of Technology, 430068 Wuhan, China

* Correspondence: yangzi1985@ctgu.edu.cn (ZhengJian Yang); lorke@uni-landau.de (Andreas Lorke)

Highlights:

- A significant change in the thermal regime of Three Gorges Reservoir has been observed after two newly upstream-located reservoirs operated.
- Spring stratification in Three Gorges Reservoir became weaker and less frequent.
- The development of thermal stratification in Three Gorges Reservoir was closely related to discharge and water residence time.
- Reservoir warming can alter the hydrodynamics and water quality in tributary bays.
-

Abstract

Despite the well-perceived fact that the thermal regimes of the Yangtze River have changed greatly due to the construction of Three Gorges Reservoir (TGR), little is known about how the thermal structure of TGR responded to the construction of two large upstream reservoirs in 2013. We investigated the seasonal variations of water temperature and discharge in the upper reaches of the Yangtze River by analyzing multi-year (2004-2018) hydrological and meteorological data. The effects of upstream dam construction on the thermal regime of TGR were examined, as well as the impacts of spring water temperature change on density currents and phytoplankton blooms in a typical tributary bay in TGR. The results show that water temperature in TGR increased in spring (+1.1 °C) and winter (+0.8 °C) seasons after construction of upstream reservoirs (2014-2018) compared to the years before (2009-2013). The development of thermal stratification in TGR was closely related to discharge and water residence time. The increase of inflow, which was at least partially due to upstream dam construction, was an important factor to the weakening of stratification during the spring season. The warmer TGR water in spring contributed indirectly to a dramatic reduction in the frequency and biomass of phytoplankton blooms in tributary bays of TGR. This is because a smaller difference in water temperature between TGR water and the tributary bay in spring changed the density-driven exchange between both water bodies and the resulting deepening of the surface mixed layer made is unfavourable for plankton blooms.

Keywords

Water temperature, reservoir operation, thermal stratification, density current, phytoplankton bloom

1 Introduction

Water temperature is an important physical property of surface waters because of its crucial role in ecological and biogeochemical processes (Caissie, 2006; Ducharne, 2008). For instance, associated with the rapid warming of lake surface water on the globe (Oreilly et al., 2015), the trophic cascade and eutrophication are expected to change dramatically (Kratina et al., 2012). Also the emissions of the greenhouse gas methane have been predicted and observed to increase in response to global warming (Aben et al., 2017; Dean et al., 2018). An improved understanding of the dynamics of thermal regimes in aquatic systems is therefore essential for addressing these challenges and for potential counter measures in anthropogenically affected water bodies. Water temperature of natural rivers is sensitive primarily to large-scale climate changes (e.g., air temperature and precipitation) (Han et al., 2019; Van Vliet et al., 2013). The gradual increases in river temperature observed during the last century are primarily induced by an increase in air temperatures and flow variation (Lammers et al., 2007). In addition to climate as a major driver, intensified human activities, e.g., flow regulation, construction of reservoirs and land use are increasingly modifying the thermal regimes of natural rivers (Cynthia, 2000; Prats et al., 2010).

Damming has substantially changed the hydrological and thermal regime of rivers both in space and time (Dickson et al., 2012; Wang et al., 2012a). The formation and operation of reservoirs can reduce the river thermal variability, including the range, frequency, duration and delay of temperature extremes (Casado et al., 2013; Olden and Naiman, 2010; Ren et al., 2020). Moreover, if thermal stratification builds up in reservoirs, the downstream water temperature can be greatly altered, if water is discharged from the warm surface layer or cold bottom layer. The thermal structure in stratified reservoirs can be affected by different operational strategies, e.g., selective withdrawal, discharge management (Çalışkan and Elçi, 2009; Mi et al., 2019). Additional complexity is added when considering the combined operational effects of reservoir cascades (Wang et al., 2018; Wei et al., 2011). The inflow water often forms density currents, e.g. underflows along the riverbed if the temperature of the discharged water from the upstream reservoir is lower than the bottom temperature in the downstream reservoir (Chen et al., 2016a; Gang et al., 2015), which affects the thermal regime and stratification in downstream reservoirs (Hocking and Straškraba, 1994; Long et al., 2019a).

Three Gorges Reservoir (TGR), the largest water control project in the world, has substantially altered the hydrological and thermal regimes of the Yangtze River by seasonal flow regulations and by the build-up of thermal stratification within the reservoir during the spring season (Cai et al., 2018; Chen et al., 2016b; Tao et al., 2020). As a consequence eutrophication and algal blooms became the widespread environmental problems in some tributaries of the TGR (Fu et al., 2010; Ye et al., 2007). Previous studies have evaluated the effect of damming on downstream water temperature, by comparing longer-term observations of river water temperature before and after the construction of TGR (Dai et al., 2012; Long et al., 2016). While regression models were applied to quantify the respective contributions of climate change and anthropogenic perturbations (Cai et al., 2018; Tao et al., 2020), it remains difficult to accurately evaluate the effects of damming on river water temperature by simply comparing the differences before and after damming. This is because two key processes are not considered: 1) thermal stratification in TGR may differ between different operational stages; 2) the effect of thermal stratification on downstream water temperature; 3) the effect of thermal stratification on algal blooms in tributaries. In addition to these knowledge gaps, the thermal and ecological impacts of the two newly built large reservoirs upstream of TGR have not been explored.

The main objectives of this study are to investigate the change of river water temperature, discharge, and thermal stratification in TGR. Long-term field data on hydrology and water quality were collected in the middle reaches of the Yangtze River, including water temperature, discharge, depth profiles of flow velocity and

Chlorophyll concentration. Additionally, a hydrodynamic model (CE-QUAL-W2) was used to simulate the response of density currents in tributary bays to changes in the thermal structure of TGR. The study will contribute to understanding of the ecological impacts of cascading reservoirs and provide information for optimization of reservoir management.

2 Materials and methods

2.1 Study area

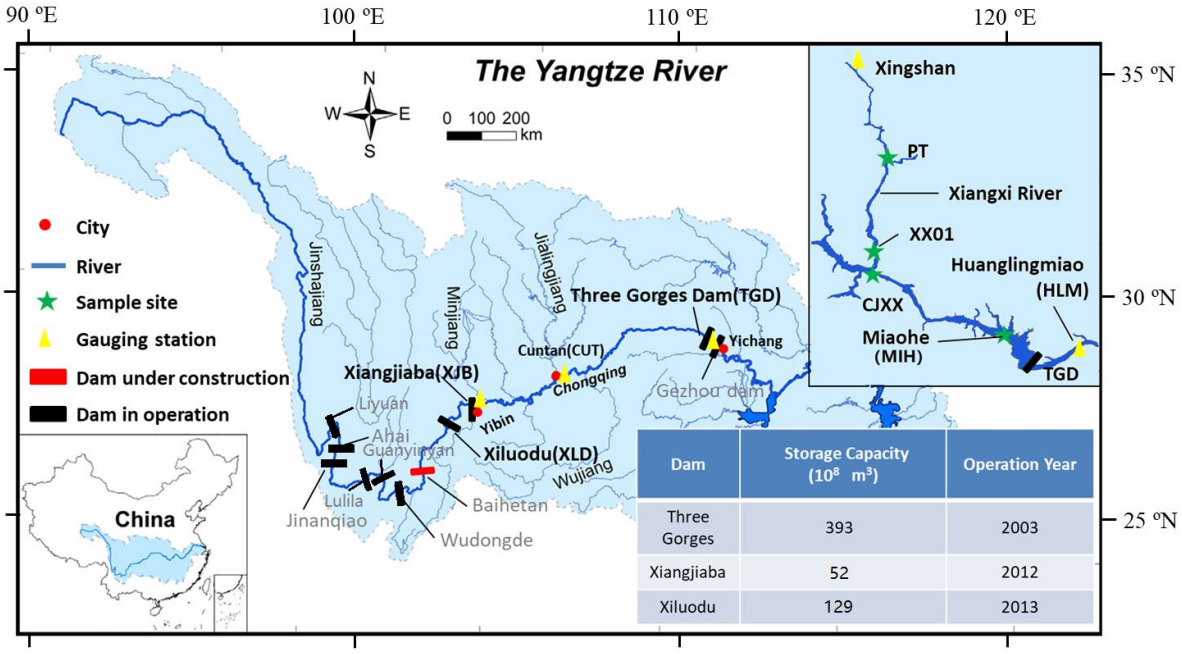

Fig. 1. Map of the upper and middle Yangtze River with names of hydropower dams in operation (black bars) and under construction (red bars). The lower left inset map shows the location of the studied region in China. The upper right inset map shows the location of sampling sites in a representative tributary (Xiangxi River) of TGR. The inset table shows the related information on completed hydropower dams. The catchment area is marked by light blue color. The three gauging stations used in the present study (Xiangjiaba, Cuntan and Huanglingmiao), and four meteorological stations (Yibin, Chongqing and Yichang, Xingshan) are marked by yellow triangles and major cities are marked by red filled circles, respectively.

The Yangtze River is the longest river in Asia and the fourth largest river in the world in terms of discharge. Its upper reach incorporates the zone upstream of Yichang city (Fig. 1), the middle reach stretches out from Yichang to Datong, and the lower reach extends from Datong to the river mouth at Shanghai. The Three Gorges Dam (TGD) is located at Yichang. Three Gorges Reservoir (TGR) is one of the largest impoundments in the world, with a storage capacity of 3.93×10^{10} m^3 at normal water level of 175 m above sea level (a.s.l.), a surface area of 1080 km^2 and watershed area of more than 1.0×10^6 km^2 (Xu et al., 2011). TGR is located along the main stream of the Yangtze River between Chongqing and Yichang (Fig. 1). The average basin-wide precipitation is 1070 mm yr^{-1}, and 70-80% of annual precipitation and > 80% of discharge occur during the flood season between May and October (Cai et al., 2018). Xiangxi River (XXR) is the largest tributary in the lower reach of the TGR (32 km upstream of the dam). It is also one of the representative eutrophic tributary bays of TGR (Yang et al., 2013).

2.2 Data and measurements

We analysed data from four sampling locations along the main stream of the upper Yangtze (Fig. 1). The sites are located at the outflow of the upstream dam (Xiajiaba, XJB, 914 km upstream of TGD), at the upstream end of TGR (Cuntan, CUT, 608 km upstream of TGD), near TGD (Miaohe, MIH, 14 km upstream of TGD), and near the outflow of TGR (Huanglingmiao (HLM), 12 km downstream of TGD). Being located upstream of TGR, XJB was chosen as a reference station that was affected by the two upstream dams (Xiangjiaba and Xiluodu), which were completed in 2012 and 2013, respectively, while CUT was chosen as a reference station that was not affected by the construction of TGD but potentially affected by the construction of upstream dams (Cai et al., 2018). In TGR, depth profiles of water temperature in the dam area were measured at MIH during spring. HLM station was used as a represent the outflow of TGR.

Daily measurements of water temperature and discharge for the period 2009–2018 at the three stations (XJB (Before it goes into service in 2012 replaced by Pingshan station, 29 km upstream of Xiangjiaba Dam, abandoned after 2012), CUT and HLM) were provided by the Yangtze Water Resources Commission (*http://xxfb.hydroinfo.gov.cn*). Monthly mean air temperature in the same time period at the three stations were obtained from the daily weather data from the nearest meteorological stations (Yibin, Chongqing and Yichang) (*http://www.data.cma.cn*). Vertical water temperature at Miaohe (MIH) were recorded by temperature loggers (HOBO MX2203) at water depths of 1, 3, 5, 7, 10, 13, 16, 20, 25, 30, 40, 50, 70, 90, 110, 130 m and at the bottom with a temporal resolution of three times in the early, middle and late ten-day period of each month in 2004-2018.

In the tributary bay of the Xiangxi River, monthly depth profiles of water temperature and flow velocity were measured at the river mouth (CJXX) and in the tributary (XX01, cf. Fig. 1) during 2010-2015, using a Hydrolab DS 5X multi-probe (Hach, USA) and an Acoustic Doppler Velocimeter (ADV, Vector, Nortek, Norway) with a vertical resolution of 2 m. Daily measurements of Chlorophyll-a (Chl.a) concentrations in XXB were conducted during sping season (March to May) using a Hydrolab DS 5X multi-probe at a water depth of 0.5 m from a moored platform (station PT, Fig. 1) from 2009 to 2017, except for 2013. In XXB, daily inflow rate and meteorological data (including air temperature, humidity, wind speed and direction, cloud cover and total incident solar radiation), and weekly measurement of inflow temperature) were obtained from 'Xingshan' gauging station, ~36 km upstream of the mouth of XXR (Fig. 1). Water level close to dam, daily outflow from TGR (from the China Three Gorges Corporation (*http://www.ctgpc.com.cn/*)), and temperature profiles at MIH were used as the downstream boundary condition for numerical modelling (see below).

2.3 Data processing

Data analysis of daily water temperature and discharge were conducted at seasonal time scale, in which we defined the four seasons as spring (March–May), summer (June–August), autumn (September–November) and winter (December–February). Vertical thermal stratification in TGR was defined using a threshold for the maximum difference between surface and bottom water temperature (MTD) of 0.5 °C. Water residence time (WRT) in TGR was calculated as reservoir storage volume divided by the mean discharge at TGD. The storage volume of TGR was estimated from water level using the reservoir capacity regression curve (Fig. S1).

2.4 Hydrodynamic model

We used a two-dimensional (longitudinal and vertical), laterally averaged, hydrodynamic and model CE-QUAL-W2, (Cole and Wells, 2013)) to simulate the density-driven exchange flows between XXR and TGR during the period 2009 to 2018. Monthly statistics of spring density current patterns at the mouth of XXR were estimated from model simulations following (Long et al., 2019b), see supplemental material for details. The XXR is river-type tributary bay that has a length-to-width ratio of ~400, which is suitable for the application of

CE-QUAL-W2. The model of XXR was represented by 64 longitudinal segments between 500 and 1000 m in length and 109 vertical layers of 1 m thickness and widths ranging from 20 to 1300 m. The accuracy of the bathymetry was confirmed by comparing the observed and simulated storage water elevation curves. The plunging points, intrusion travel distances and flow velocities agreed well with observations, indicating that the model can accurately simulate the important features of density currents in the tributary bay (Long et al., 2019b; Ma et al., 2015). According to the depth of plunging points, three different density currents were distinguished: underflow, interflow and overflow (see Fig. S2 for examples). The frequency of occurrence of each type of density currents in spring was calculated from 2009 to 2018.

3 Results

3.1 Overview of the TGR operation

The water level management of TGR during filling and operation can be divided into four stages (Fig. 2). TGR was initially filled from 70 to 139 m in October 2003 and then maintained the levels between 135-139 m until 2006 (stage I). During a transitional period between October 2006 and October 2008, the water level varied between 145-156 m (stage II). Starting from 2009, the reservoir has been in full operation with seasonal water level variations between 145–175 m. We divide this normal operation period into stage III (2009-2013) and stage IV (2014-2018), representing the time before and after two upstream located dams (Xiangjiaba and Xiluodu) became operative in October 2012 and May 2013, respectively. Since 2010 TGR started to operate at a seasonal mode, i.e., 1) flood season - the reservoir operates at the lowest level of 145 m during the flood season (June-August); 2) impoundment - the reservoir is filled rapidly up to the normal water level of 175 m in September-October; 3) dry season - the reservoir operates at normal water level during November-January and 4) drawdown - water level decreases slowly until mid-June.

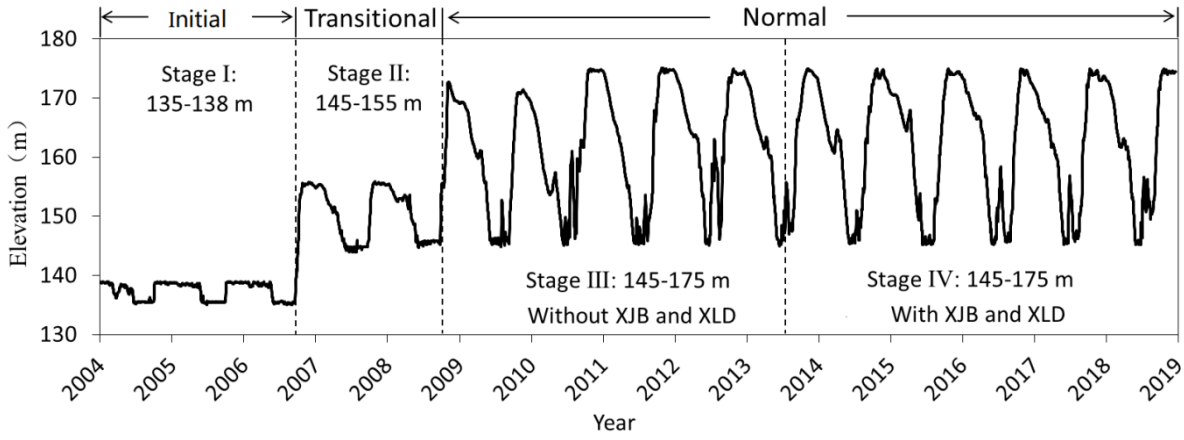

Fig. 2. Daily measurements of water level near to Three Gorges Dam in 2004–2018. Different operational stages are distinguished by vertical dotted lines, see text labels for explanation (numbers represent the range of water level fluctuations during each stage).

3.2 Changes in the thermal regime of TGR in response to the completion of upstream reservoirs

At XJB, the seasonal mean values of water temperature differed significantly between stage III and stage IV, i.e. before and after dam construction ($p < 0.01$, Fig. 3). The temperature of the outflowing water from XJB was lower in spring (-2.6 °C) and summer (-0.7 °C), and higher in autumn (+1.2 °C) and winter (+1.7 °C), compared to the average water temperature during stage III. At the inflow of TGR (CUT station), the increase in water temperature was smaller (+0.8 °C in autumn and +1.2 °C in winter), while no significant difference was

observed in spring and summer. This indicates a high recovery ability of the natural rivers section between the reservoirs in respect to temperature. At the outflow of TGR (HLM), mean water temperature increased in winter (+0.8 °C) and in spring (+1.1 °C). While increase in winter is consistent with the trends observed at the two upstream sites, the temperature increase in spring is opposite to the observed trend at XJB. There were no significant changes in mean water temperature at HLM in summer and autumn (Fig. 3)

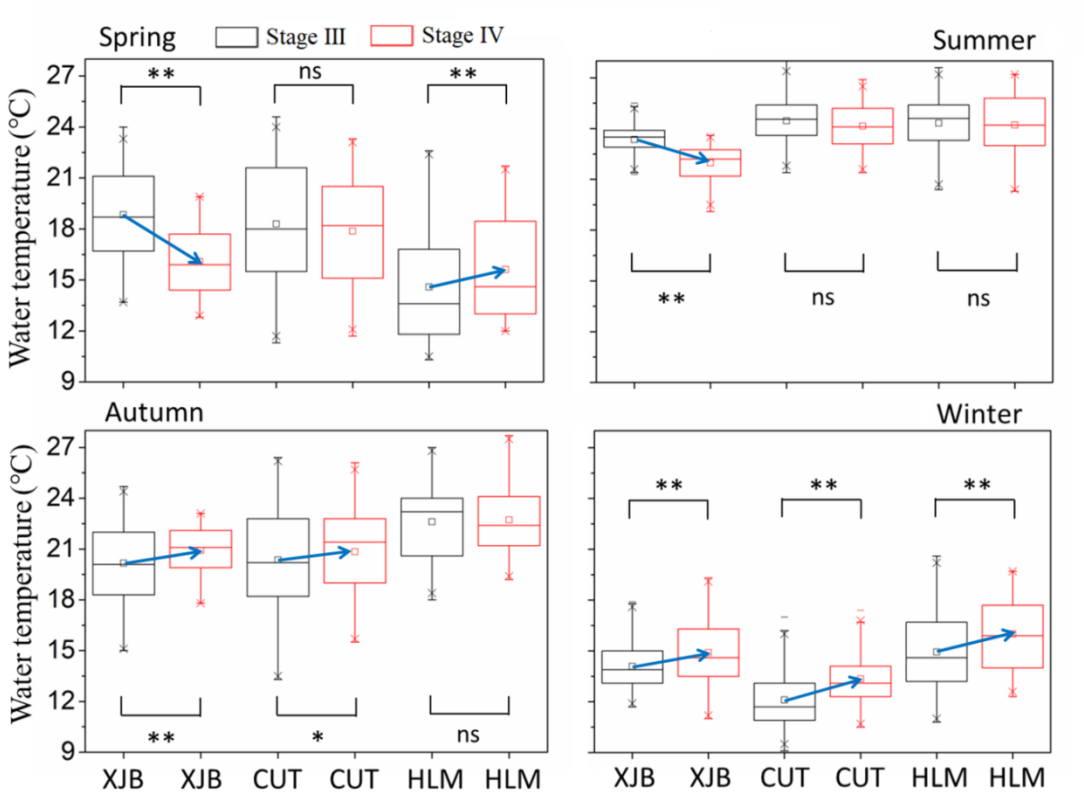

Fig. 3. Seasonal changes in water temperature at XJB, CUT and HLM sites during stage III (2009–2013) and stage IV (2014–2018). The box plots show the variability of daily water temperature (boxes mark the range between the first and third quartiles, crosses outside the box show the minimum and maximum values, the horizontal line is the median value and square symbols are mean values). Significant differences in water temperature were tested using a *t*-test: *: $p < 0.05$; **: $p < 0.01$; ns: not significant. Blue arrows indicate trends in water temperature.

The spring thermal regime in the dam area changed from non-stratified in the initial filling stage, to strong stratification in the transitional stage, then to weak stratification in stage III stage and finally to further weakening in stage IV (Fig. 4). During the analysed period, the bottom cold water was present below the elevation of 80 m, which was far below the position of intakes (elevation: 110 m). No vertical temperature differences (< 0.1 °C) were observed during the initial period except 2006. The first short-term thermal stratification appeared in April 2006 and was gradually intensified (MTD up to 6.6 °C) with a maximum vertical temperature gradient of 0.16 °C m^{-1}, and then faded rapidly associated with the increasing water temperature in May. The strongest stratification occurred during the transitional period with a maximum temperature difference of 10.3 °C and a vertical gradient of 0.42 °C m^{-1} until mid-June, when the discharge substantially increased. The days of stratification increased to three full months during this period (Fig. 4, detailed statistics of stratified days and MTD is presented in Table S1). The thermal stratification was gradually weakened since TGR started to operate at high water levels in normal operation period, particularly during stage IV. Stratification with MTD between 4.7 and 7.6 °C persisted for 39 to 66 d in stage III (Table S1), whereas MTD was reduced to 2.8 to 1.5 °C with shorter duration of stratification (10–39 d) in stage IV.

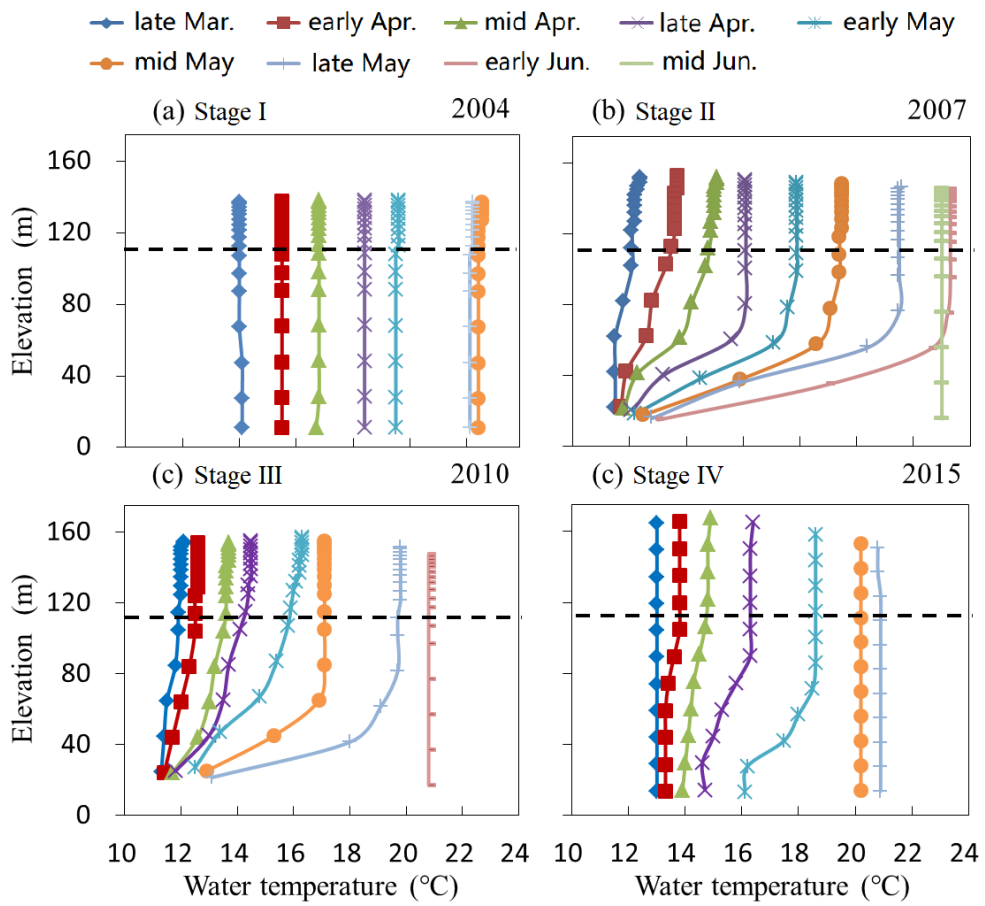

Fig. 4. Development of spring thermal stratification in Three Gorges Reservoir (station MIH) during four selected years, representative for stage I to IV, respectively. Coloured lines with symbols show water temperature profiles measured during spring (see legend, the exact sampling dates varied among the ears). The horizontal black dotted line marks the elevation of the water intake at Three Gorges Dam.

3.3 Effects of upstream dams on discharge dynamics

The impact of upstream reservoirs on TGR was not only reflected by water temperature, but also by discharge (Fig. 5). A significant ($p < 0.01$) increase in discharge in spring and winter at all stations was observed in stage IV, compared to stage III. The increments of spring discharge along the river were 806, 2062, and 1751 $m^3 s^{-1}$, respectively. The upstream dams accounted for ~39% of the changes in inflow of TGR (at CUT). The mean increase of discharge in winter was 443, 1361, 514 $m^3 s^{-1}$, respectively. In summer, the discharge at XJB decreased lightly, but not significantly ($p > 0.05$), while discharge at CUT and HLM dropped by ~2000 $m^3 s^{-1}$. This indicates that a part of the water could have been stored by smaller dams at tributaries entering the Yangtze River between XJB and CUT. In autumn, the increases of discharge at XJB and CUT in stage IV were 950 and 2000 $m^3 s^{-1}$, respectively, but no significant change was found at HLM. As a whole, after upstream dams came to operation, river discharge downstream of TGR was greatly modified, with higher discharge in spring and winter and a reduction in summer.

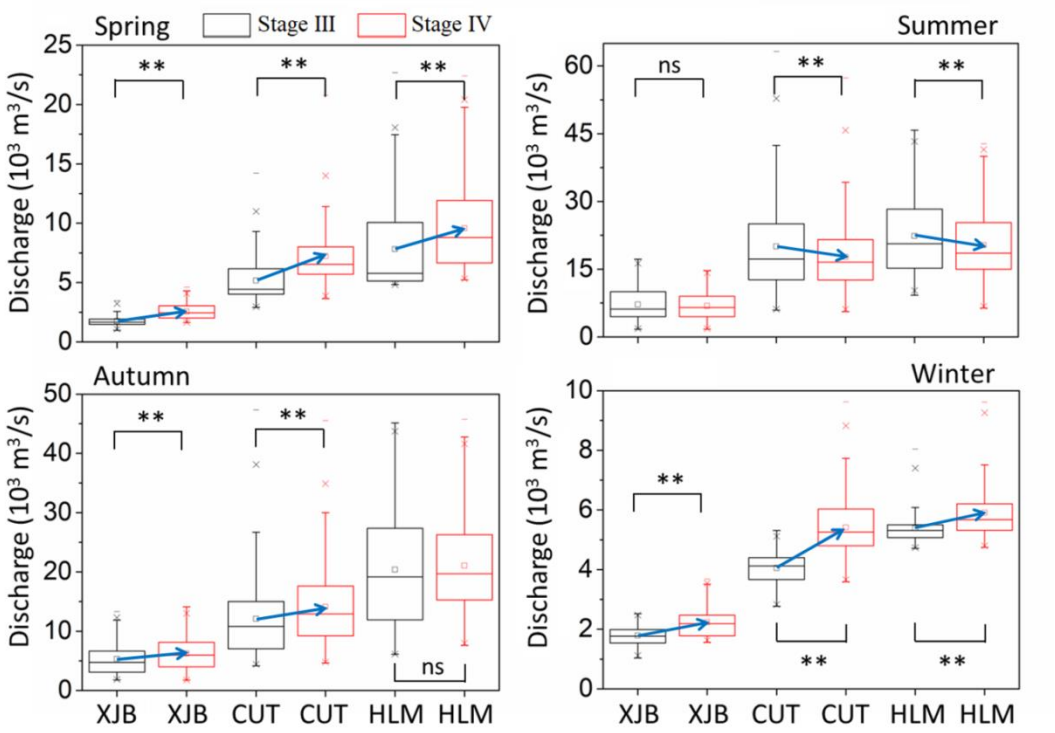

Fig. 5. The seasonal changes in discharge at XJB, CUT and HLM between stage III (2009-2013) and stage IV (2013-2018). Box plots show statistics of daily discharge measurements (see caption of Fig. 3 for explanation of the box elements). Significance levels (*t*-test) are indicated: *: $p < 0.05$; **: $p < 0.01$; ns: no significant. Blue arrows represent trends in mean discharge between both operational stages.

3.4 Impacts of TGR operation on thermal stratification

Spring thermal stratification in TGR was affected by reservoir operation. This is evidenced by the strong correlation between maximum temperature difference between surface and bottom (MTD) and number of days with stratification on one hand, and discharge and water residence time (WRT) on the other hand (Table 1 and Fig. 6). Spring stratification in TGR did not significantly correlate with inflow water temperature and air temperature at Yichang, but MTD and stratified days were both correlated to discharge at CUT and TGD ($p < 0.05$). In addition, both parameters describing stratification (MTD and number of stratified days) were strongly correlated with each other ($p < 0.01$). A linear regression between discharge at CUT and number of stratified days for the period 2009-2018 suggests that the critical inflow discharge for no stratification is 7602 $m^3 s^{-1}$ (Fig. 6a). But this threshold is inappropriate for the period 2004–2008, because of the large difference of mean water level in spring during the two operational stages (Table S1). The water residence time at different stages was both closely related to the number of stratified days, but the slopes differed between both stages, which were probably due to too few data points in 2004–2008 (Fig. 6b). For the same WRT, the number of stratified days was higher in the transitional period because of lower discharge with less storage capacity. During the first two years (2014–2015), shallow water depth with extremely low water level promoted persistent vertical mixing. From 2009 to 2018 spring average water level varied between 155–162 m. Because the WRT was reduced in stage IV compared to stage III, the stratification got weakened with the decreasing MTD and stratified days. Besides, downstream water temperature (WT_{HLM}) was closely related to discharge (Q_{TGD}) and surface water temperature in the reservoir (WT_{MIH}, Table 1).

Table 1 Correlation matrix (correlation coefficients) for variables related to reservoir operation and thermal regime in stage III and stage IV: discharge at XJB (Q_{XJB}), CUT (Q_{CUT}), and TGD (Q_{TGD}, outflow at TGD), water temperature (WT) at CUT, MIH, HLM stations, air temperature (AT) at Yichang, stratification (maximum temperature difference (MTD) and number of stratified days and water residence time in TGR (WRT). Numbers above the diagonal are Pearson correlation coefficients, numbers below the diagonal are significant levels (*p*-values, double-tailed *t*-test). Significant correlations are marked as: ** at 0.01 level and * at 0.05 level.

	Q_{CUT} (m^3/s)	Q_{TGD} (m^3/s)	WT_{CUT} (°C)	WT_{MIH} (°C)	WT_{HLM} (°C)	$AT_{Yichang}$ (°C)	MTD (°C)	Stratified (day)	WRT (day)
Q_{CUT} (m^3/s)		0.85**	-0.25	0.76*	0.50	-0.16	-0.87**	-0.86**	-0.81**
Q_{TGD} (m^3/s)	0.00		-0.08	0.64*	0.69*	-0.18	-0.70*	-0.76*	-0.93**
WT_{CUT} (°C)	0.49	0.83		0.05	0.26	0.57	0.39	0.44	0.20
WT_{MIH} (°C)	0.01	0.05	0.89		0.80**	-0.01	-0.76*	-0.67*	-0.69*
WT_{HLM} (°C)	0.14	0.03	0.47	0.01		-0.05	-0.50	-0.49	-0.70*
$AT_{Yichang}$ (°C)	0.67	0.61	0.09	0.98	0.89		0.19	0.28	0.36
MTD (°C)	0.00	0.02	0.26	0.01	0.14	0.59		0.97**	0.68*
Stratified (day)	0.00	0.01	0.20	0.03	0.15	0.44	0.00		0.70*
WRT (day)	0.00	0.00	0.58	0.03	0.02	0.31	0.03	0.03	

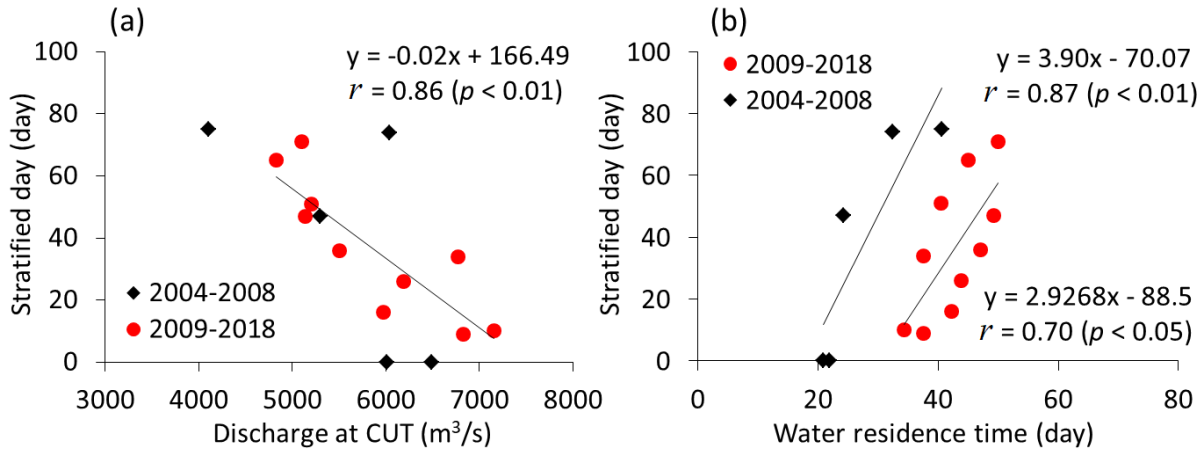

Fig. 6. (a) Linear regression between number of stratified days in TGR and spring average discharge at CUT in 2004-2008 (black symbols) and 2009-2018 (red symbols and line). For the first period, the Pearson correlation coefficient (*r*) was not significant (no regression line shown). For the second period, the regression equation and correlation statistics is shown in the legend. The intercept of the regression line corresponds to a critical discharge for no stratification (zero stratified days) of 7602 m^3 s^{-1}. (b) Linear regression between the number of stratified days and spring average water residence time in 2004-2008 and 2009-2018. Regression equations and correlation statistics are shown in the legend.

3.5 The effect of thermal structure on tributary bays

Consistent with previous studies, observations of flow velocity in the tributary bay (XXB) revealed persistent, bidirectional density currents, which were driven by the temperature differences between the tributary bays and TGR (Fig. 7). The faster warming of TGR mainstream (CJXX) than in the tributary (XX01) during spring, caused a gradual uplift of the intrusion from TGR from the bottom (2010 March, Fig. 7) to the middle of the water column (2010 April, Fig. 7), and eventually to the water surface (2010 May, Fig. 7). In 2015, for example, the warming-induced lift-up of the intrusion occurred one month earlier than in 2010. The statistics of

density currents in spring obtained from the modelling results indicate a dramatic increase (from 33 to 91%) of the likelihood of overflows after 2015 (Fig. 8a).

In close synchrony with the notable change in intrusion depth since 2015, a sharp decrease in both frequency and biomass of phytoplankton blooms (represented by chlorophyll-a concentration) was observed in XXB (Fig. 8b and c). For example, high concentrations of Chl.a were observed in spring 2010, which exceeded the threshold of algal bloom (30 μg L^{-1}) (Zheng et al., 2006) in TGR on late March and mid, late April. In spring 2015, in contrast, the chlorophyll concentrations were strongly reduced and algal blooms occurred on only mid-May (Fig. 8b). Generally, a sharp reduction of mean Chl.a concentration was observed since 2014 (Fig. 8c), in agreement with the density pattern changes (Fig. 8a) except 2014. During advantageous condition of density current, the decrease in Chl.a in 2014 could be caused by uncertain factors, eg., weather, nutritions. The reduction in phytoplankton blooms was not only found in this particular tributary bay, but has been reported for almost all tributary bays of TGR (Fig. S4).

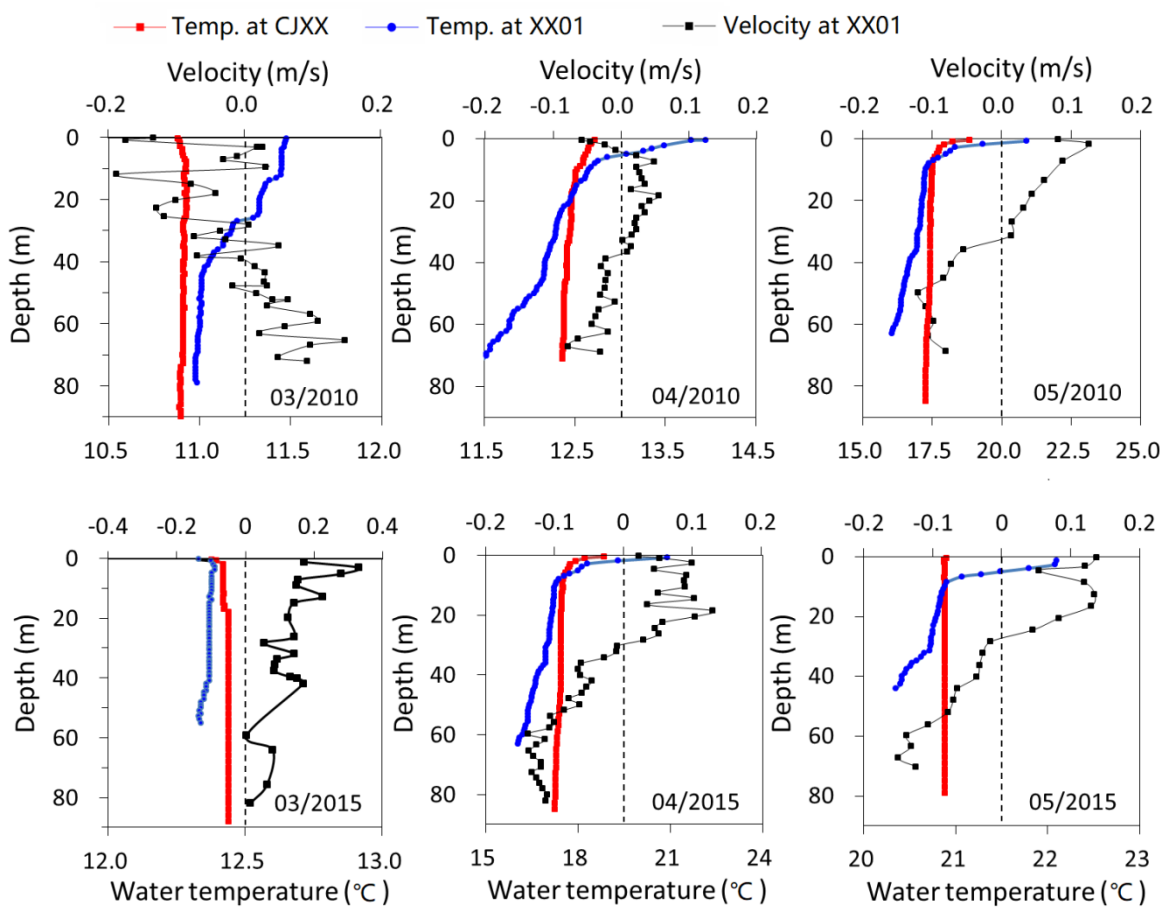

Fig. 7. Flow velocity and temperature profiles measured at the mouth of the Xiangxi River in stage III (March, April and May 2010, upper row) and stage IV (March, April and May 2015, lower row). Temperature profiles are shown for TGR (red colour) and in the bay (station XX01, blue colour). Positive flow velocity corresponds to upstream flow (from TGR into the tributary. Negative velocity represents water flowing into TGR.

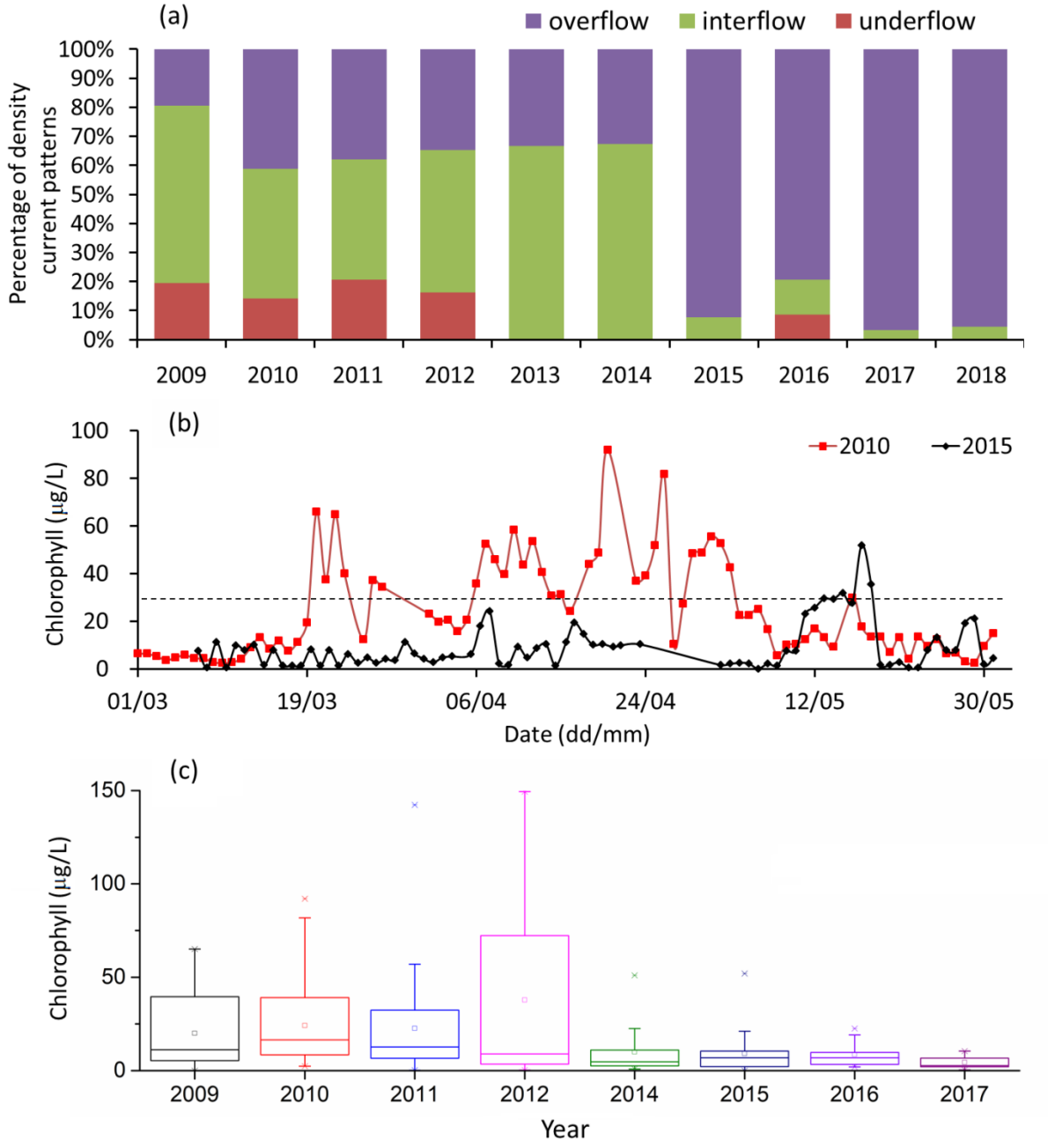

Fig. 8. (a) Relative frequency of occurrence of different patterns of density currents (overflow, interflow and underflow, see legend) in Xiangxi bay during spring season for the period 2009 to 2018. (b) Daily measurements of chlorophyll-a in the surface water of the bay (station PT) during spring in 2010 (red colour) and in 2015 (black colour). The black dotted line indicates a threshold concentration for algal blooms (30 µg L^{-1}). (c) Box plots of daily mean chlorophyll-a concentration during spring for the period 2009–2017. Boxes mark the range between the first and third quartiles, crosses outside the box show the minimum and maximum values, the horizontal line is the median value and square symbols are mean values.

4 Discussion

4.1 Changes of the thermal regime of TGR

A dramatic shift in the thermal regime of TGR was observed since 2014, when two upstream reservoirs were completed. The upstream reservoirs caused a significant cooling in spring (-2.6 °C) and summer (-0.7 °C), and warming in autumn (+1.2 °C) and winter (+1.7 °C) at the outflow of the lower new reservoir (XJB station). The upstream cooling effects in spring and summer were not detected at the upstream end of TGR (CUT, Fig. 3), while the warming effects were transmitted downstream with decreasing amplitude (e.g., the magnitude of winter warming decreased from +1.7 °C at XJB, to +1.2 °C at CUT and +0.8 °C at TGR outflow (HLM). It is noteworthy, that the spring inflow water temperature of TGR did not change significantly, but the outflow temperature increased by +1.1 °C at HLM. Simultaneously, spring stratification in TGR became weaker and less frequent. By analysing water temperature observations over prolonged periods (1975–2014), Cai et al, (2018) quantified the effects of TGR dam on water temperature in the Yangtze River at Yichang as a reduction by -1.8 °C in spring and an increase of +3.1 °C in winter. The recent changes of the thermal regime are therefore further amplifying the effect of hydropower developments on water temperature downstream of TGD.

The causes of changes in the thermal regime in reservoirs can be manifold: 1) changes in inflow due to the upstream reservoirs (Gang et al., 2015; Long et al., 2019a); 2) reservoir discharge operation (Prats et al., 2010; Wang et al., 2012a; Winton et al., 2019); and 3) regional climate change (Johnson et al., 2004; Wang et al., 2012b). In cascading reservoirs, cumulative impacts can be additive, as it has been found for the Mekong River (Lauri et al., 2012; Trung et al., 2018) and Yangtze River (Ali et al., 2019; Wang et al., 2018). Compared to a solitary reservoir, inflowing water often forms a density current along the channel bottom due to lower release temperature of the upstream reservoir (Chen et al., 2016a), which can strengthen thermal stratification in the cascade reservoir (Hocking and Straškraba, 1994). This effect has been observed in Xiangjiaba reservoir, where the upstream located Xiluodu reservoir affected vertical stratification (Long et al., 2019a). We found that the cooling effect of the two upstream located reservoirs are not further transmitted to downstream reservoirs, after the Yangtze river flows along a 400 km long undeveloped section between XJB and CUT. This is in agreement with analyses by He et al., (2020), who estimated a recovery of 61% from the thermal impacts of the upstream dams along this free-flowing river section. The temperature at the outflow of TGR, however, increased of +0.8 °C during spring, suggesting that other mechanism contributed to the changes in thermal regime than inflow temperature. Compared to stage III, the inflow discharge of TGR in stage VI increased in spring (1430 m^3/s), autumn (1523 m^3/s), and winter (912 m^3/s) but decreased (2280 m^3/s) in summer. The flow modifications by upstream dams accounted for about 39, 13, 48 and 33% of the inflow changes at CUT from spring to winter, respectively. In addition to discharge from Jinsha River basin, which accounts for 26.3 % of the Yangtze River Basin in terms of it drainage area (Lu et al., 2019), other inflows major enter the Yangtze river between XJB and CUT, e.g., the Minjiang River (~8.9 % in terms of its water yield) (Cui et al., 2012), the Jialing River (~9 % in terms of it drainage area) (Zeng et al., 2015)). Unfortunately, no data were available for these tributaries.

Previous studies have shown that reservoir stratification is affected by discharge operations (Johnson et al., 2004; Wang et al., 2012b). Statistical analyses suggested that the spring stratification in TGR was closely related to discharge. The decrease of the number of stratified days from 55 to 22 d and the reduction of the mean vertical temperature difference between surface and bottom from 5.9 to 2.0 °C from stage III to stage IV were related to the higher discharge in spring and shorter WRT. Previous analysis for stage I to III already demonstrated that differences of WRT caused by water level differences led to the drastic changes of stratification in T GR (Cao et al., 2012). We estimated a critical discharge (inflow in TGR) of 7602 $m^3 s^{-1}$, for which the number of stratified days would approach zero. This estimate in approximate agreement with a theoretical prediction of 6000 $m^3 s^{-1}$ in April (Huang, 1999). The thermal regime is not only influenced by human activities, but also by climate change. Previous studies have estimated a climatically-driven increase of water temperature in the Yangtze river basin of 0.4 °C between the 1950s and the pre-TGD decade (1993–2002) and an additional increase by 0.4 °C in the

post-TGD decade (2003–2012) (Othman Ali et al., 2019; Yang et al., 2015). This increase in water temperature agrees with the global land temperature increase of the same period (Stocker et al., 2013). On the other hand, reservoir cooling impacts on downstream temperatures can offset climate-related warming (Cheng et al., 2020). The observed spring (1.1 °C) and winter (0.8 °C) warming downstream at TGR during stage IV, however, is significantly higher than the effect of climate warming. Moreover, statistical analyses showed that there was no significant change of the air temperature in the study area (Fig. S3) and water temperature (WT_{MIH}) was not significantly correlated to air temperature ($AT_{Yichang}$) ($p > 0.05$) during the course of 10 years (2009–2018). This suggests, that the observed warming can rather be attributed to alteration of the hydrological regime. Dam operation and cascade dam construction therefore play important roles in the thermal regime and stratification in TGR.

4.2 Ecological impacts of changes in the thermal structure

The change in thermal structure of TGR is a likely reason for the observed dramatic changes in aquatic ecology in tributary bays of TGR since 2013. Our simulations showed the warmer TGR water in spring caused a three-fold increase of the frequency of occurrence of overflows. This change in density-driven exchange resulted in alterations of the mixing regime in the tributary bay, i.e., deepening of the surface mixed layer (Long et al., 2019b). The deeper mixed layer results in a reduction of the ratio of thickness of euphotic zone to mixing depth and therewith to unfavourable conditions for phytoplankton blooms in the Xiangxi River (Fig. 8c) and potentially also in other tributary bays (Fig. S4).

Previous studies demonstrated that density currents have significant effects on the thermal structure, transformation and transport of nutrients, phytoplankton blooms, and aquatic ecosystem succession in the tributaries (Ji et al., 2017; Liu et al., 2012; Yang et al., 2010). Further studies have shown that the risk of algal bloom in TGR will be different during different density currents (Long et al., 2019b). Overflow can increase surface water velocity, causing more intense mixing and rapid break-up of thermal stratification. Interflows provide more favourable hydrodynamic conditions for phytoplankton, such as a stagnant and stratified surface layer with longer residence time (Long et al., 2019b).

The mechanism of bloom control in tributary bays of TGR by density currents has been described by Liu et al. (2012), who observed a change in intrusion depth from TGR from mid depth to the water surface in response to a rapid water level rise in summer, which caused a sharp decrease in phytoplankton biomass in the tributary bay. Flow regulation with larger-amplitude diel water level fluctuations have been proposed for TGR for the purpose of phytoplankton control (Liu et al., 2012; Yang et al., 2013), but large fluctuations of water levels like it in storage period are difficult to implement due to flood control requirements. Our results suggest that spring warming has a similar effect on the pattern of density current and hydrodynamics in the tributary bay.

Besides changes in the thermal structure of the reservoir and its tributary bays, the effect of dam construction on the thermal regime of downstream rivers have attracted widespread attention (Maheu et al., 2016; McCartney et al., 2001). The warming or cooling effect can alter water quality, habitat conditions and biological communities (Mbaka and Wanjiru Mwaniki, 2015; Zhou et al., 2014), as well as on fish migration and availability of suitable spawning grounds (Barbarossa et al., 2020). For TGR, it has been reported that shifts in the seasonal timing of water temperature reaching 20 °C can have a great influence on fish spawning (Gao et al., 2014; Lu et al., 2013). Wang et al., (2020) estimated by modelling that water temperature changes after cascade dam operation in the Yangtze River will result in a further delay of fish spawning times. Thus, accurately and timely understanding of the dynamic of the thermal regime in TGR is important for assessing the impacts of cascading hydropower development on the river ecosystem.

5 Conclusions

A significant change in the thermal regime of TGR has been observed since the year 2013, when two newly created upstream-located reservoirs became operative. The results show that the TGR water was warmer in spring (+1.1 °C) and winter (+0.8 °C) during 2014-2018, compared to the years 2009-2013. A reduction of water temperature during spring was observed at the upstream dams, but not in the inflow of TGR. Spring thermal stratifications near to dam became weaker, with reductions of the number of stratified days and the maximum temperature difference between surface and bottom. The change in thermal stratification in TGR in spring was mainly caused increasing inflow discharge, which was only partially caused by flow modification from the new upstream dams and additionally affected other tributaries. Reservoir warming not only changed the downstream water temperature, but also altered the hydrodynamics and water quality in tributary bays. As a result of increasing water temperature in TGR in spring, the intrusion depth of water from the main reservoir in the tributary bay (XXB) was more frequently lifted to the surface, causing a sharp reduction in both magnitude and frequency of phytoplankton blooms in the bay.

Acknowledgments

This work is financially supported by the Natural Science Foundation of China (grant No. 91647207, 51779128, 51879099, 52079075). The Hubei province Chutian Scholar program (granted to Andreas Lorke) provided additional financial support for the field measurements.

Reference

Aben, R.C.H. et al., 2017. Cross continental increase in methane ebullition under climate change. Nature Communications, 8(1): 1682. DOI:10.1038/s41467-017-01535-y

Ali, R., Kuriqi, A., Abubaker, S., Kisi, O., 2019. Hydrologic Alteration at the Upper and Middle Part of the Yangtze River, China: Towards Sustainable Water Resource Management Under Increasing Water Exploitation. Sustainability, 11(19): 5176.

Barbarossa, V. et al., 2020. Impacts of current and future large dams on the geographic range connectivity of freshwater fish worldwide. Proceedings of the National Academy of Sciences, 117(7): 3648-3655. DOI:10.1073/pnas.1912776117

Cai, H. et al., 2018. Quantifying the impact of the Three Gorges Dam on the thermal dynamics of the Yangtze River. Environmental Research Letters, 13(5): 054016-.

Caissie, D., 2006. The thermal regime of rivers: a review. Freshwater Biol., 51(8): 1389-1406. DOI:10.1111/j.1365-2427.2006.01597.x

Çalışkan, A., Elçi, Ş., 2009. Effects of Selective Withdrawal on Hydrodynamics of a Stratified Reservoir. Water Resources Management, 23(7): 1257-1273. DOI:10.1007/s11269-008-9325-x

Cao, G., Hui, E., Hu, X., 2012. Analysis of the vertical structure of water temperature in the vicinity area of Three Gorges Dam since the Three Gorges Reservoir impounds. Journal of hydraulic Engineering, 39(10): 1254-1259(in Chinese).

Casado, A., Hannah, D.M., Peiry, J.-L., Campo, A.M., 2013. Influence of dam-induced hydrological regulation on summer water temperature: Sauce Grande River, Argentina. Ecohydrology, 6(4): 523-535.

Chen, G., Fang, X., Devkota, J., 2016a. Understanding flow dynamics and density currents in a river-reservoir system under upstream reservoir releases. Hydrological Sciences Journal, 61(13): 2411-2426. DOI:10.1080/02626667.2015.1112902

Chen, J. et al., 2016b. Changes in monthly flows in the Yangtze River, China – With special reference to the Three Gorges Dam. Journal of Hydrology, 536: 293-301. DOI:https://doi.org/10.1016/j.jhydrol.2016.03.008

Cheng, Y., Voisin, N., Yearsley, J.R., Nijssen, B., 2020. Reservoirs Modify River Thermal Regime Sensitivity to Climate Change: A Case Study in the Southeastern United States. Water Resources Research, 56.

Cole, T.M., Wells, S.A., 2013. CE-QUAL-W2: A Two-dimensional, Laterally Averaged, Hydrodynamic and Water Quality Model, Version 3.71. Department of Civil and Environmental Engineering, Portland State University, Portland, OR.

Cui, X., Liu, S., Wei, X., 2012. Impacts of forest changes on hydrology: A case study of large watersheds in the upper reaches of Minjiang River watershed in China. Hydrology and Earth System Sciences, 16: 4279-4290. DOI:10.5194/hess-16-4279-2012

Cynthia, L.L., 2000. Stream temperature variation in regulated rivers: Evidence for a spatial pattern in daily minimum and maximum magnitudes. Water Resources Research, 36(10): 2947-2955.

Dai, L., Dai, H., Jiang, D., 2012. Temporal and spatial variation of thermal structure in Three Gorges Reservoir: A simulation approach. Journal of Food Agriculture & Environment, 10(2): 1174-1178.

Dean, J.F. et al., 2018. Methane Feedbacks to the Global Climate System in a Warmer World. Reviews of Geophysics, 56(1): 207-250. DOI:10.1002/2017rg000559

Dickson, N.E., Carrivick, J.L., Brown, L.E., 2012. Flow regulation alters alpine river thermal regimes. Journal of Hydrology, 464-465: 505-516. DOI:https://doi.org/10.1016/j.jhydrol.2012.07.044

Ducharne, A., 2008. Importance of stream temperature to climate change impact on water quality. Hydrology and Earth System Sciences, 12(3): 797-810.

Fu, B. et al., 2010. Three Gorges Project: Efforts and challenges for the environment. Progress in Physical Geography: 1-14.

Gang, C., Xing, F., Devkota, J., 2015. Understanding flow dynamics and density currents in a river-reservoir system under upstream reservoir releases. Hydrological Sciences Journal/journal Des Sciences Hydrologiques, 61(13): 2411-2426.

Gao, X. et al., 2014. Effects of Water Temperature and Discharge on Natural Reproduction Time of the Chinese Sturgeon, Acipenser sinensis, in the Yangtze River, China and Impacts of the Impoundmentof the Three Gorges Reservoir. Zoological Science, 31(5): 274.

Han, Z., Long, D., Fang, Y., Hou, A., Hong, Y., 2019. Impacts of climate change and human activities on the flow regime of the dammed Lancang River in Southwest China. Journal of Hydrology, 570: 96-105. DOI:https://doi.org/10.1016/j.jhydrol.2018.12.048

Hocking, G., Straškraba, M., 1994. An analysis of the effect of an upstream reservoir by means of a mathematical model of reservoir hydrodynamics. Water Science and Technology, 30(2): 91-98. DOI:10.2166/wst.1994.0032

Huang, Z., 1999. Some Issues on Envirronmental Hydraulics of TGP. China Three Gorges Construction, 09: 36-39 (in chinese).

Ji, D. et al., 2017. Impacts of water level rise on algal bloom prevention in the tributary of Three Gorges Reservoir, China. Ecological Engineering, 98: 70-81. DOI:10.1016/j.ecoleng.2016.10.019

Johnson, B.M. et al., 2004. Effects of climate and dam operations on reservoir thermal structure. Journal of Water Resources Planning and Management, 130(2): 112-122.

Kratina, P., Greig, H., Thompson, P., Carvalho-Pereira, T., Shurin, J., 2012. Warming modifies trophic cascades and eutrophication in experimental freshwater communities. Ecology, 93: 1421-30. DOI:10.2307/23213771

Lammers, R.B., Pundsack, J.W., Shiklomanov, A.I., 2007. Variability in river temperature, discharge, and energy flux from the Russian pan-Arctic landmass. Journal of Geophysical Research Biogeosciences, 112(G4): 1-15.

Lauri, H. et al., 2012. Future changes in Mekong River hydrology: impact of climate change and reservoir operation on discharge. Hydrol. Earth Syst. Sci., 16(12): 4603-4619. DOI:10.5194/hess-16-4603-2012

Liu, L., Liu, D., Johnson, D.M., Yi, Z., Huang, Y., 2012. Effects of vertical mixing on phytoplankton blooms in Xiangxi Bay of Three Gorges Reservoir: implications for management. Water Resources, 46(7): 2121-30. DOI:10.1016/j.watres.2012.01.029

Long, L.-H. et al., 2016. Characteristic of the water temperature lag in Three Gorges Reservoir and its effect on the water temperature structure of tributaries. Environmental Earth Sciences, 75(22). DOI:10.1007/s12665-016-6266-1

Long, L., Ji, D., Liu, D., Yang, Z., Lorke, A., 2019a. Effect of Cascading Reservoirs on the Flow Variation and Thermal Regime in the Lower Reaches of the Jinsha River. Water, 11(5): 1008. DOI:10.3390/w11051008

Long, L. et al., 2019b. Density-driven water circulation in a typical tributary of the Three Gorges Reservoir, China. River Research and Applications, 35(5): 1-11. DOI:10.1002/rra.3459

Lu, C.-h., Dong, X.-y., Tang, J.-l., Liu, G.-c., 2019. Spatio-temporal trends and causes of variations in runoff and sediment load of the Jinsha River in China. Journal of Mountain Science, 16(10): 2361-2378. DOI:10.1007/s11629-018-5330-6

Lu, S.S., Dai, L.Q., Dai, H.C., Mao, J.Q., 2013. Effect of Release Temperature from Three Gorges Reservoir on the Procreation of Chinese Sturgeons. Applied Mechanics & Materials, 361-363: 958-961.

Ma, J. et al., 2015. Modeling density currents in a typical tributary of the Three Gorges Reservoir, China. Ecological Modelling, 296: 113-125. DOI:10.1016/j.ecolmodel.2014.10.030

Maheu, A., St-Hilaire, A., Caissie, D., El-Jabi, N., 2016. Understanding the Thermal Regime of Rivers Influenced by Small and Medium Size Dams in Eastern Canada. River Research and Applications, 32(10): 2032-2044. DOI:10.1002/rra.3046

Mbaka, J.G., Wanjiru Mwaniki, M., 2015. A global review of the downstream effects of small impoundments on stream habitat conditions and macroinvertebrates. Environmental Reviews, 23(3): 257-262. DOI:10.1139/er-2014-0080

McCartney, M., Sullivan, C., Acreman, M., 2001. Ecosystem Impacts of Large Dams. School of Arts and Social Sciences Papers.

Mi, C., Sadeghian, A., Lindenschmidt, K.-E., Rinke, K., 2019. Variable withdrawal elevations as a management tool to counter the effects of climate warming in Germany's largest drinking water reservoir. Environmental Sciences Europe, 31(1): 19. DOI:10.1186/s12302-019-0202-4

Olden, J.D., Naiman, R.J., 2010. Incorporating thermal regimes into environmental flows assessments: modifying dam operations to restore freshwater ecosystem integrity. Freshwater Biology, 55(1): 86-107.

Oreilly, C. et al., 2015. Rapid and highly variable warming of lake surface waters around the globe. Geophysical Research Letters, 42. DOI:10.1002/2015GL066235

Othman Ali, R., Abubaker, S.R., Islam, S., 2019. Overview effect of three gorges reservoir on the changing water temperature in the Yangtze river, China. International Journal of Hydrology, 3(3): 230-237. DOI:10.15406/ijh.2019.03.00185

Prats, J., Val, R., Armengol, J., Dolz, J., 2010. Temporal variability in the thermal regime of the lower Ebro River (Spain) and alteration due to anthropogenic factors. Journal of Hydrology, 387(1): 105-118. DOI:https://doi.org/10.1016/j.jhydrol.2010.04.002

Ren, L., Song, C., Wu, W., Guo, M., Zhou, X., 2020. Reservoir effects on the variations of the water temperature in the upper Yellow River, China, using principal component analysis. Journal of Environmental Management, 262: 110339. DOI:https://doi.org/10.1016/j.jenvman.2020.110339

Stocker, T.F. et al., 2013. Climate Change 2013: The Physical Science Basis. Cambridge University Press, Cambridge.

Tao, Y. et al., 2020. Quantifying the impacts of the Three Gorges Reservoir on water temperature in the middle reach of the Yangtze River. Journal of Hydrology, 582: 124476. DOI:https://doi.org/10.1016/j.jhydrol.2019.124476

Trung, L. et al., 2018. Assessing Cumulative Impacts of the Proposed Lower Mekong Basin Hydropower Cascade on the Mekong River Floodplains and Delta – Overview of Integrated Modeling Methods and Results. Journal of Hydrology. DOI:10.1016/j.jhydrol.2018.01.029

Van Vliet, M.T.H. et al., 2013. Global river discharge and water temperature under climate change. Global Environmental Change, 23(2): 450-464. DOI:10.1016/j.gloenvcha.2012.11.002

Wang, Q.G., Du, Y.H., Su, Y., Chen, K.Q., 2012a. Environmental Impact Post-Assessment of Dam and Reservoir Projects: A Review. Procedia Environmental Sciences, 13: 1439-1443. DOI:https://doi.org/10.1016/j.proenv.2012.01.135

Wang, S., Qian, X., Han, B.P., Luo, L.C., Hamilton, D.P., 2012b. Effects of local climate and hydrological conditions on the thermal regime of a reservoir at Tropic of Cancer, in southern China. Water Research, 46(8): 2591-2604.

Wang, Y., Zhang, N., Wang, D., Wu, J., Zhang, X., 2018. Investigating the impacts of cascade hydropower development on the natural flow regime in the Yangtze River, China. Science of The Total Environment, 624: 1187-1194. DOI:https://doi.org/10.1016/j.scitotenv.2017.12.212

Wei, O., Hao, F., Song, K., Xuan, Z., 2011. Cascade Dam-Induced Hydrological Disturbance and Environmental Impact in the Upper Stream of the Yellow River. Water Resources Management, 25(3): 913-927.

Winton, R.S., Calamita, E., Wehrli, B., 2019. Reviews and syntheses: Dams, water quality and tropical reservoir stratification. Biogeosciences, 16(8): 1657-1671. DOI:10.5194/bg-16-1657-2019

Xu, Y., Zhang, M., Wang, L., Kong, L., Cai, Q., 2011. Changes in water types under the regulated mode of water level in Three Gorges Reservoir, China. Quaternary international, 244(2): 272-279.

Yang, S.L., Xu, K.H., Milliman, J.D., Yang, H.F., Wu, C.S., 2015. Decline of Yangtze River water and sediment discharge: Impact from natural and anthropogenic changes. Scientific Reports, 5(1): 12581. DOI:10.1038/srep12581

Yang, Z., Liu, D., Ji, D., Xiao, S., 2010. Influence of the impounding process of the Three Gorges Reservoir up to water level 172.5 m on water eutrophication in the Xiangxi Bay. Science China Technological Sciences, 53(4): 1114-1125. DOI:10.1007/s11431-009-0387-7

Yang, Z. et al., 2013. An eco-environmental friendly operation: An effective method to mitigate the harmful blooms in the tributary bays of Three Gorges Reservoir. Science China Technological Sciences, 56(6): 1458-1470.

Ye, L., Han, X., Xu, Y., Cai, Q., 2007. Spatial analysis for spring bloom and nutrient limitation in Xiangxi bay of three Gorges Reservoir. Environmental monitoring and assessment, 127(1): 135-145.

Zeng, X., Zhao, N., Sun, H., Ye, L., Zhai, J., 2015. Changes and Relationships of Climatic and Hydrological Droughts in the Jialing River Basin, China. PLoS One, 10(11): e0141648-e0141648. DOI:10.1371/journal.pone.0141648

Zheng, B., Zhang, Y., Fu, G., Liu, H., 2006. On the assessment standards for nutrition status in the Three Gorge Reservoir. Acta Scientiae Circumstantiae, 26(6): 1022-1030 (in chinese).

Zhou, J., Zhao, Y., Song, L., Bi, S., Zhang, H., 2014. Assessing the effect of the Three Gorges reservoir impoundment on spawning habitat suitability of Chinese sturgeon (Acipenser sinensis) in Yangtze River, China. Ecological informatics, 20: 33-46.

Supporting Information for "Recent changes of the thermal structure in Three Gorges Reservoir and its ecological impacts on tributary bays"

L.H. Long[1,2], Z.J. Yang[2], D.B. Ji[2], L. Liu[3], D.F. Liu[4], A. Lorke[1*]

[1]Institute for Environmental Sciences, University of Koblenz-Landau, Fortstrasse 7, 76829, Landau, Germany

[2]College of Hydraulic and Environmental Engineering, China Three Gorges University, 443002 Yichang City, Hubei Province, China

[3]Department of Experimental Limnology, Leibniz-Institute of Freshwater Ecology and Inland Fisheries, 16775 Stechlin, Germany

[4]Hubei Key Laboratory of River-lake Ecological Restoration and Algal Utilization, Hubei University of Technology,430068 Wuhan City, Hubei Province, China

Contents of this file

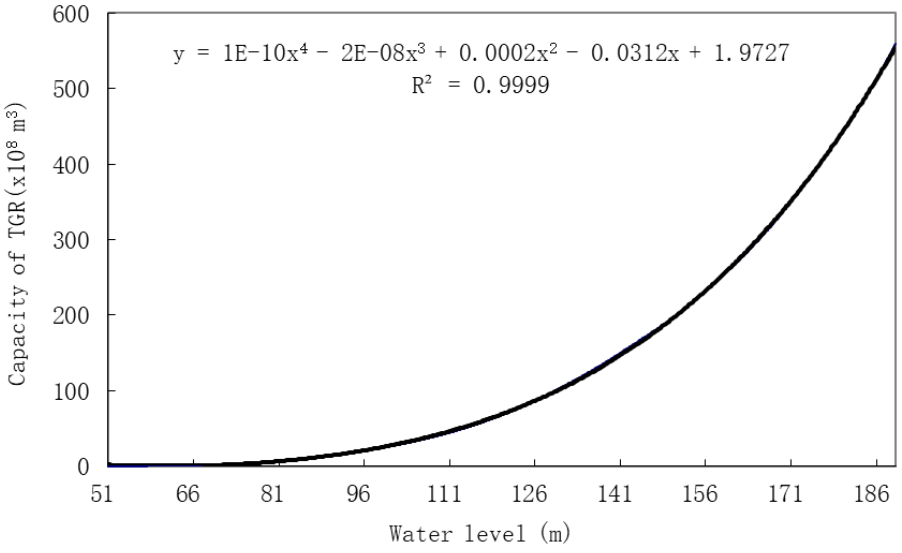

Fig. S1. Polynomial regression curve of reservoir capacity and water level near to the dam in Three Gorges reservoir (TGR).

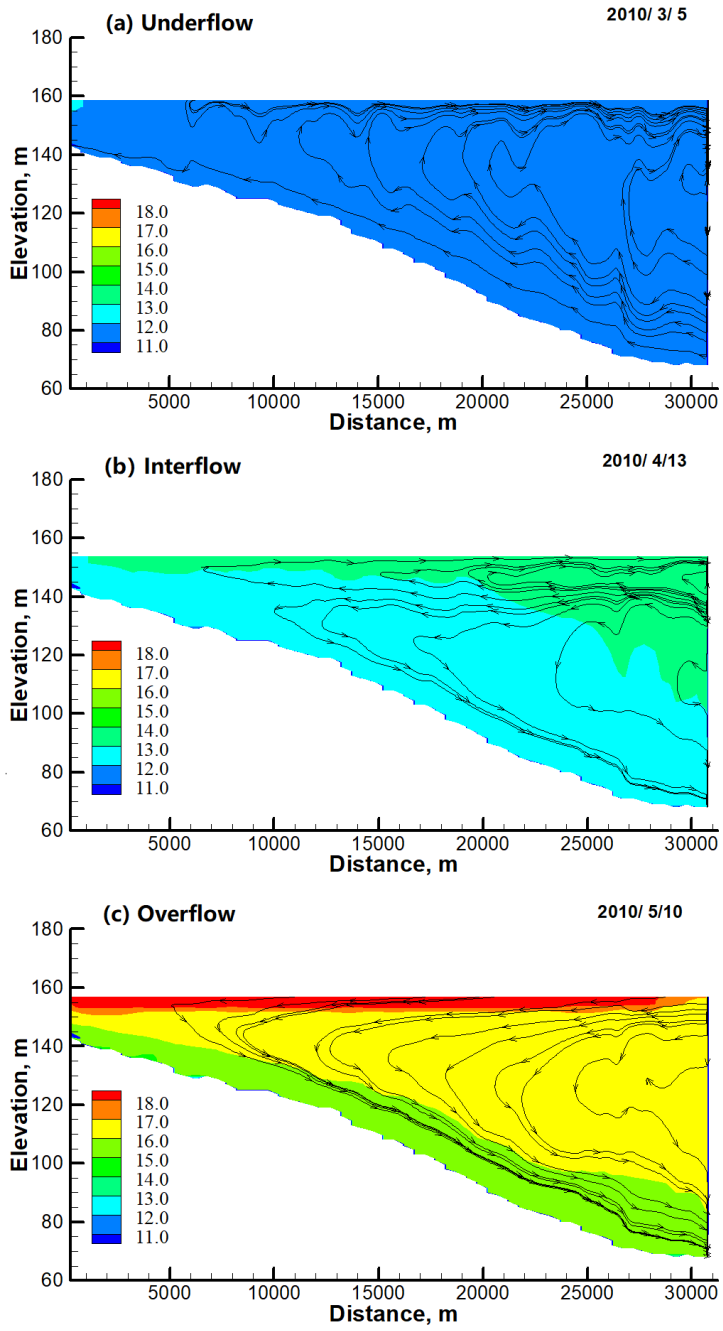

Fig. S2: Longitudinal cross-sections of Xiangxi Bay showing temperature contours (colour) and streamlines (black lines with arrows). The three examples illustrate seasonally changes in density-driven exchange flows between the main reservoir at the deep end of the cross section, and the inflowing river at the shallow end: (a) Underflow (5 March 2015), (b) interflow (13 April 2015), (c) overflow (10 May 2015). Water temperature and flow velocity was simulated using the CE-QUAL-W2 model.

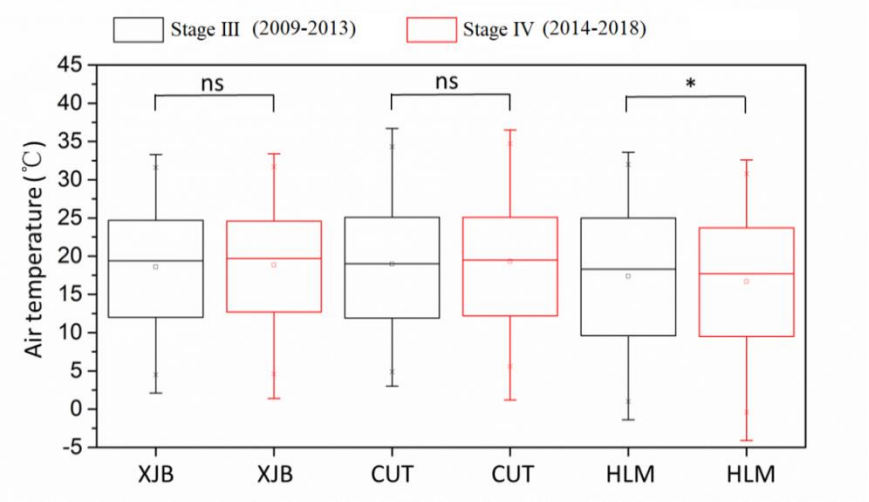

Fig. S3. Variations of daily mean temperature with significance tests during stage III (2009 to 2013) and stage IV (2014 to 2018) periods at Yibin (XJB), Chongqing (CUT) and Yichang (HLM). Boxes mark the range between the first and third quartiles, crosses outside the box show the minimum and maximum values, the horizontal line is the median value and square symbols are mean values.

Multi-year mean air temperature at Yibin, Chongqing and Yichang were 18.7, 19.1 and 17.0 ℃, respectively. No significant changes in air temperature ($p > 0.05$) were observed at the three weather stations, except for a slight decrease (-0.70 °C) at HLM after the upstream cascading reservoirs were filled (Fig.S3). This indicates that the rise of water temperature was not climate driven. Instead, the effect of upstream cascading reservoirs on water temperature of TGR was observed (Fig. 4). At stage III (before the completion of the two upstream reservoirs), water temperature was linearly correlated to air temperature at XJB and CUT throughout the year. In contrast, at stage IV (after the upstream reservoirs came into operation), water temperature decreased in spring and summer and increased in autumn and winter at XJB. A consistent linear correlation between air temperature and water temperature was observed at CUT, while a clear seasonality was found because of the operation of TGR and no obvious distinction between the two periods at HLM (Fig. S4).

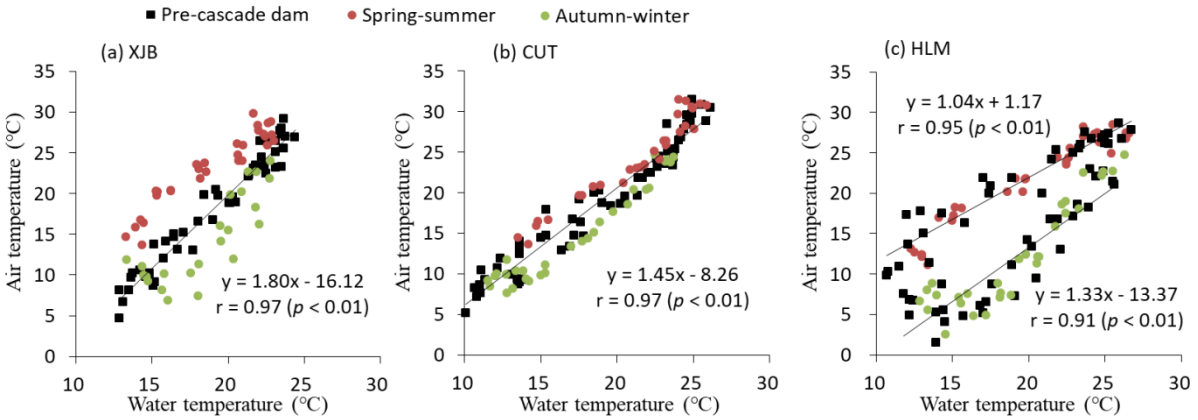

Fig. S4. Monthly mean air temperature versus water temperature: (a) at the locations of the upstream dam (XJB), (b) at the inflow of TGR (CUT), and (c) at the outflow of TGR (HLM). Black symbols mark data from construction of the upstream dam (2009-2013), red and green symbols show data from after dam construction (2014-2018) for spring and summer, respectively. Black lines show linear regressions of pre-cascade dam period (2009-2013), with the regression equation, Pearson correlation coefficient (r) and significance level (p) as labels.

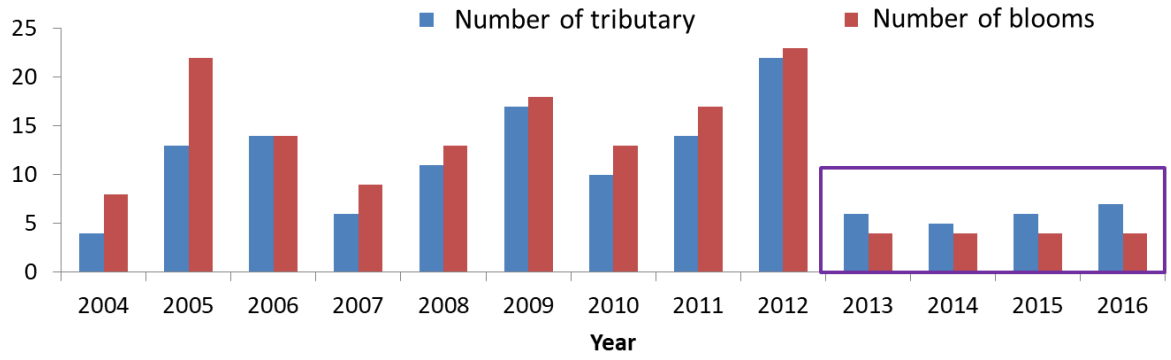

Fig. S5. Number of tributaries of TGR where algae blooms were detected (blue bars) and number of blooms in each year (red bars) for the period 2004 to 2016. Data are available online from the ‘‘Bulletin on ecological and environmental monitoring for Three Gorges Project’’ *http://webinterface.cnemc.cn/*).

Table S1 Statistics (mean ± standard deviation) of hydrological and physical properties of TGR during four operational stages in spring (March to May). Q_{XJB} and Q_{TGD} are the discharge from XJB dam and TGD dam, respectively. WT_{MIH} is water temperature measured near the water surface (0.5 m depth) close the dam (station MIH). MTD is maximum temperature difference between surface and bottom and stratified days represents the number of days with MTD > 0.5 °C. WRT is hydraulic water residence time.

Stage	Year	Q_{XJB} (m^3/s)	Q_{TGD} (m^3/s)	Water level in TGR (m)	WT_{MIH} (℃)	MTD at MIH (℃)	Stratified days (d)	WRT (d)
I	2004	2285±542	8371±3087	137.6±0.7	16.8±4.2	0.1	0	22
	2005	2194±463	8872±4082	138.3±0.5	16.4±5.0	0.1	0	21
	2006	1964±356	7980±2930	138.3±0.7	16.3±4.1	6.6	47	24
II	2007	1831±729	7036±2405	149.7±2.3	15.5±3.6	10.3	96	41
	2008	2189±663	8604±3134	151.4±2.3	15.2±4.6	10.0	71	32
III	2009	1788±305	9457±4182	159.2±3.5	14.9±3.4	5.9	51	40
	2010	1841±466	6963±2792	155.2±2.0	14.3±2.9	6.7	66	45
	2011	1801±326	6924±1342	159.6±4.7	13.9±3.2	7.6	71	50
	2012	1630±619	8244±4955	162.3±4.0	13.6±3.5	4.7	39	47
	2013	1681±218	7468±4179	160.8±3.6	15.2±3.3	4.7	49	49
IV	2014	1970±308	8420±2821	160.1±4.2	15.1±3.0	1.5	20	42
	2015	2768±628	8508±1813	162.2±5.8	15.9±3.3	2.5	25	44
	2016	2629±437	11516±4134	162.0±6.2	15.7±3.1	1.5	10	34
	2017	2817±763	9792±3208	161.1±4.8	15.9±2.7	1.5	12	38
	2018	2588±641	9573±4548	160.5±3.8	16.0±3.4	2.8	39	38